In memory of my brother, the late S.T. Balasubramanian

ABSTRACT

A STUDY OF SHEAR DIAPHRAGMS
AND CLAD MULTISTORY FRAMES

Sithambaram Chockalingam, Ph.D.
Concordia University, 1979.

The research reported in this study forms part of an overall project on the shear behaviour of cold-formed shear diaphragms and their application as stiffening elements in multistory frames. Because of their inherent economy, light-gage steel panels are widely used in many buildings as shear resisting elements. When used in combination with steel frames, they offer considerable shear resistance to lateral loads.

The objective of this study is to develop a simplified method for the elastic analysis of the entire structural system consisting of the frame and the claddings. The investigation consists of two parts: The first part is concerned with the analysis for the shear stiffness and strength of claddings (also referred to as shear diaphragms). Based on an assumed deformation mode, simple expressions are developed for fastener forces and shear stiffness of diaphragms. Since the ultimate shear strength may be controlled by failure of the connections or by overall shear buckling, theories for prediction of both modes of failures are presented. The accuracy of the proposed expressions are verified by

comparing the predicted shear stiffnesses and strengths with the measured values of several diaphgragms having a wide range of variables.

The second part of the investigation deals with the response of multi-story frames stiffened with corrugated steel claddings. A simple technique is developed to derive the stiffness matrix of the cladding. The analysis of the overall structure is carried out by using the conventional direct stiffness approach. The lateral load responses of three different clad frames are predicted by the new approach and the results are compared to those from other theories. Design curves are developed for the rapid analysis of clad frames. Recommendations for further research are also included.

5. EXPERIENCE (RESEARCH OR RELATED EXPERIENCE)

DATES	INSTITUTION	SUBJECT
1963-1965	Design Engineer, Highways Dept., Government of Madras, India	Structures
1965-1968 1970-1972	Faculty of Civil Engineering A.C. College of Engineering Karaikudi, Tamilnadu, India	Structural Engineering
1972-1974	Part time instructor and Research Assistant, University of Toronto, Toronto, Canada	Structures and Mechanics
1974 to date	Instructor and Research Assistant, Concordia University, Montreal, Canada	Civil Engineering

LIST OF PUBLICATIONS

1. Fazio, P., Ha, H.K. and Chockalingam, S.; "Literature Survey on the Behaviour of Light Gage Steel Diaphragms", Report No. SBC-27-CE75-1, Dept. of Civil Engg., Concordia University, Montreal, Canada.

2. Fazio, P., Ha, H.K. and Chockalingam, S.; "Shear Flexibility of Light Gage Steel Corrugated Diaphragms", Report No. SBC-28-CE-75-2, Dept. of Civil Engg., Concordia University, Montreal, Canada.

3. Fazio, P., Ha, H.K. and Chockalingam, S.; "Strength of Light Gage Steel Corrugated Diaphragms", Report No. SBC-29-CE-75-3, Dept. of Civil Engg., Concordia University, Montreal, Canada.

4. Fazio, P., Ha, H.K. and Chockalingam, S.; "Buckling Formulas for Corrugated Metal Shear Diaphragms", Discussion in the Journal of the Structural Division ASCE, Proc. ST-3, March 1976.

5. Fazio, P., Ha, H.K. and Chockalingam, S.; "Design of I-shaped Beams with Diaphragm Bracing", Discussion in the Journal of the Structural Division ASCE, December 1976.

6. Ha, H.K., Chokalingam, S. and Fazio, P.; "The Analysis and Design of Multistory Frames with Light-Gage Corrugated Panels", Report No. CBS 66, Centre for Building Studies, Concordia University, Montreal, March 1977.

7. Fazio, P., Ha, H.K. and Chockalingam, S.; "Strength of Light-Gage Steel Corrugated Shear Diaphragms", Report No. CBS 30, Centre for Building Studies, Concordia University, Montreal, August 1977.

8. Chockalingam, S., Fazio, P. and Ha, H.K.; "Ultimate Torque of Reinforced Concrete Beams", Discussion in the Journal of the Structural Division ASCE, June 1977.

9. Chockalingam, S.; "Experimental Study of the Behaviour of Reinforced Concrete Coupling Slabs", Discussion in the Journal of the American Concrete Institute, September 1977.

10. Ha, H.K., Fazio, P. and Chockalingam, S.; "The Effect of Light Gage Partitions on Multistory Buildings", Discussion in the Journal of the Structural Division, ASCE, August 1977.

11. Chockalingam, S., Ha, H.K. and Fazio, P.; "Strength and Stiffness of Corrugated Metal Shear Diaphragms", Discussion in the Journal of the Structural Division, ASCE, January 1978.

12. Chockalingam, S., Ha, H.K. and Fazio, P.; "Strength of Light Gage Steel Corrugated Shear Diaphragms", Proceedings of the Fourth International Specialty Conference on Cold-Formed Steel Structures, University of Missouri, Rolla, June 1978.

13. Fazio, P., Ha, H.K. and Chockalingam, S.; "Strength of Cold-Formed Steel Shear Diaphragms", Canadian Journal of Civil Engineering. (Appearing in March 1979).

14. Ha, H.K., Chockalingam, S. and Fazio, P.; "Further Study on the Strength of Cold-Formed Steel Shear Diaphragms", International Conference on Thin Walled Structures, University of Strathclyde, Glasgow, Scotland. (Appearing in April 1979).

15. Chockalingam, S., Fazio, P. and Ha, H.K.; "Overall Buckling of Corrugated Metal Shear Diaphragms". Tentatively accepted for publication, Journal of the Structural Division, ASCE.

16. Chockalingam, S., Ha, H.K. and Fazio, P.; "Simplified Analysis of Cold-Formed Steel Shear Diaphragms". Submitted for publication in the Canadian Journal of Civil Engineering.

17. Chockalingam, S., Fazio, P. and Ha, H.K.; "Buckling of Cold-Formed Shear Diaphragms". Submitted for presentation at the Canadian Society of Civil Engineering Annual Conference, June 1979.

ACKNOWLEDGEMENTS

I wish to place on record my profound thanks and gratitude to Professors Kinh Ha and Paul Fazio for introducing the topic of shear diaphragms and for their valuable guidance, criticisms and suggestions throughout this study.

I am also thankful to Professors Cedric Marsh and Alan Russell for their interest in this study.

I also extend my special thanks to Professor P. Venkataraman for his valuable time in proofreading this thesis.

My special thanks are also due to my colleagues, Jaya Raman, Denis Prud'homme, Louis Stankevicius and Jane St. Pierre for their ever-willing assistance during the course of this project.

I would like to express my thanks to Mr. L. Krishnan, Reserve Bank of India, for all his encouragement and help during the period of study.

I gratefully acknowledge the assistance of Pam O'Cain and Mrs. Elizabeth Horwood for the typing of this thesis.

I wish to express my deep sense of appreciation and sincere thanks to my wife Arumugam and to my children, Seethalatchimi, Poongodi, Renuga and Siva Sithambaram, for their extreme patience, without which it would have been very difficult to complete my study.

TABLE OF CONTENTS

LIST OF TABLES

LIST OF FIGURES

NOMENCLATURE

a = Total width of diaphragm (perpendicular to corrugation)

a_s = Spacing of seam attachments

A = Cross-sectional area of purlins

b = Length of diaphragm (parallel to the corrugations)

b' = Width of one panel in Eq. 4.20.

c_2, c_3 = Unity for seam clinches (see Ref. 41)

D_x, D_y and D_{xy} = Orthotropic constants in Eqs. 5.7 to 5.9

E = Modulus of elasticity of the material

F_{si} = Force in the side fastener

F_{se} = Force in the seam fastener

F_R = Horizontal component of end fastener force

F_{pi} = Force in the girt fastener

F_{vi} = Vertical component of end fastener force

F_e = Resultant force in end fastener

F_p = Ultimate strength of one girt fastener

F_u = Ultimate strength of one side fastener

F_v = Ultimate strength of one seam fastener

F_w = Ultimate strength of one end fastener

I_D = Gross moment of inertia of deck unit about vertical centre line axis in inch^4

I_y = Moment of inertia of the cross section of panel per unit length about the horizontal neutral axis in inch^4

G' = Diaphragm shear modulus (shear stiffness according to Ref. 12)

I_{eo}, I_{go} = Second moment of end fastener and girt fastener patterns about point 0 in Fig. 3.4

K = Sheeting constant from Ref. 42

K_{si}, K_{se} = Stiffnesses of one side and seam fastener respectively

K_e, K_g = Stiffnesses of one end and girt fastener respectively

L_c = Height of one story in multistory frame

L_v = Vertical span of panels (distance between the purlins)

M_c, M_b = Moments in clad frame and bare frame respectively

m = Number of buckled waves in a diaphragm

N = Shear load per unit width of diaphragm

N_{cr} = Critical buckling load of diaphragm per unit width

N_4 = Ultimate shear load per unit width of diaphragm

P = Total shear load in diaphragm perpendicular to corrugations

P_i = Lateral forces at each floor level of multistory frame

q = Horizontal projection of a single width of panel

q_1, q_2 = Components of working shear in lbs/ft/

Q_{ult} = Ultimate shear load of diaphragm (parallel to corrugations)

r = Shear stiffness ratio defined by Eq. 6.13

R_i = Restraining forces offered by the cladding

s = Developed width of a single panel

S = Shear stiffness of diaphragm or cladding

T_{fsi}, T_{fse} = Total force along the sides and seams

T_{si}, T_{se} = Ultimate strength of the fasteners along the sides and seams

t_s, t = Thickness of sheeting

t_1 = Thickness of sheeting at the bottom of vertical ribs

t_2'/t_2 = Effective thickness ratio of fluted element in inches (Ref.41)

w = Width of one panel

x_o = Location of zero force in Fig. 3.4

Δ_c, Δ_b = Lateral deflection of clad frame and bare frame respectively

α_s = Tangent of the angle between y-axis and the direction of buckled waves

γ = Total shear strain of the diaphragm

Δ = Shear deflection of the diaphragm

CHAPTER 1

INTRODUCTION

1.1 General

The introduction of light gage steel for structural components in recent years could be regarded as a major step in the evolution of structural forms from their primitive massiveness to the modern types of structures which are slender, lighter and more economical. Extensive use of light gage steel can be seen in the construction of roofs, walls and internal partitions of many types of buildings, both on this continent and abroad. The first large light gage steel roof deck in Canada was erected about 40 years ago in Toronto by Westeel-Rosco Ltd, one of the largest steel deck manufacturers in this country. Since that time, steel roof deck has grown in popularity and it has been reported that over 80% of all non-domestic roofing installations employ steel deck systems [1]. The same trend has been noticed in countries like the United States, England and Sweden.

When used primarily as a means of enclosing the space, roof covering and wall sheathing are usually referred to as claddings. It has been customary to treat these claddings as non-structural elements in the design of steel buildings. The structural use of light gage steel in buildings started only after the introduction of corrugated panels. Many different sizes and shapes of panels can be obtained from light gage steel by cold forming (Figs.1.1 and 1.2)

Corrugated panel, because of its increased flexural rigidity, could support and sustain large forces normal to its plane. In addition, if the panels are properly fastened to each other and to the supporting frame, the resulting structure would offer substantial resistance to in-plane forces.

As early as 1947, tests were performed in the United States [2] to investigate the shear behaviour of isolated panels and panel assemblies and their effects on framed buildings [3-6]. The results have proved that the calculated values of stresses and deflections of frames without considering the claddings, were much higher than their corresponding measured values. This provided strong evidence to support the fact that the supposedly non-structural elements offer considerable shear resistance to loads acting in their plane. Because the cladding is connected to the frame, interaction of the cladding and the frame will always be there, even if the building is not designed for the effect of the cladding. By virtue of its shear stiffness, the cladding will attract its share of the applied load and hence, a proper and safe design procedure would have to consider the effect of the cladding in the overall behaviour of the entire building. However, there was some hesitation among the engineers in the past to consider the effects of these non-structural elements. The reasons for this may be stated as follows:

i) Cladding had been traditionally treated as a component which could be removed later during the life time of the building;

ii) There was no generally accepted theory to calculate the stiffening effect.

Thus, if the roof sheeting and wall sheathing are to be taken into account in the design, they must be regarded as permanent structural elements and proper attention must be given in the design of the connections. When treated as structural elements and designed to resist in-plane forces, claddings are generally referred to as "shear diaphragms".

1.2 Shear Diaphragm Action in Structures

Buildings may be subjected to lateral loads from a variety of sources such as wind, earthquakes and blasts. Referring to Fig.1.3, the building is subjected to horizontal forces at the level of the roof and can be designed as a pin-jointed frame with x-bracing (Fig.1.4a) or as a moment resistant frame (Fig.1.4b). Alternately, the roof sheathing or cladding could be designed as a shear diaphragm to provide the required lateral stiffness (Fig.1.4c). By utilising the inherent shear strength of the cladding one could obtain a lighter structure with considerable saving in the overall cost of the building. The roof diaphragm, when properly connected to the supporting frame, would act as the web of a deep plate girder with the framing members AB and CD as the flanges (Fig.1.3). Similarly, walls may also be designed to incorporate diaphragmic action with panels spanning between girts as shown in Fig.1.5 and thus eliminating diagonal bracing in the end frames. Many shed type buildings have

been constructed by utilising the concept of shear diaphragms and have proved to be safe and economical. The use of shear diaphragms is, however, not restricted to single story shed type buildings. Research is underway to utilise the stiffening effect of cladding on multistory frames and is discussed in the next section.

1.3 Effect of Cladding on Multistory Frames

Shear resistance of light gage steel cladding may also be used for controlling the lateral deflection of multistory structures. The contribution of the cladding and internal partitions to the strength and stiffness of the structure has been generally ignored in the design because proper design methods were not available to account for the integrated behaviour. As in single story buildings, measured deflections in the case of tall buildings were considerably smaller than the computed deflections. In a study conducted by Rathbburn[7] on the lateral deflection of the Empire State Building in New York, it was observed that the actual deflection was about one fifth of the calculated value. This large difference arises from ignoring the effect of the heavy stone and masonry walls in the calculations. In another study on a 56 story concrete framed structure apartment building, Wiss and Curth [8] found that the measured deflection of the top story was only 3.3 inches as compared to the calculated value of 8.9 inches. These studies indicate that the cladding elements do haye a significant effect on the stiffness of multistory frames.

Since, in the design of tall buildings, the member sizes in the lower stories are often controlled by lateral deflection limitations rather than by stress considerations, accurate prediction of the lateral deflection is of paramount importance. Only recently, some attempts have been made to include the effect of shear diaphragms in the analysis of multistory frames and it has been found that the lateral deflections are considerably reduced with even the lightest form of claddings [9, 10]. As an example, Fig. 1.6 shows the lateral deflections of a 3 bay, 26 story frame with and without cladding. The infilled frame consisted of light gage steel panels (thickness of sheeting 16-gage or 0.0635 inch) placed at the central bay. The overall dimensions of the frame and member sizes are shown in Fig.1.7. In addition to the significant reduction of the lateral deflections due to the infills, substantial reduction in bending moments and stresses has also been observed [9].

1.4 Components of a Structural Cladding

A typical structural cladding or a shear diaphragm is a two-dimensional structure consisting of four different components as described below (see Fig.1.8):

1) Corrugated Panels: The panels are made of galvanized light gage steel sheet or aluminium sheeting and are available in different sizes and shapes. The width of the panels vary from 18 to 40 inches and the length from 12 to 50 feet. Thickness of the sheet metal could vary from 8 gage to 31 gage (8 gage corresponds to 0.1681 inch and 31 gage corresponds to 0.0142 inch). Panels with sheet thickness less than

20 gage (0.0396 inch) are usually referred to as light gage panels. (Table 1 gives the Gage Number and the corresponding thickness in inches). Corrugated panels available in Canada are of standard widths, 24, 32 and 40 inches and thicknesses ranging from 20 gage to 26 gage (0.0396 to 0.0217 inch).

ii) Panel to Panel Fastener: These are seam connectors or side lap fasteners. For panels with sheet thickness less than 20 gage, the seam fasteners are usually mechanical clinches made by a special tool as an alternative to welds which are often used for heavier gages. In England and other European countries, however, the fasteners are either rivets or screws. The main function of the seam fasteners in a shear diaphragm is to transfer the shear from one panel to the next, and because of their critical function, these fasteners could be regarded as the most important component in a diaphragm.

iii) Connection between the Panels and the Framing Members: These fasteners are referred to as edge and end connectors. The fasteners between the panel sides and the framing members are called edge fasteners (sometimes as side fasteners) and those between the framing members and the panel ends as end fasteners (sheet-purlin fasteners). In North America, screws, rivets and most often welding are used for these fasteners. However, in Europe, welding is seldom in favour. The end and edge fasteners provide the shear transfer from the panel to the framing members.

iv) Marginal Framing Members or Perimeter Members - Framing members or supporting members are usually hot rolled steel sections of suitable size. In recent years, however, cold formed structural sections are also used in the construction of decking. The purpose of the framing members in a shear diaphragm is to carry axial forces.

Some of the most commonly employed panel shapes and the various types of welded connections are shown in Fig.1.9. When welding is used for seam connections, they are of 1 to 2 inches long. The end and edge welds are generally of 3/4 to 1 inch diameter puddle welds.

When all the above components are connected together and the resulting structure is subjected to a load as shown in Fig. 1.10, the deflection at the loaded edge is the measure of the 'shear flexibility' of the diaphragm. In addition to the 'shear flexibility', another important characteristic known as the 'shear strength' representing the diaphragm capacity, is also required for the design of the clad building. Since these two characteristics depend upon a large number of variables [6], their predictions are not a trivial matter and many attempts have been made in the past 25 years. A review of the related studies is presented in the next chapter. Most of the reported research on shear diaphragms are either from North America or England and hence they are discussed under different sections for the sake of comparison.

CHAPTER 2

REVIEW OF PREVIOUS STUDIES AND OBJECTIVES OF THE RESEARCH PROGRAMME

2.1 Research on Shear Diaphragms in North America

Research on light gage steel cladding started almost 30 years ago, when engineers recognized the substantial effect of cladding on the behaviour of the structure. The first test related to diaphragm action of cladding was conducted in 1947 by C.B. Johnson and J.F. Converse [2]. This test was carried out on a full-size clad building subjected to lateral loads applied through cables attached to the side of the building. Johnson presented the results of the tests in the 1950 ASCE meeting in Los Angeles and called for more research pertaining to diaphragm action. As reported in Ref. [11], the next group of tests were performed in 1950 by S.B. Barnes and associates using cellular type of panels.

In 1955, a major research project was sponsored by the Fenestra, Inc. of Bufallo and by the American Iron and Steel Institute and many full-scale tests were carried out by Nilson[11] at Cornell University. This was the first systematic research program on the complex problem of shear diaphragms. After conducting a number of tests on large size diaphragms, Nilson suggested that the shear strength and stiffnes could be obtained more consistently from a cantilever test set-up (Fig.1.10). Various factors influencing the performance of diaphragms such as the connections, panel length, thickness of sheet, panel width, orientation of the panels are discussed. Nilson recognised that the flexibility

of the diaphragm is caused by:

i. the deformation of the connections;

ii. shear deformation of the sheeting; and

iii. deformation of the perimeter members due to bending in the plane of the panel.

One of the major contributions of Nilson is that the cantilever test set-up adopted in his research project has been incorporated as a standard testing procedure and is now being used all over the world. The plan view of a typical cantilever frame with panels is shown in Fig.1.10.Complete details of the testing procedure and design aspects are included in the manual for the "Design of Light Gage Steel Diaphragms", published by the American Iron and Steel Institute [12]. Recently, the American Society for Testing Materials has included the above testing procedure in the ASTM Standards [13] for testing shear diaphragms.

Nilson's work was continued by Luttrell [6] and Apparao [14] to isolate the contribution of the different variables to the overall load-displacement behaviour of diaphragms. Panels with box ribs, trapezoidal and sinusoidal corrugations were used in the test diaphragms. The effects of the following parameters have been investigated: type and size of panel sheet; spacing and type of fasteners (both screw type fasteners and welded connections); number of purlins; and the size of the framing members. Over 100 tests have been performed with some tests to include the various combinations of the above variables. For the first time, behaviour of

panel assembly was subjected to repeated and reversed loading. Although it was not possible to formulate a general theory, an empirical expression and design chart was established to determine the shear stiffness of the cladding. Part of the recommendations for the design of shear diaphragms reported in Ref. 12 is from the work of Luttrell [6].

Easley proposed a new theory [15] for the analysis of shear diaphragms, after conducting a number of full-scale tests [16, 17]. The theory is based on the assumption that all the fasteners would have identical load-deformation characteristics. This assumption makes it difficult, if not impossible, to adopt the theory for diaphragms where the seams and side fasteners are different from the end fasteners. A more simplified approach has been suggested in Ref. 18 for predicting the shear stiffness and strength of diaphragms. Further, Easley's theory has been modified [19] to diaphragms where the fasteners may have different load-deformation behavior.

By using the finite element technique, Ammar and Nilson [20] analysed the shear behaviour of diaphragms and reported that the test results of some diaphragms were in good agreement with the predicted values for the shear stiffness and strength. It is worth mentioning that Ammar and Nilson were the first to employ the finite element method for the analysis of shear diaphragms.

From the assumed deformation modes of the panels and framing members, Ha [21] has developed a new technique for the analysis of corrugated shear diaphragms. The method is based on the stiffness approach and the load-deformation curves for the fasteners are represented in multi-linear forms. The analysis is carried out by using a special computer program and the method has the advantage that it can be easily incorporated into conventional frame programs for the analysis of clad multistory frames. The computed values of shear stiffness and strength are in good agreement with the finite element analysis and test data. However, the method involves the use of special computer programs which are not readily available to designers.

2.2 Research on Shear Diaphragms in England

In England, studies related to the shear behaviour of diaphragms started almost at the same period as in America. While the experimental approach [12] has been successfully used in the U.S.A., researchers in England attempted to solve the problem analytically. Bryan and Jackson [22] suggested a simplified approach for calculating the shear flexibility based on certain simplifying assumptions on the distribution of forces in the diaphragm. The energy approach was used to evaluate the flexibility of a single rectangular corrugated panel. The flexibility components of the connections were obtained from individual tests. The total flexibility of the diaphragm was obtained as the sum of the flexibilities contributed by the panel distortion and the slippage of the connections. Good agreement between the theory and the test results was reported.

The above approach by Bryan and Jackson could be regarded as the

first attempt to study the problem analytically. However, the effects of intermediate purlins and the end fasteners were not considered in this theory. The work was extended further by Bryan and Dakhakhni [5] to include the above mentioned effects. The total shear flexibility was again obtained as the sum of the different components and simple expressions have been proposed for calculating the shear strength of a diaphragm from the strength of the fasteners.

Recently, Davies [23] reported that the expressions proposed by Bryan et al [5] could give erroneous values for the strength of certain types of diaphragms and proposed modified expressions for the ultimate strength and for the flexibility components due to purlin rafter connections. The results obtained from these modified expressions compare favourably with those given by the finite element method [23]. Davies has also presented a simplified approach [24] by modelling the diaphragm as a frame-truss system with appropriate member stiffnesses.

2.3 Empirical Approach for the Design of Shear Diaphragms

The design data for diaphragms could be obtained either by the experimental approach [12] or the analytical methods [5, 15, 20] as mentioned previously. In addition to these approaches, empirical equations [25] are available for predicting the shear flexibility and strength of diaphragms. These equations are derived on the basis of limited test data and are lengthy and complex. Current design procedure in Canada [26], however, is based on design tables prepared from the empirical equations.

2.4 Research on Shear Buckling of Diaphragms

In many diaphragm tests, it has been observed that the failure of the diaphragm occured due to overall buckling of the panels without any sort of rupture at the fasteners. This type of overall buckling would occur when the fasteners are strong and closely spaced. Some attempts have been made to predict the critical load in overall buckling of the diaphragm. As early as 1930, Bergmann and Reissner [27] treated the corrugated plate as an orthotropic plate and developed design curves for the buckling load. Easley and McFarland [28] also used the concept of equivalent orthotropic plate and derived an expression for the shear buckling load by using the principle of minimum potential energy. The expression when applied to full-size diaphragms, resulted in error ranging from 15 to 30%. Easley [29] extended his previous study with some modifications and the new formula predicts well the buckling load of idealized specimen where the shear load is applied along the neutral plane. To account for the restraining effect of special end taps in the idealized specimen, Easley introduced a correlation factor in his expression. However, in practice, evaluation of such a factor would be difficult, if not impossible. Hence, the formula is not of much use for design purpose. Hlavacek [30] has proposed an expression for the buckling load of stiffened plate and reported that the formula could also be used for corrugated panels.

Ellifritt and Luttrell [31] tested a number of welded diaphragms in order to study the effect of the following variables on the shear behaviour:

i. size and type of panel;

ii. fastener arrangements;

iii. purlin spacing;

iv. thickness of sheet; and

v. yield strength of the material.

The major contribution was the derivation of simple formulas for predicting the critical load for local buckling of the panel. Correlating the critical buckling load to the panel span and gage thickness, design curves have been developed. In addition to the design charts for strength, empirical equations were also presented for determining the shear stiffness. In most of the tests, failure of the diaphragm occured either due to tearing of the sheeting around the weld or by strut-like buckling of an edge flute between purlins. It must be mentioned here that the design equations were derived considering only the gage thickness and purlin spacing as the major variables and, therefore, correction factors were introduced to account for other parameters.

Amos [32] carried out a study on the buckling of corrugated panels subjected to in-plane shear forces. By using the shallow shell theory Amos has developed formulas for calculating the local buckling load of a corrugation and reported that the formula predicted well the critical load of panels having sinusoidal corrugation.

Studies related to the shear behaviour of isolated corrugated panels have also been reported by Libove et al [33], McKenzie [34] and Horne and Raslan [35]. However, these works are of little use for

large size diaphragms with many panels and intermediate purlins or girts.

In addition to the above works, research is in progress in Sweden at the Royal Institute of Technology, Stockholm [36] to obtain design procedures for shear diaphragms. The objective is to develop analytical and experimental methods to predict the strength and stiffness of diaphragms. Other projects are also aimed at standardising the procedure for testing of connections under static and dynamic loads.

The next section is concerned with the research reported on the behaviour of clad multistory frames.

2.5 Studies Related to Clad Multistory Frames

While considerable attention is given to the structural behaviour of isolated panels, very few attempts have been made to study the integrated behaviour of multistory frames infilled with light gage steel panels. The need for more research in this area was recognized by the engineering profession as exemplified by the following statement of the Research Committee of the Structural Division of the American Society of Civil Engineers [37] :-

> "Increased use of light-gage metal as the exterior panels of high-rise buildings has revealed the gap in our knowledge of the influence of the exterior covering of such structures. Ordinary design procedures do not consider the exterior structures as primary structural elements.

Such elements do, however, contribute significantly to the lateral stiffness, damping and vibration characteristics. Openings in light-gage exterior surfaces can have a considerable effect. Contributions of the exterior covering to the properties of structures must be evaluated to develop more rational design procedures. Primary among such considerations should be the required thickness and minimum attachment for effective use of these elements as contributing structural elements."

" ..... It should be recognised that the individual elements of a structure do not behave independently of those to which they are connected. Rather, the entire structure responds to the environment and the forces and motions to which the structure is subjected to. Hence, greater attention must be given in the future to the behaviour of the entire structural system and to the development of analytical design procedures and concepts that take this into account."

Reinforcing the above view is a statement by J.F. Baker: "The most unsatisfactory feature in the design of orhtodox buildings has been the small account taken of the strength and stability provided by the cladding".[38].

Among the high-rise structures that are widely used and that will find greater application in the near future are the modern apartment and office buildings with 20 to 30 storys. Construction of many high-rise buildings has increased the necessity for more

refined and rational method of analysis. In most of the tall buildings, the introduction of curtain walls and light-gage steel panels has replaced the traditional use of heavy masonry walls. High-rise structures designed according to the strength requirements are slender and in most cases do not satisfy the lateral deflection requirement. All these factors have aroused interest in more accurate analysis technique for clad multistory frames. Fortunately, the development of digital computers and the matrix methods provided the necessary tools with which the more refined techniques could be developed.

Although a great amount of work has been done on the behaviour of multistory frames during the past 15 years, most of these are related to the analysis and design of either the bare frames or frames infilled with concrete panels. Very few studies are reported on the analysis of multistory frames clad with light gage steel panels. Miller [9] developed a computer programme for the linear elastic analysis of infilled frame. In this approach the panel stiffness is obtained by using the finite element technique [22]. Miller has also presented a general review of the various studies related to the analysis of multistory frames. In another study, Oppenheim [39] investigated the behaviour of clad frames subjected to static and dynamic loading. The shear stiffness of the panel is derived from the finite element technique. However, he suggested that if the stiffness is obtained from approximate method [5], one must be sure that the formulas derived are applicable to the particular construction. Recently, Dakhakhni [10] presented a new method based on the flexibility approach for the analysis

of clad multistory frames and discussed some design aspects related to the control of lateral deflection of frames infilled with light gage panels. Dakhakhni obtained the flexibility of the panel from approximate expressions [40]. Both Oppenheim and Dakhakhni did not consider the effect of the axial deformation of columns in their theory and this has resulted in an error of 10 to 35% in the lateral deflection.

2.6 General Comments

The methods presented by Bryan and Davies have been found to be satisfactory for diaphragms where the fasteners are of screws or rivets. There is no evidence that the theory could be used for welded diaphragms. In fact, it has been observed [19] that the equations proposed by Bryan do not predict well the strength of diaphragms with welded connections. The expressions developed by Davies, though an improvement over Bryan's method, are again only suitable for diaphragms with mechanical fasteners.

The finite element technique, though attractive and a major step in the analysis technique for shear diaphragms, the necessary computer program is not available to design engineers. Further, it has been observed [20] that the approach does not predict well the stiffnesses of diaphragms with longer panels. In addition, the method would involve considerable amount of time for the preparation of input data and hence, may be inconvenient to use in routine design problems.

From the brief review presented in this chapter, it is clear that there is need for a simplified general approach for evaluating the

shear strength and stiffness of steel cladding. The method should be rational and simple so that it can be used for diaphragms with mechanical fasteners as well as welded connections. Further, a practical method is to be developed for the analysis of clad multistory frames, especially when the effect of column shortening affects the behaviour of frames significantly. The objective of the present research programme is outlined in the following section.

2.7 Research Programme and Objectives

The current research programme deals with the analysis and some design aspects of multistory frames clad with cold-formed light gage steel panels. The work is divided into two phases:

i. A study on the behaviour and analysis of isolated shear diaphragms; and

ii. Investigation of the effects of shear diaphragms on the overall behaviour of multistory frames.

The first part of the study involves the development of simplified techniques for the evaluation of the shear characteristics of the diaphragm, namely, the shear stiffness and usable strength. The accuracy of the different formulas are checked by comparing with many test results. The second phase deals with the development of an approach for incorporating the diaphragm stiffness to the frame. The results of the analysis are compared with those obtained from other methods. Finally, an approximate method has also been suggested to obtain appropriate panel stiffness to control the lateral deflection of multistory frames.

CHAPTER 3

SHEAR STIFFNESS OF METAL DIAPHRAGMS

3.1 General

The design of a diaphragm is mainly concerned with two aspects: the shear stiffness and the strength. The overall shear stiffness, defined as the shear load per unit shear displacement, depends on the type of panel, the strength, and stiffness of the various fasteners. The different components of a typical shear diaphragm have been described in detail in Chapter 1. Because of the multitude of interconnected parts, the determination of the forces and deformations in these components is not a trivial problem. Rigorous analysis of the structure would require a detailed finite element analysis. Most of the current methods are often based on an assumed fastener force distribution, which would render the structure statically determinate. A brief review of the most important methods is included in the previous chapter. Based on the actual behaviour of the fasteners and panels observed during testing of full size diaphragms, this chapter presents a new method for the analysis of diaphragms. Simplified formulas are derived for calculating the overall shear displacement and fastener forces. Examples are also included to illustrate the application of the method to calculate the shear displacements of both welded and screw connected diaphragms. Further, the results from the proposed approach are compared with those from other theories and to published test data. The aspect of shear strength of diaphragms is treated separately in other chapters.

3.2 Theoretical Development

A typical shear diaphragm with all the fasteners is shown in Fig. 3.1 . The fasteners being the major components of the shear carrying system of a diaphragm, accurate determination of their contribution to the overall rigidity of the structure is of prime importance. Accordingly, this section is devoted to the evaluation of the contribution of the fasteners to the shear deformation. Since the theory is based on test evidence, it is proposed to present a brief description of the deformation pattern of a typical diaphragm with mehcanical fasteners (see Fig.3.1). Under the action of a load P, the diaphragm is rotated about the supports an amount represented by the angle γ, as shown in Fig.3.2. It can be seen from Fig.3.3 that the angle, γ, consists of two parts, namely, an amount γ_1, entirely due to the deformation of the fasteners and an angle γ_2, due to the following components:

i. the horizontal slip at the sheet-purlin fasteners;

ii. the bending of the sheet profile;

iii. shear strain in the sheeting itself; and

iv. bending of the framing members.

The primary objective of this section is to develop expressions for the angle γ_1 and for the fastener forces.

The following observations may be made from the deformation pattern of the fasteners indicated in Fig.3.3. i) The configuration of deformations gives an indication of the direction of the forces in the various fasteners. For example, the deformation $2\Delta_{se}$ at each of the seam fasteners shows that the seam forces are uniform and parallel to the sides of the panel; ii) The tilting of the panels and end fastener deformations pro-

vide more information about the type of forces acting on the end fasteners. The inclined directions of the end fastener deformations indicate the presence of forces acting both parallel and perpendicular to the ends of the panels. One could also note that the vertical components of the end fastener deformations vary linearly within the panel while the horizontal components remain uniform and equal throughout the panel. (The terms vertical and horizontal are used with reference to the directions shown in Fig.3.3). The above observations lead to the following assumptions:

i. The seams and side fastener forces are constant along the panel seams and are directed along the seams.

ii. The vertical components of end fastener forces vary linearly along the panel ends.

iii. The horizontal components of end fastener forces are uniform and equal in magnitude and these components add up to the total shear force, P, indicated in Fig.3.1.

3.2.1 Shear Strain due to Deformation at the Fasteners

Consistant with the above assumptions, the diaphragm deformation, γ_1, caused solely by the deformation at the fasteners is shown in Fig.3.4. The deformation of the side fasteners is denoted by Δ_{sf}, while that at the seam fasteners as $2\Delta_{sf}$. Extensive finite element studies have also shown that there is little variation of the seam fastener forces throughout the diaphragm (Refs.20,23). Thus, a constant seam fastener deformation $2\Delta_{se}$ is imposed as shown in Fig. 3.4.

Free body diaphragms of an end and intermediate panel of a shear diaphragm are shown in Fig.3.5. Horizontal equilibrium of these panels is

automatically satisfied and so is the vertical force equilibrium of the intermediate panel. This leaves three equations corresponding to the moment equilibrium of the two panels and vertical equilibrium of the end panel to be considered. Unfortunately, the number of unknowns are only two, chosen among Δ_{si}, x_o and Δ_{se} from the assumed deformation mode in Fig.3.5. Thus, there is a possibility of violation of one of the equilibrium conditions. In order to simplify this situation, Easley [15] has assumed that all panels experience identical deformations, i.e., $x_o = w/2$ and $\Delta_{si} = \Delta_{se}$. The consequence of the above assumptions is the violation of the two equilibrium conditions for the end panel. On the other hand, Davies [23] ensures complete equilibrium of the intermediate panels and allows violation of moment equilibrium of the end panel. However, extensive experimental evidence has shown that shear diaphragm failures invariably occured at the end panel [41] and the failures in most cases were due to tearing of the sheeting at the fastener locations. Hence, it is felt that greater emphasis must then be placed on the end panel by ensuring its complete equilibrium.

The vertical component of the force in an end fastener shown in Fig. 3.5, may be written as:

$$F_{vi} = k_e \cdot \frac{(x_o - x_i)}{x_o} \cdot \Delta_{si} \qquad (3.1)$$

where K_e = stiffness of one end fastener; x_i = distance of the fastener, i, measured from the left side of the panel; Δ_{si} = vertical component of the deformation of the side fasteners. x_o is as shown in Fig. 3.3. The vertical forces in the intermediate girt fasteners can also be obtained from Eq.3.1 by replacing K_e with K_g, the stiffness of one girt fastener. By making use of Eq. 3.1 and by assuming that all the upward

forces are positive, the vertical force equilibrium of the end panel may be expressed as follows:

$$n_{si}.F_{si} + \frac{2\Delta_{si}.K_e}{x_o} \sum_{i=1}^{n_e} (x_o - x_i) + \frac{n_g K_g \Delta_{si}}{x_o} \sum_{i=1}^{n_{ge}} (x_o - x_i)$$

$$- n_{se}.F_{se} = 0 \qquad (3.2)$$

in which n_{si}, n_{se}, n_e and n_{ge} are the number of side, seam, end and girt fasteners respectively; F_{si} and F_{se} are the vertical forces in the side and seam fasteners; n_g = number of intermediate girts or purlins. For the assumed deformation mode of Fig.3.5 the vertical displacements of the side and seam fasteners are Δ_{si} and $2\Delta_{se}$ respectively. Then, the corresponding forces are:

$$F_{si} = K_{si}.\Delta_{si} \qquad (3.3)$$

$$F_{se} = K_{se}.2\Delta_{se} = K_{se}.2\frac{\Delta_{si}}{x_o}(w - x_o) \qquad (3.4)$$

in which w = distance between the centre lines of side and seam fasteners. The values of F_{si} and F_{se} may now be substituted from Eqs. 3.3 and 3.4 into Eq. 3.2 which, when solved, would give the value of x_o as:

$$x_o = \frac{2K_e \sum_{i=1}^{n_e} x_i + n_g K_g \sum_{i=1}^{n_{ge}} x_i + n_{se}.2K_{se}.w}{n_{se}.K_{se} + n_g.n_{ge}.K_g + n_{se}.2K_{se} + 2n_e K_e} \qquad (3.5)$$

Next, the moment equilibrium of the forces acting on the end panel may be considered about point 'o' in Fig.3.5 as:

$$n_{si}F_{si}x_o + n_{se}.F_{se}(w - x_o) + 2M_{eo} + n_g M_{go} - F_h.n_e.b = 0 \qquad (3.6)$$

where $F_h = \frac{P}{a} \cdot \frac{w}{n_e} = \frac{N.w}{n_e}$ (3.7)

Equation 3.7 gives the horizontal force in each end fastener and N is the applied shear load per unit width of the diaphragm. M_{eo} and M_{go} in Eq. 3.6 are the moments (taken about point 0) due to the vertical forces acting at the end and girt fasteners and are given by:

$$M_{eo} = K_e \cdot \frac{\Delta_{si}}{x_o} \cdot I_{eo} \qquad (3.8)$$

and

$$M_{go} = K_g \cdot \frac{\Delta_{si}}{x_o} \cdot I_{go} \qquad (3.9)$$

where

$$I_{eo} = \sum_{i=1}^{n_e} (x_i - x_o)^2 \qquad (3.10)$$

and

$$I_{go} = \sum_{i=1}^{n_{ge}} (x_i - x_o)^2 \qquad (3.11)$$

Equations 3.3, 3.4 and 3.5, when combined with Eqs. 3.6 to 3.11 would yield the following expression for Δ_{si}:

$$\Delta_{si} = \frac{N.w.b}{n_t} \qquad (3.12)$$

where

$$n_t = n_{si} K_{si} . x_o + \frac{n_{se} . 2K_{se}}{x_o} (w - x_o)^2 + \frac{2K_e I_{eo}}{x_o} + \frac{n_g K_g I_{go}}{x_o} \qquad (3.13)$$

The shear strain, γ_1 may be obtained from Δ_{si} as:

$$\gamma_1 = \frac{\Delta_{si}}{x_o} \qquad (3.14)$$

Since the value of γ_1 is derived for the end panel, it can be easily seen from Fig.3.2 that the rotation of the end panel about the hinge would also be equal to γ_1. This component of shear strain is solely due to the deformation of the fasteners.

3.2.2 Forces in the Fasteners

The expressions for the fastener forces may be derived by combining Eq. 3.12 with Eqs. 3.1 to 3.4 as:

$$F_{si} = K_{si} \cdot \frac{N.w.b}{n_t} \tag{3.15}$$

$$F_{se} = K_{se} \cdot \frac{2N.w.b}{n_t} \frac{(w-x_o)}{x_o} \tag{3.16}$$

$$F_{vi} = K_e \cdot \frac{N.w.b}{n_t} \frac{(x_o-x_i)}{x_o} \tag{3.17}$$

and

$$F_{pi} = K_g \cdot \frac{N.w.b}{n_t} \frac{(x_o-x_i)}{x_o} \tag{3.18}$$

Equation 3.18 gives the force in the girt fasteners. The force in the end fastener consists of a horizontal component, F_h, and a vertical component, F_{vi}, and the resultant force in the end fastener is obtained as:

$$F_e = [F_h^2 + F_{vi}^2]^{\frac{1}{2}} \tag{3.19}$$

$$= N[(\frac{w}{n_e})^2 + (K_e \cdot \frac{N.w.b}{n_t} \frac{(x_o-x_i)}{x_o})^2]^{\frac{1}{2}} \tag{3.20}$$

3.3 Determination of Shear Strain, γ_2

As already mentioned, the overall shear strain, γ is composed of two parts, namely, γ_1 and γ_2. By using Eq. 3.14, the value of γ_1 may be evaluated. Since the angle γ_2 depends upon many factors, the effect of these are considered separately and expressions are developed in the following sections for calculating their contributions to the overall shear strain.

3.3.1 Shear Strain due to Horizontal Forces in End Fasteners

This part of the shear strain is due to the horizontal components of the slip at the end fasteners and is denoted as $\gamma_{2.1}$. The following expression may be written for the horizontal force in the end fastener as:

$$F_h = K_e.\Delta_h \tag{3.21}$$

where K_e = the stiffness of the end fastener and Δ_h = horizontal slip at each end fastener. The value of Δ_h may be obtained by combining Eqs. 3.21 and 3.7 as:

$$K_e.\Delta_h = \frac{N.w}{n_e} \tag{3.22}$$

or $$\Delta_h = N.w/K_e.n_e \tag{3.22}$$

The shear strain $\gamma_{2.1}$ may now be obtained easily by using Eq. 3.22 and from Fig. 3.6 as:

$$\gamma_{2.1} = \frac{2.\Delta_h}{b} = \frac{2.N.w}{b.K_e.n_e} \tag{3.23}$$

in which b = depth of the diaphragm (parallel to the corrugations).

3.3.2 Shear Strain due to Bending of Profile

A major component of the shear strain γ_2 is due to the distortion of the panel profile. This component is represented by $\gamma_{2.2}$ and is caused by the bending and twisting of the corrugation. The amount of shear strain due to this effect depends upon the arrangement of fasteners, ie. whether the panel is fixed to the ends in every trough or alternate troughs of the corrugation and also on the geometry of the profile.

Because of the complex nature of the phenomenon, a precise and rigorous analysis is not available to predict this component. However, one could estimate the shear deformation in the sheeting by using the equation proposed by Bryan [42]. By assuming that the shear deformation is linear across the depth of the panel as shown in Fig. 3.7, and by treating the shear flow around the corrugation as constant, the following expression has been derived [42], from simple energy principle, for calculating the shear displacement as:

$$\Delta_{2.2} = \frac{0.144\ a\ d^4 f_1 K.Q}{Et^3 b^3} \tag{3.24}$$

Referring to Fig.3.8, the shear strain $\gamma_{2.2}$ may be obtained as:

$$\gamma_{2.2} = \frac{\Delta_{2.2}}{a} = \frac{0.144\ d^4 f_1 K.Q}{Et^3 b^3} \tag{3.25}$$

in which a = width of the diaphragm; Q is the shear load applied parallel to the corrugation; E = Young's modulus of the material of the sheeting; t = thickness of the sheeting; b = depth of the diaphragm panel, measured parallel to the corrugation; d = pitch of corrugations; f_1 = the correction factor to account for the effect of intermediate purlins; and K is a sheeting constant which depends on the property of the cross-section of the corrugation. The values of f_1 and K are available in Ref. [42] for various profiles and purlin arrangements. Equation 3.25 gives the shear strain $\gamma_{2.2}$ when the load Q is applied parallel to the corrugations as shown in Fig.3.8. However, if the load is placed perpendicular to the corrugation as shown in Fig.3.9, then the value of Q in Eq. 3.25 would be P.b/a and the resulting expression for the shear strain would be given by:

$$\gamma_{2.2} = \frac{0.144\ d^4 f_1 KP}{Et^3.b^2a} \qquad (3.26)$$

3.3.3 Contribution of Shear Strain from the Sheeting

Another component which affects the shear angle γ_2 is the shear strain in the sheeting itself and is designated as $\gamma_{2.3}$. When the panel is loaded in its plane, each face of the corrugation will be subjected to shear strain which will tend to distort the rectangles into a parallelogram.

By using the energy principle, the value of $\gamma_{2.3}$ may be easily derived. A typical shear panel subjected to load P is shown in Fig.3.10. The shear displacement due to shear strain alone is indicated as Δ. The strain energy per unit volume, u, may be written as follows:

$$u = \frac{q^2}{2G} \qquad (3.27)$$

where q = the shear stress and G = the shear modulus. For a sheet thickness of t, the value of q is given by

$$q = \frac{P}{at} \qquad (3.28)$$

The total strain energy, u is obtained as

$$u = \frac{q^2}{2G}\,[b.t.n_c(d+2h)] \qquad (3.29)$$

where n_c = number of corrugations in the width, a, and is given by:

$$n_c = a/d \qquad (3.30)$$

in which d = the pitch of the corrugation. Substitution of n_c in Eq. 3.29 would yield:

$$u = \frac{q^2}{2G}\left[a\ b\ t\ \left(\frac{d+2h}{d}\right)\right] \tag{3.31}$$

Now, equating the total strain energy given by Eq. 3.31 to the external work done 1/2 $P.\Delta_{2.3}$ would yield the following:

$$\frac{1}{2}\,P.\Delta_{2.3} = \frac{P^2}{a^2t^2.2G}\,[a\ b\ t]\left[\frac{d+2h}{d}\right] \tag{3.32}$$

or

$$\Delta_{2.3} = \frac{P}{atG}\,b\,\left(\frac{d+2h}{d}\right) \tag{3.33}$$

Next, the shear strain $\gamma_{2.3}$ may be obtained from Fig.3.10 as:

$$\gamma_{2.3} = \frac{\Delta_{2.3}}{b} = \frac{P}{Gat}\,(d+2h/d) \tag{3.34}$$

The effect of intermediate purlins may be included by multiplying Eq. 3.34 by the factor f_2 which can be obtained from Ref. 43. In Eq. 3.34, the term P/a is the shear load per unit width of diaphragm and may be replaced by N . The ratio of (d+2h)/d is simply the ratio of the developed width to the projected width of one corrugation. It is of interest to see that Eq. 3.34 would then reduce to that reported by Easley [15] for this component of shear strain.

3.3.4 Shear Strain due to Bending of the Framing Members

When the diaphragm is loaded in shear, as shown in Fig.3.11, the end framing members are subjected to bending in the plane of the diaphragm and axial forces are introduced. These axial forces will tend to change the length of the members, thereby causing additional shear deflection. The component of shear strain due to this deflection alone is designated as $\gamma_{2.4}$ and is derived as follows:

In Fig.3.11, the axial forces in the edge members increase linearly from 0 to a maximum value of P.b/a for an applied load of P. The force at any distance is P.y/a and the strain energy of each vertical member would be

$$u = \int_0^b \frac{P^2 y^2 . dy}{2a^2 AE} = \frac{P^2 . b^3}{6Aa^2 E} \qquad (3.35)$$

By equating the total strain energy to the external work done, $\frac{1}{2}P.\Delta_{2.4}$, the following relation may be written :

$$\frac{1}{2}P.\Delta_{2.4} = \frac{2}{6} \cdot \frac{P^2 . b^3}{A_v E a^2}$$

or
$$\Delta_{2.4} = \frac{2}{3} \frac{P}{A_v E} \frac{b^3}{a^2} \qquad (3.36)$$

The shear strain $\gamma_{2.4}$ can now be evaluated as

$$\gamma_{2.4} = \frac{\Delta_{2.4}}{b} = \frac{2P}{3A_v E} \cdot \frac{1}{b} \cdot \frac{b^3}{a^2} \qquad (3.37)$$

For the case of loading parallel to the corrugation, a similar expression may be derived for $\gamma_{2.4}$ as

$$\gamma_{2.4} = \frac{2.P.l.}{3.EA_h a} \cdot \frac{a^3}{b^2} \qquad (3.38)$$

The terms A_h and A_v in Eqs. 3.38 and 3.37 are the cross-sectional areas of the horizontal and vertical members. The effect of intermediate purlins may be taken into account by multiplying Eq. 3.38 by the factor f_3, obtained from Ref. 43.

3.4 Overall Shear Displacement of Diaphragm

The total shear strain is the sum of all the components derived above

and may be expressed as

$$\gamma = \gamma_1 + \gamma_{2.1} + \gamma_{2.2} + \gamma_{2.3} + \gamma_{2.4} \tag{3.39}$$

The overall deflection Δ_t may be obtained as

$$\Delta_t = \gamma.b \tag{3.40}$$

Next, the shear stiffness S, by definition, is the shear load per unit shear deflection and is expressed as

$$S = \frac{P}{\Delta_t} \tag{3.41}$$

3.5 Effect of Panel Orientation Relative to Load

The shear deflection of the diaphragm depends whether the corrugations are parallel or perpendicular to the direction of the applied load. For the purpose of deriving the overall shear deflection in the previous section, it was assumed that the load was applied perpendicular to the direction of the corrugations (see Fig.3.1). However, one could obtain the shear displacement for the case of loading parallel to the corrugations from simple expressions as explained below.

Shown in Fig.3.12 are the two cases of loading under discussion. The load, P and Δ_h are for the case of corrugations perpendicular to the applied load while the load Q and Δ_v are for the other case where the loading is parallel to the corrugations. The value of Q may be written in terms of P as

$$Q = P.b/a \tag{3.42}$$

Since the shear strain γ, is the same in both cases, the shear deflec-

tions, Δ_v and Δ_h may be related as

$$\gamma = \frac{\Delta_v}{a} = \frac{\Delta_h}{b} \tag{3.43}$$

or $$\Delta_v = \Delta_h . b/a \tag{3.44}$$

Similarly, the shear stiffnesses for these cases may also be related to each other:

Shear Stiffness for Case i) $= S_h = \frac{P}{\Delta_h} = \frac{P}{\gamma . b}$ (3.45)

Shear Stiffness for Case ii) $= S_v = \frac{Q}{\Delta_v} = \frac{Q}{\gamma . a}$ (3.46)

Since γ is the same in both cases, S_h and S_v may be related as

$$\gamma = \frac{S_h . b}{P} = S_v . \frac{a}{Q} \tag{3.47}$$

Substitution of $Q = P.b/a$ in the above equation would yield

$$\frac{S_h . b}{P} = \frac{S_v . a}{P . b} . a$$

or $$S_h = S_v . \frac{a^2}{b^2} \tag{3.48}$$

The term stiffness, S_h, in the above equation is the inverse of the shear flexibility. The American Iron and Steel Institute [12] defines the shear stiffness, denoted by G', as the ratio of the shear load per unit length at 40% of the ultimate load ($0.4P_u$) to the corresponding shear strain, γ. Accordingly, G' may be written as

$$G' = \frac{0.4P_u}{b} . \frac{a}{\Delta_s} = \frac{0.4N_u}{\gamma} \tag{3.49}$$

where N_u is the shear load per unit length of the diaphragm, Δ_s = the

shear deflection at a load of 0.4 P_u; P_u = ultimate strength of the diaphragm; and a and b are the width and length of the diaphragm. The term G', as defined by AISI, should be carefully interpreted and should not be understood as the inverse of the shear flexibility. The term "Diaphragm Shear Modulus" would be more appropriate to represent G'. The relationship between the "shear stiffness", S, and the "shear modulus", G', however, can be derived by replacing the term $\frac{0.4\ P_u}{\Delta_s}$ by s, in Eq. 3.49 and this would lead to the following expression:

$$G' = S.a/b \qquad (3.50)$$

In this study, G' is referred to as diaphragm shear modulus and S as the shear stiffness, the inverse of the shear flexibility.

3.6 Correlation with Test Results

The proposed theory for predicting the shear deflection is now applied to two types of diaphragms which have been tested experimentally as well as subjected to finite element analysis. These diaphragms cover a wide range of variables with respect to the type of fasteners, diaphragm size and loading configuration. The first two diaphragms were fabricated with panels having a continuous flat sheet, stiffened by two hat sections as shown in Fig.3.13. These types of panels are usually referred to as closed cellular deck panels. All the connections were of welds in these diaphragms. In the second type of diaphragm, the panel profile is of open trapezoidal cross-section as shown in Fig.3.14. Such a profile is more susceptable to distortion, especially when the ends are not fastened in every trough of the corrugations. All the fasteners in these diaphragms were of self tapping screws. A brief description of these diaphragms is presented in the following sections.

3.6.1 Welded Diaphragms

Two different sizes of diaphragms are considered under this category. The first one is of 12'0" x 30'0" and the second is of 30'0" x 30'0". The first diaphragm, designated as 57.2, was tested over a simple span of 30'0" with the two point loads at third points. The test was performed as part of an overall project at Cornell University and reported by Nilson [12]. The diaphragm assembly consists of 3 bays as shown in Fig.3.13 and each bay in turn contains six 2'0" wide panels. The diaphragm panels were manufactured by Fenestra, Inc. of Bullafo, New York and are designated as Type D [20]. The longitudinal edge at one side of the flat sheet was made into an upturned lip while that of the other side was formed into a vertical hook in order to connect the adjacent panel. The panels were fabricated by using 16 gage sheet (thickness 0.0598") for both the flat sheet and the hat sections. The details of the welded connections are given below:

Seam welds: 1 1/2" long burnthrough welds @ 18" c/c

Side welds: 1" diameter puddle welds @ 24" c/c

End welds : 1" diameter puddle welds, 3 numbers per panel at each end.

3.6.2 Calculation of Shear Deflection for 12'0" x 30'0" Diaphragm

Most of the data for the fasteners are obtained from the original test results [12] and the stiffness values for the welded connections are taken from the work of Ammar and Nilson [20]. The shear deflection is calculated for a load of 50% of the ultimate load and compared with the corresponding value observed during test.

Diaphragm Data: Length of panel, b = 12'0"; width of an equivalent cantilever diaphragm, a = 10'0"; width of one panel, w = 2'0"; number of side fasteners, n_{se} = 8; stiffness of side fastener, K_{si} = 800 kips/inch; stiffness of seam fastener, K_{se} = 500 kips/inch; stiffness of end fastener, K_e = 1000 kips/inch; ultimate strength of diaphragm per foot length, N_u = 3220 lbs/ft; 50% of the ultimate load, 0.5 N_u = 1610 lbs/ft.

Solution:

i) Shear strain due to deformation of fasteners:

Using Eq. 3.5, the value of x_o is obtained as 1.17 feet; the deformation at the side fasteners, Δ_{si} is obtained from Eq. 3.12 as 0.001731 N; where N = 1.61 kip per foot.

From Eq. 3.14 $\gamma_1 = \frac{\Delta_{si}}{x_o} = \frac{0.001731 \times 1.61}{1.17 \times 12} = 0.000198$

ii) Shear strain due to horizontal slip at fasteners:

From Eq. 3.23, $\gamma_{2,2} = \frac{2.N.w}{b \cdot K_e.n_e} = \frac{2 \times 1.61 \times 2}{12 \times 12 \times 1000 \times 3}$

$= 0.0000149$

iii) Contribution of shear strain from profile distortion, $\gamma_{2,2}$:

This component may be neglected since the value of the sheeting constant K is zero [42] in Eq. 3.25.

iv) Contribution due to shear strain from sheeting, $\gamma_{2,3}$:

From Eq. 3.34, $\gamma_{2,3} = \frac{P}{aGt}\left(\frac{d+2h}{d}\right) = \frac{1.61 \times 27}{12 \times 11 \times 10^3 \times 0.0598 \times 24}$

$= 0.000229$

v) Shear strain due to bending of the framing members, $\gamma_{2.4}$:

From Eq. 3.38, $\gamma_{2.4} = \frac{2.P}{3 \times a^2 b} [\frac{b^3}{AE}]$

$$= \frac{2}{3} \times \frac{1.61}{12} \times \frac{1}{120} \times \frac{1 \times 120^3}{144\ 7.97} \times \frac{1}{30} \times 10^3$$

$$= 0.000037.$$

Total shear strain $\gamma = \gamma_1 + \gamma_{2.1} + \gamma_{2.2} + \gamma_{2.3} + \gamma_{2.4}$

$$= 0.000197 + 0.000049 + 0.0 + 0.000229$$
$$+ 0.000037 = 0.000513$$

Shear deflection $\Delta_v = \gamma \times b = 0.000513 \times 120 = 0.061"$

Measured shear deflection at 50% ultimate load = 0.060" [12]

$$\frac{\Delta_{measured}}{\Delta_{calc}} = \frac{0.060}{0.061} = 1.00$$

3.6.3. Welded Diaphragm - 30'0" x 30'0"

This diaphragm, designated as 58-5, was tested on a cantilever frame with a single load applied as shown in Fig.3.15. The diaphragm had 15 panels of 2'0" width and were also tested by Nilson [12] at Cornell University. The spacing of the fasteners, panel shape and welding patterns were identical to that of the previous test specimen. Using the equations presented in Section 3.4, the shear deflection was computed at 50% of the ultimate load and the results are compared below:

$$\Delta_{calculated} = 0.157"$$

$$\Delta_{test} = 0.145"$$

$$\frac{\Delta_{(test)}}{\Delta_{(calc)}} = \frac{0.145}{0.157} = 0.92$$

3.6.4 Diaphragms with Mechanical Fasteners

Welded diaphragms are generally stiffer than mechanically fastened diaphragms; however, good workmanship is required. Most of the diaphragm construction in England is done with mechanical fasteners, such as rivets or screws. The first two diaphragms under type 2, designated as A_1 and A_2 were fabricated by using 97.5 cm wide trapezoidal panels. Each diaphragm was of 390 x 378 cm size with two intermediate purlins. The major difference between the diaphragms A_1 and A_2 was the number of end fasteners. The panels were fixed to the purlins in every corrugation in A_1 while the fasteners in A_2 were in alternate corrugations. The general layout of the panels, location of shear connectors and loading arrangement are shown in Fig.3.14. The last two diaphragms designated as C_1 and C_2 had only one intermediate purlin (Fig. 3.16). The sizes of these diaphragms were of 720 cm x 370 cm with 8 panels of 90 cm width. The general arrangement of the panels and the loading direction are shown in Fig.3.16. Apart from the difference in the overall size of the diaphragms, the major difference between these diaphragms and A_1 and A_2 is in the loading direction. The load is applied perpendicular to the direction of corrugations in the case of C_1 and C_2. The end fasteners were at every corrugation in C_1 while the fasteners were provided in alternate corrugations in the case of diaphragm C_2. These four diaphragms, with screw connections, (A_1, A_2, C_1 and C_2) have been tested by Davies [23] at the University of Salford. Davies has also reported the results from the finite element analysis and simplified approximate methods for all these diaphragms. Complete details of these results are available in Ref. (23).

The shear deflection for all these four diaphragms are predicted at a load of 4450 lbs (1kN) and the results are compared to test data in Table 3.1. Further, the results from the proposed approach are also compared to that obtained from the finite element method.

3.7 Conclusions

By assuming a single mode of deformation, closed form expressions are developed for the analysis of shear diaphragms. In order to verify the accuracy of the various formulas, the shear deflection of many diaphragms are predicted and the results are compared to test data and finite element results where these are available. The diaphragms selected cover a wide range of variables, such as the diaphragm size, panel profile, type and arrangement of fasteners and the orientation of the panels relative to the load. It is observed that the equations developed here, apart from their simplicity, predict well the shear deflection of the various diaphragms chosen form the available literature. The expressions derived for the fastener forces form the basis for predicting the shear strength of metal diaphragms and the details of these are presented in the next chapter.

CHAPTER 4

STRENGTH OF SHEAR DIAPHRAGMS

4.1 General

The shear stiffness of a diaphragm plays a dominant role in the allowable stress design approach of clad buildings and the strength is of importance only to check whether the load factor is within the limits specified by the codes [12, 42]. One should then know the ultimate strength of a diaphragm to calculate the load factor. Further, the shear capacity of a diaphragm plays a more dominant role in the plastic design procedure of clad buildings. The strength of a diaphragm is greatly affected by the mode of failure which in turn is governed by the strength and spacing of the fasteners. There are three main failure modes for a shear diaphragm.

Firstly, the failure may occur due to shearing of the fasteners, especially when the size of the fastener is small. Shear failures of fasteners is most undesirable since they occur suddenly. The second type of failure is by tearing of the sheeting at the seam fasteners or end fasteners. This type of failure is more ductile and is often noticed in many full scale tests. The third and last type of failure is due to overall buckling of the entire diaphragm with a number of diagonal waves. This type of overall buckling failure might occur when the fasteners are closely spaced and of high strength. In addition to these three basic modes, the diaphragm might exhibit a combination of all the above failure modes. This chapter deals only with the first two types of failures. The third type, i.e., failure in buckling, will be treated separately in the next chapter. Simplified expressions are developed for the

strength calculation of diaphragms. The formulas are applicable only to diaphragms whose capacities are governed by the strength of the fasteners. A typical full-scale diaphragm test is chosen and the shear capacity is predicted by the new method and also by using the other methods currently available and the results are compared to test data. Finally, the present theory is applied to a series of diaphragms with welded connections and several diaphragms with mechanical fasteners. The results obtained from the proposed theory are also compared with those from other theories where these are availalbe.

4.2 Prediction of Shear Strength of Diaphragms

Simplified expressions are presented here to determine the approximate shear capacity of diaphragms. It is assumed that the expressions for the fastener forces developed in the previous chapter remain valid at the collapse stage. In other words, if the connections have an elasto-plastic behaviour, as shown in Fig.4.1, the strength of the diaphragm may be obtained from simple expressions as outlined in the next section. The equations are derived by assuming that all the fasteners located along a particular seam or side would fail simultaneously. Failure could occur either at the seam fasteners, side fasteners or at the end fasteners. Accordingly, equations are derived to cover all these possible failures at the fasteners.

4.2.1 Failure of Side Fasteners

The connections between the panel and the side framing members are called side fasteners. If there are sheet-purlin fasteners in line with the side fasteners, then the following equation may be written

for the total force along the side fasteners, T_{fsi} is

$$T_{fsi} = n_{si}F_{si} + n_g F_{pi} + 2F_{vi} \tag{4.1}$$

where n_{si} and n_g are the number of side fasteners and intermediate purlins respectively. The values of F_{si}, F_{pi} and F_{vi} may be substituted from Eqs. 3.15 - 3.18 and when this is done, Eq. 4.1 would become:

$$T_{fsi} = [n_{si}K_{si} + n_g K_g + 2K_e]\frac{w.b.N}{n_t} \tag{4.2}$$

The total capacity of all these fasteners is given by:

$$T_{si} = n_{si}F_u + n_g F_p + 2F_w \tag{4.3}$$

in which F_u, F_p and F_w are the strength of a single side fastener, sheet-purlin fastener and end fastener respectively. These values may be obtained by conducting simple tests on these connections. Equating the total force to the capacity, the shear strength may be obtained as

$$N_u = \frac{[n_{si}F_u + n_g F_p + 2F_w]\, n_t}{wb[n_{si}K_{si} + n_g K_g + 2K_e]} \tag{4.4}$$

When there are no sheet-purlin fasteners in line with the side fasteners, Eq. 4.4 would reduce to the following form:

$$N_u = \frac{F_u.n_t}{w.b.K_{si}} \tag{4.5}$$

4.2.2 Failure of Seam Fasteners

If the failure of the diaphragm is caused by the seam fasteners, then the shear capacity may be obtained from the strength of the seam fasten-

ers. In addition to the seam fasteners, if there are sheet-purlin fasteners in line with the seams, then the total force along a given seam may be written as, T_{fse}

$$T_{fse} = (n_{se}.F_{se} + n_g F_{pi} + 2F_{vi}) \tag{4.6}$$

where n_{se} is the number of seam fasteners. The values of F_{se}, F_{pi} and F_{vi} may be substituted from Eqs. 3.16-3.18 and this would result in the following equation for the total force along a seam as:

$$T_{fse} = [n_{se}2K_{se} + n_g K_g + 2K_e](\frac{w-x_o}{x_o}) \cdot \frac{N.w.b}{n_t} \tag{4.7}$$

Again, the total capacity of the fasteners along the seam is

$$T_{se} = n_{se}F_v + n_g F_p + 2F_w \tag{4.8}$$

in which F_v is the strength of one seam fastener. The shear capacity, N_u, may be obtained by equating the above two expressions

$$N_u = \frac{n_{se}F_v + n_g F_p + 2F_w}{(\frac{w-x_o}{x_o})\frac{w.b}{n_t}[2n_{se}K_{se} + n_g K_g + 2K_e]} \tag{4.9}$$

Equation 4.9 may be simplified if there are no sheet-purlin fasteners in line with the seams and the resulting equation would be

$$N_u = \frac{F_v.x_o.n_t}{K_{se}.2.w.b(w-x_o)} \tag{4.10}$$

4.2.3 Failure of End Fasteners

Finally, if the failure of the diaphragm is due to the failure of end fasteners, then the shear capacity of the diaphragm can be evaluated from the strength of the end fastener by using an elastic analysis. It was shown in the previous chapter that the end fasteners are subjected to both horizontal and vertical forces. The resultant force in the end fastener was obtained as

$$F_e = N\left[\left(\frac{w}{n_e}\right)^2 + \left(K_e \cdot \frac{w.b}{n_t}\left(\frac{x_o - x_i}{x_o}\right)\right)^2\right]^{\frac{1}{2}} \qquad (4.11)$$

The shear strength may be obtained by replacing F_e with F_w, the strength of one end fastener and this would yield

$$N_u = \frac{F_w}{\left[\left(\frac{w}{n_e}\right)^2 + \left(\frac{K_e w.b}{n_t}\left(\frac{x_o - x_i}{x_o}\right)\right)^2\right]^{\frac{1}{2}}} \qquad (4.12)$$

in which K_e is the stiffness of one end fastener; x_i is the distance of the end fastener where the force F_{vi} is maximum; and x_o is as shown in Fig.3.5. The shear capacity of the diaphragm would be the lowest of the three values given by Eqs. 4.4, 4.9 and 4.12.

The above procedure ignores possible redistribution of the fastener forces due to yielding of some of the fasteners. A more accurate theoretical evaluation of the shear strength may be carried out by an incremental load procedure where changes in the fastener stiffness are taken into account at each load increment. However, this procedure might involve many steps to evaluate the shear strength. Further, such procedure may not be necessary nor practical for the following additional reasons:

Firstly, the seam and side fasteners would fail almost simultaneously; and

Secondly, the approximate or average values of the fastener stiffness and strength would make such a procedure meaningless.

The accuracy of the proposed method will be verified next by predicting the shear capacity of a welded diaphragm and the results will be compared to test data and other theoretical predictions.

4.3 Details of Tested Diaphragm

The plan view of the diaphragm test set up is shown in Fig.4.2. The test frame consisted of four 14" WF 34 lbs through beams spaced at 12'0" centres and six 12" WF 36 lbs beams set at 8'0" centres. All these beams were connected by bolts. The two end beams were extended beyond the test panel by about 2'0" and were bolted to a longitudinal beam which served as a reactor beam for the application of the loads. The reactor beam was in turn supported by the two columns as shown in Fig.4.2. The panels were laid with corrugations running parallel to the 8'0" direction. The diaphragm consisted of 3 bays with 6 panels each of 2'0" width in the end bays and 4 panels laid as shown in the central bay. The panels were connected to the framing members by 3/4" plug welds at 12" centres at the ends and at 17" centres along the sides. The seams between the panels were button punched at 24" centres. The diaphragm was loaded monotonically to failure with two point loads located at the third points of the simple beam testing rig. The testing was done according to the AISI recommendations [12] and the ultimate strength of the diaphragm was noted as 7700 lbs. This load is equivalent to a

load of 963 lbs/ft. The diaphragm test presented here is taken from a report on steel deck diaphragms by Levelt and Fung [41].

4.4 Load-deformation Curves for the Fastener

Since the analytical prediction of the shear behaviour of a diaphragm depends primarily on the behaviour of the fasteners, the load-slip curves for the fasteners must be obtained accurately from separate tests. There are two types of fasteners in the diaphragm shown in Fig.4.2 namely,

i) the seam fasteners between the panels made by mechanical clinching (button punching); and

ii) the end fasteners consisting of 3/4" diameter puddle welds.

Many tests were conducted on typical connections and the load-slip curves were obtained.

4.4.1 Behaviour of Seam Fasteners

In many diaphragms constructed in North America, the seams between the panels are connected by mechanical clinching and care must be taken to ensure that the panels are properly aligned vertically. Otherwise, poor connections might result. Many test specimens were made and tested as shown in Fig.4.3. Some typical load-slip curves are shown in Figures 4.4 and 4.5. It can be seen from these curves that the ultimate strength F_u varies from 290 lbs. to 470 lbs. The initial slope of the load-slip curve is denoted by K_s and varies from 2040 lbs/inch to 2540 lbs/inch. The reasons for these variations may be attributed to error in vertical alignment of the panels. The following average values of K_s and F_u have been used in the analytical methods for predicting the shear

strength: K_s = 2290 lbs/inch and F_u = 380 lbs. Tests were also conducted on specimens with 22 gage sheet and the load-deformation curves are shown in Figs.4.6 and 4.7.

4.4.2 Behaviour of End Fasteners

The connections between the panels and the supports (end fasteners or sheet-purlin fasteners) were of 3/4 inch puddle welds, two welds per panel. Test specimens were made by welding 2" x 8" sheet (18 gage thick) to a base plate of 2" x 8" x ¼" with 3/4 inch puddle welds as shown in Fig.4.8. Many samples were tested and it was observed that the strengths and the stiffnesses of the welded connections were reasonably uniform. The behaviour of the connections was linear up to about 80% of the ultimate load. Since there was some slippage in the grips at the beginning, the value of stiffness, K_e, for the welded connection is taken in the linear range, slightly above the origin as marked in Figures 4.9 and 4.10. The values of F_e and K_e are taken as 5500 lbs and 75,000 lbs/inch respectively for the welded connections. Additional tests were also performed on specimens with 22 gage sheet and the load-deformation curves are shown in Figs.4.11 and 4.12.

4.5 Shear Strength from the Proposed Method

The shear capacity of the diaphrgm may now be predicted from the equations developed in Section 4.2 and by using the data for the fasteners. The average values of the ultimate load and stiffness of the fasteners are summarized below:

Ultimate strength of one side fastener, F_u = 5500 lbs.

Ultimate strength of one seam fastener, F_v = 380 lbs.

Ultimate strength of one end fastener, F_w = 5500 lbs.

Stiffness of side connection, K_{si} = 75000 lbs/inch

Stiffness of seam connection, K_{se} = 2270 lbs/inch

Stiffness of end connection, K_e = 75000 lbs/inch

The various steps involved in calculating the shear capacity are explained in the next section.

4.5.1 Failure of Side Fasteners - Using Eq. 4.5

$$N_u = \frac{F_u \quad n_t}{K_{si}.w.b}$$

where F_u = 5500 lbs; K_{si} = 75000 lbs/inch, w = 2'0"; b = 8'0".

$$n_t = n_{si}K_{si}.x_o + n_{se}.K_{se}\frac{2(w-x_o)^2}{x_o} + \frac{2K_e.I_{eo}}{x_o} + \frac{n_g K_g I_{go}}{x_o}$$

where n_g = 0; since there are no intermediate girts and x_o is obtained from Eq. 3.5 as

$$x_o = \frac{2K_e \sum_{i=1}^{n_e} x_i + n_{se}.2K_{se}.w}{n_{si}K_{si} + n_{se}2K_{se} + 2.n_e.K_e}$$

$$= \frac{2x75[0.5 + 1.5] + 5x2x2.27x2}{6x75 + 5x2x2.27 + 2x2x75} = 0.447 \text{ feet}$$

$$I_{eo} = \sum_{1}^{n_e} (x_i-x_o)^2 = (0.5-0.447)^2 + (1.5-0.447)^2$$

$$= 1.1128 \text{ ft}^2$$

Substitution of x_o, I_{eo} in the equation for n_t would result in

$$n_t = 6x75x0.447 + 5x2x2.27\frac{(2-0.447)^2}{0.447} + \frac{2x75x1.112}{0.447}$$

$$= 695.9 \text{ kips}$$

Therefore,

$$N_u = \frac{5500 \times 695.9}{75 \times 2 \times 8} = 3189.5 \text{ lbs/ft.}$$

4.5.2 Failure of Seam Fasteners - Using Eq. 4.10

$$N_u = \frac{F_v . x_o \cdot n_t}{K_{se} \cdot 2.w.b(w-x_o)} = \frac{380 \times 0.447 \times 695.9}{2.27 \times 2.x\ 2 \times 8 \times 1.053}$$

$$= 1047.8 \text{ lbs/ft.}$$

4.5.3 Failure of End Fastener - Using Eq. 4.12

$$N_u = F_w / [(w/n_e) + (\frac{K_e w.b(x_o - x_{imax})}{n_t \cdot x_o})^2]^{\frac{1}{2}}$$

$$= \frac{5500}{[(\frac{2}{2})^2 + (\frac{75 \times 2 \times 8 \times 1.053}{659.9 \times 0.447})^2]^{\frac{1}{2}}}$$

$$= 5500/4.18 = 1314 \text{ lbs/ft.}$$

The lower of the above three values should be taken as the shear capacity, i.e., N_u = 1048 lbs/ft.

$$N_{u(test)} = 963 \text{ lbs/ft.}$$

$$\frac{N_{u(test)}}{N_{u(calc)}} = \frac{963}{1048} = 0.92$$

It can be seen that the simplified method predicts well the shear capacity of the diaphragm tested. The error is of the order of about 8%. Next, the shear capacity of the same diaphragm is predicted by using the other existing methods.

4.6 Bryan's Method

In England, the design procedure for light gage steel shear diaphragms is based mostly on the work of Bryan. It could be easily mentioned that the work of Bryan laid the foundation for a systematic research programme by using both the analytical techniques and experimental methods. The aim of this section is to verify the accuracy of the formulas originally proposed by Bryan [6] in the year 1966. Based on the type of construction, Bryan has classified diaphragms into two major types:

i) Diaphragms with panels connected to the framing members on all four sides; and (Fig. 4.13)

ii) Diaphragms where the panels are connected only to the purlins which in turn are connected to the rafters (Type ii).

For each of the above types, a simple distribution of the fastener forces is assumed. The load which first causes failure in any of the fasteners is taken as the shear capacity of the diaphragm.

The type of diaphragm considered here could be classified as Type i, since the panels are connected on all four sides to the framing members. Assuming a uniform distribution of forces in the seam fasteners, Bryan has proposed the following equation for the force in the seam fastener, F_{se} as:

$$F_{se} = N.b/n_{se} \qquad (4.13)$$

where N = shear force per unit length; b = depth of the panel; n_{se} = number of seam fasteners between two panels. Similarly, the end fasteners are also assumed to carry equal forces and the force in the end

fastener is given by:

$$F_e = N.w/n_e \qquad (4.14)$$

where w = width of one panel; and n_e = number of end fasteners per panel. The shear capacity of the diaphrgm is determined from Eqs. 4.13 and 4.14 by replacing F_{se} and F_e by F_v and F_w respectively. The values of F_v and F_w are found from separate tests and the data for the fasteners are taken from Section 4.4.

4.6.1 Strength from Seam Fasteners - Using Eq. 4.13

$$F_v = 380 = N_u.b/n_s = N_u(8/5)$$

Hence

$$N_u = 238 \text{ lbs/ft.}$$

4.6.2 Strength from the End Fasteners - From Eq. 4.14

$$F_w = 5500 = \frac{N_u w}{n_e} = \frac{N_u.2}{2}$$

Therefore

$$N_u = 5500 \text{ lbs/ft.}$$

The lower of the above two values of N_u = 238 lbs/ft.

$$\frac{N_{u(test)}}{N_{u(calc)}} = 963/238 = 4.04$$

4.7 Davies' Equations

It can be seen from the above section that the simple distribution of fastener forces as proposed by Bryan [5] would yield results in gross error. Davies [23] has also observed certain deficiencies with respect

to Bryan's expressions. Based on the finite element analysis and the observations made during the testing of diaphragms, Davies employed an improved internal force distribution for the fasteners. By assuming that each panel in a diaphragm would resist equal load and that failure would occur due to tearing of the sheeting along a vertical line of fasteners (parallel to corrugations), Davies [23] proposed the following equation for calculating the shear strength when the diaphragm capacity is controlled by the capacity of the seam fasteners.

Case i - Failure at an Internal Seam:-

When the failure occurs at the seam fasteners, the ultimate load is given by:

$$Q_{ult} = \frac{(n_s F_s + n_p F_p)(2n_s s + g_1 n_p . s_s)}{(2n_s s + n_p s_s)} \qquad (4.15)$$

where n_s = number of seam fasteners per side lap;

F_s = ultimate load of one seam fastener;

n_p = number of purlins (end and intermediate);

F_p = ultimate load of one sheet purlin-fastener;

s, s_s = slip per sheet - purlin fastener and seam fastener

g_1 = correction factor for the number of end fasteners [43]

Equation 4.15 has been derived by assuming a sheet-purlin fastener in line with the seam fasteners. Since there is no sheet-purlin fastener in line with the seams of the diaphragm shown in Fig.4.2, Eq. 4.15 would reduce to

$$Q_{ult} = \frac{n_s F_s (2n_s s + g_1 n_p . s_s)}{2n_s s} \qquad (4.16)$$

Case ii - Failure at End of Panel:-

If the failure occurs along the side welds, then the following equation may be written for the ultimate load:

$$Q_{ult} = n_{si} \cdot F_{si} \qquad (4.17)$$

where n_{si} = number of side fasteners; and F_{si} is the ultimate load of one side fastener. Equations 4.16 and 4.17 are sufficient for the diaphragm specimen considered here in Fig.4.2. However, the values of s and s_s are required to use the formulas presented above. These values may be obtained from the stiffness values of the end and seam fasteners as follows:

$$s = \frac{1}{K_e} = \frac{1}{75000} = 1.33 \times 10^{-3} \text{ inch/lb.}$$

$$s_s = \frac{1}{K_s} = \frac{1}{2270} = 4.405 \times 10^{-4} \text{ inch/lb.}$$

F_s = 380 lbs

$F_{si} = F_e$ = 5500 lbs

g_1 = 0.25 taken from the European Recommendations [43]

n_s = 5; n_{si} = 6 and n_p = 2

4.7.1 Strength from Davies' Method

Case i - Failure at internal seam using Eq. 4.16:-

$$Q_{ult} = \frac{5 \times 380[2 \times 5 \times 0.0000133 + 0.25 \times 2 \times 0.0004405]}{2 \times 5 \times 0.0000133}$$

$$= 5043 \text{ lbs}$$

$$N_u = \frac{5043}{8} = 630 \text{ lbs/ft}$$

Case ii - Failure along side welds using Eq. 4.17:-

$$Q_{ult} = 6x5500 = 33000 \text{ lbs}$$

$$N_u = \frac{33000}{8} = 4125 \text{ lbs/ft.}$$

Hence, failure would occur along the seams and the ultimate load would be 630 lbs/ft.

$$\frac{N_{u(test)}}{N_{u(calc)}} = \frac{963}{630} = 1.52$$

It is observed that the expressions proposed by Davies [23], though an improvement over Bryan's [5] approach, tend to underestimate the shear capacity of the type of diaphragm considered here. It must be mentioned here that the equations of Davies have been derived for a particular fastener arrangement and loading condition and hence, one should be careful to modify the equations as explained in this section, before applying to any specific problem.

4.8 Shear Strength from Empirical Approach

At present, the design of shear diaphragms in Canada is based either on design tables supplied by various steel deck manufacturers [44] or by using the design booklet published by the Canadian Sheet Steel Building Institute [26]. The design tables included in the above references are prepared by using the empirical equations given in the Manual for Seismic Design of Buildings [25]. The formulas for the allowable shear capacity are derived on the basis of limited test data and based on an assumed factor of safety of 3. The equations for calculating

the allowable shear capacity, q_d, are given below (notations are explained in section 4.8.1 with reference to the diaphragm shown in Fig. 4.2.)

$$q_d = [q_1 + q_2]\, q_3 / q_2 \tag{4.18}$$

where

$$q_1 = \frac{92\, A[t_1 + t_2^1]\, k}{bL_v} \tag{4.19}$$

$$q_2 = \frac{a'b'\, t_s^{\frac{1}{2}}\, c_2}{2}\left[q_1\left[\frac{500}{I_D} + \frac{1}{L_v dA(t_1 + t_2^1)^2}\right]\right]^{\frac{1}{2}} \tag{4.20}$$

$$q_3 = \frac{3600\, t_s a' c_3}{L_v} \tag{4.21}$$

$$k = \frac{1000}{\left[1 + A\left[\frac{1}{\frac{(t_1 + t_2)\, t_1 + 100 n_v^{\frac{1}{2}}\, t_2^2 (43/h)^{\frac{1}{2}} \left(\frac{t_2}{t_1 + t_2}\right)^3}{t_2^2}}\right]\right]^{2}}^{\frac{1}{2}} \tag{4.22}$$

The shear capacity of the diaphragm per unit length, N_u, is taken as 3 times q_d. The above equations are used for calculating the shear capacity of the diaphragm shown in Fig.4.2.

4.8.1 Diaphragm Data

Width of panel, b' = 2 feet; vertical span, L_v = 8 feet; spacing of button punches, a_s = 24 inch c/c; number of end welds per panel = two 3/4" ϕ puddle welds; t_1 = 0 (for single deck profile without any flat bottom sheet); thickness of fluted sheet, t_s = 0.048" (18 gage); $a' = L_v/a_s$;

$\frac{t_2'}{t_2} = 1$; distance of the extreme end weld from the centre of the panel, $y_o = 0.5$ feet; number of vertical ribs per foot transversely supported by end welds, $n_v = \frac{4}{2} = 2$ (see Fig. 4.13).

4.8.2 Solution from Empirical Approach

$$A = \Sigma \frac{y^2}{y_o} = \frac{2 \times 0.5^2}{0.5} = 1.0$$

$$a' = \frac{L_v}{a_s} = \frac{8}{2} = 4; \quad I_D = 82.9 \text{ in}^4;$$

$$d = 2 y_o = 2 \times 0.5 = 1.0;$$

$$c_2 = c_3 = 1.0 \text{ (refer to notations for details)}$$

Substituting these values in Eqs. 4.18 - 4.22, we obtain

$$k = \frac{1000}{[1 + 1\ [1/(0+100\sqrt{2} \times 0.048^2\sqrt{43/1.5}(1)^3)]^2]^{\frac{1}{2}}}$$

$$= 867$$

$$q_1 = \frac{92 \times 1(0 + 0.048) \times 867}{2 \times 8} = 239$$

$$q_2 = \frac{4x2x(0.048)}{2} \times 1\{239[\frac{500}{82.9} + \frac{1}{8x1x1(0.048)}]\}^{\frac{1}{2}}$$

$$= 105$$

$$\frac{q_3}{q_2} = \frac{86.4}{105} = 0.823$$

$$q_d = (q_1 + q_2) \frac{q_3}{q_2} = (239 + 105)\ 0.823 = 283 \text{ lbs/ft.}$$

Assuming a factor of safety of 3,

$$N_u = 3 \times 283 = 849 \text{ lbs/ft.}$$

$$\frac{N_{u(test)}}{N_{u(calc)}} = \frac{963}{849} = 1.13$$

It is observed that the empirical approach provides a conservative estimate of the shear capacity; but the formulas are rather lengthy and complex. Further, the equations have the following limitations, namely:

i) The deck profile should be similar to the one shown in Fig. 4.13 and the spacing of the ribs should not exceed 12".

ii) The sheet thickness of the profile should be greater than 22 gage.

iii) The spacing of the seam fasteners should be within 3 feet centres and in the case of short lengths there shall be at least one seam fastener located at the centre of the panel length.

iv) The spacing of welds at the ends should be less than or equal to 16".

v) The deck should be connected to all the framing members parallel to the corrugation with spacings not exceeding 3 feet on centres.

4.9 Comparison of Results

The predicted values of the shear capacities from all the available methods are compared to test data in Table 4.1. While it is difficult to draw any firm conclusions based on just one comparison, it is observed that the shear strength of the diaphragm is predicted well by the simplified method proposed.

In addition to the diaphragm shown in Fig.4.2, the shear capacities of many welded diaphragms are predicted by the simplified method and the results are compared to test data in Table 4.2. The test results are taken from reported investigations [11] and cover a wide range of variables. From Table 4.1, it can easily be seen that the simplified method predicts well the strength of many welded diaphragms. The strength and stiffness values for the welded connections are taken from the work of Ammar and Nilson [20] and from Figs. 4.9 - 4.12. Some typical results [20] for the welded connections are shown in Figs. 4.14 and 4.15.

Comparison of Results

No.	Name of Method	Predicted Value of in N_u in lbs/ft
1	Full scale testing	963
2	Proposed method	1048
3	Bryan's method	238
4	Davies' equations	630
5	Empirical approach	849

4.10 Application of the Theory to Screw Connected Diaphragms

The proposed expressions for the fastener forces and shear strength are equally valid for diaphragms with rivets and screws. These fasteners are usually referred to as mechanical fasteners. A number of diaphragms with riveted connections are considered to verify the accuracy of the

method. These diaphragms have been taken from the work of Davies [23] and Luttrell [6] and cover a wide range of variables like panel span, number and arrangement of fasteners, panel orientation relative to the load and number of intermediate purlins. Complete details of the panels and fasteners for the diaphragms tested by Davies are included in Chapter 3. The diaphragms tested by Luttrell had screws as fasteners both at the ends and the seams (No. 14 screws at the ends and No. 10 screws at the seams). The strength and stiffness values for these screw fasteners are taken from the work of Ammar and Nilson [20] and from that of Davies [23]. Some typical load deformation curves are shown in Figs. 4.16-4.19. The predicted shear capacities of several screw connected diaphragms are compared to test data in Table 4.2. Further, the forces at the seam fasteners of Davies' diaphragms are predicted by using the proposed formula (Eq. 3.16) and are compared to the results from Davies' equations and finite element approach in Table 4.3. The close agreement between the calculated values and test results of many diaphragms provides strong evidence for the accuracy of the various formulas developed in this study.

4.11 Conclusions

Simplified formulas are developed for calculating the shear capacity and fastener forces of corrugated metal diaphragms. The shear strength of a full-size diaphragm is first evaluated by using the simplified approach and also by all the available analytical methods and the results are compared to test data. In addition, the shear strengths of several welded and screw connected diaphragms are predicted by the proposed theory. Comparisons are made between the calculated values and test results. It is observed that the correlation between the theoretical predictions

and test results is good. The method proposed in the present study, apart from its simplicity, is more general and is applicable for diaphragms with any types of fasteners, whether welds, screws or rivets. The proposed formulas for predicting the shear strength are applicable only where the diaphragm capacity is controlled by the capacity of the fasteners. However, there are situations where the diaphragm could fail in overall shear buckling and this is covered in the next chapter.

CHAPTER 5

BUCKLING OF SHEAR DIAPHRAGMS

5.1 General

In most applications, diaphragm failure is due to localized failure of the fasteners and the shear capacity may be obtained from the strength of the fasteners, as outlined in the previous chapter. However, if there is no failure of the connections, then the diaphragm will fail in overall buckling with a number of diagonal waves, as shown in Fig.5.1. This type of buckling failure has been observed in certain diaphragms where the fasteners are strong and closely spaced. Although the shear behaviour of diaphragms has been studied [1-23] extensively, few investigators [28-30] have attempted to study the buckling behaviour of corrugated steel diaphragms. Among the available methods, the one proposed by Easley [29] appears to be simple. However, there is no evidence for the applicability of the method for predicting the buckling loads of large size diaphragms.

The main objective of this chapter is to develop a simpler formula for calculating the buckling load of shear diaphragms. The new expression for the critical load is derived by making certain simplifications to the expression proposed by Easley and McFarland [28]. The proposed formula has been used to predict the critical buckling loads of several large size diaphragms and the results are compared to test data and those obtained by Easley's equation [29]. Application of the proposed formula is also illustrated with the aid of a numerical example.

5.2 Simplified Buckling Formula

By treating the corrugated panel as an orthotropic plate and by using the principle of minimum potential energy, Easley and McFarland [28] studied the buckling behaviour of shear diaphragms. The following expression has been proposed for the critical buckling load, N_{cr}, as:

$$N_{cr} = \pi^2 D_y \left[\frac{a^2}{2\alpha m^2 b^4} + \frac{3\alpha}{b^2} + \frac{\alpha^3 m^2}{2a^2}\right] + \pi^2 D_x \frac{m^2}{2\alpha a^2}$$

$$+ \pi^2 D_{xy} \left[\frac{1}{2\alpha b^2} + \frac{\alpha m^2}{2a^2}\right] \qquad (5.1)$$

in which m = the number of buckled half waves and is given by

$$m = \frac{a}{b}\left[\frac{D_y}{\alpha^4 D_y + \alpha^2 D_{xy} + D_x}\right]^{1/4} \qquad (5.2)$$

where D_y and D_x are the bending stiffnesses and

D_{xy} is the twisting stiffness

a,b = the dimensions of the diaphragm (see Fig. 5.1).

α = the tangent of the angle between the Y-axis and the direction of the buckled waves, shown in Fig.5.1.

Equation 5.1, in its present form, is very lengthy and the values of m and α must be known to calculate the buckling load. Unfortunately, the value of α is to be obtained from an eighth order complex equation. In spite of all these complexities, the results obtained from Eq. 5.1 are not in good agreement with test data [28].

From many diaphragm tests [28], it has been observed that the values of α are usually small. Thus, the terms involving the powers of α,

namely $\alpha^4 D_y$ and $\alpha^2 D_x$ may be neglected in Eq. 5.2 and simplified as:

$$m = \frac{a}{b}\left[\frac{D_y}{D_x}\right]^{1/4} \qquad (5.3)$$

Extensive numerical calculations were made for certain profiles shown in Fig.5.2 and the value of m was calculated by using Eq.5.3. The predicted values are compared with the measured values of m in table shown below. Also shown in that table are the values of m obtained from Eq. 5.2. The close agreement between the measured values and calculated values using Eq. 5.3, provides strong evidence that Eq. 5.3 could be used instead of Eq. 5.2.

Predicted and Measured Values of m and α

Diaphragm Size (axb) in inches	Panel Stiffnesses in lb. inch D_y	D_x	Predicted Values m from Eq.5.3	m from Eq.5.2	θ* in degrees	Measured Values m	θ* in degrees
180 x 163	153000	21.8	10	10	6.32	10	6.45
180 x 115	153000	21.8	14	14	6.40	14	6.45
108 x 115	153000	21.8	9	9	5.97	8†	6.45
108 x 163	153000	21.8	6	6	6.32	6	6.45

* $\theta = \tan^{-1} \alpha$

Next, the value of α, may be determined approximately from the buckled geometry of the diaphragm as: (see Fig.5.1)

$$\alpha = \frac{a}{bm} \qquad (5.4)$$

Again, the values of θ ($\theta = \tan^{-1}\alpha$) were calculated by using Eq. 5.4 and the results are compared to the measured values. There is close agreement between the test data and the predicted values of α.

Now, the value of α, may be directly substituted from Eq. 5.4 in Eq. 5.1 and simplified as follows:

$$N_{cr} = D_y\pi^2\left[\frac{a^2bm}{2am^2b^4} + \frac{3a}{bmb^2} + \frac{a^3m^2}{2b^3m^3a^2}\right] +$$

$$+ D_x\pi^2\left[\frac{bmm^2}{2aa^2}\right] + D_{xy}\pi^2\left[\frac{bm}{2ab^2} + \frac{am^2}{2bma^2}\right]$$

$$= D_y\pi^2\left[\frac{1}{2}\frac{a}{mb^3} + \frac{3a}{mb^3} + \frac{a}{2mb^3}\right] + D_x\pi^2\left[\frac{1}{2}\frac{am^4b^4}{mb^3a^4} +\right.$$

$$\left. + D_{xy}\pi^2\left[\frac{1}{2}\frac{a}{mb^3}\frac{m^2b^2}{a^2} + \frac{a}{2mb^3}\frac{m^2b^2}{a^2}\right]\right.$$

$$= D_y\pi^2\frac{4a}{b^3m} + \frac{D_x\pi^2}{2}\frac{a}{b^3m}\left[\frac{m^4b^4}{a^4}\right] + D_{xy}\pi^2\left[\frac{a}{mb^3}\frac{m^2b^2}{a^2}\right]$$

$$N_{cr} = \frac{\pi^2a}{mb^3}\left\{4D_y + \frac{m^2b^2}{a^2}\left[D_{xy} + \frac{D_x}{2}\frac{m^2b^2}{a^2}\right]\right\} \qquad (5.5)$$

In the case of practical diaphragms, the value of D_y is generally extremely large when compared to the values of D_x and D_{xy}. For such cases, Eq. 5.5 may be simplified further after omitting certain terms and the resulting equation may be written as:

$$N_{cr} = \frac{4\pi^2a}{mb^3} \cdot D_y \qquad (5.6)$$

The value of m must be calculated from Eq. 5.3 and the nearest integer must be substituted in Eqs. 5.4 and 5.6.

5.3 Calculation of Panel Stiffness

The bending stiffnesses D_y and D_x and the twisting stiffness D_{xy} may be obtained from the panel properties. The following equations have been used for calculating the stiffness values:

$$D_y = \frac{EI_y}{q} \quad \text{(Referred to as major bending stiffness)} \tag{5.7}$$

$$D_x = \frac{Et^3}{12s} \quad \text{(Referred to as minor bending stiffness)} \tag{5.8}$$

and

$$D_{xy} = \frac{Et^3}{6(1+u)} \frac{s}{q} \quad \text{(Referred to as twisting stiffness)} \tag{5.9}$$

where I_y = the moment of inertia of one repeating section of corrugation about the neutral axis;

t = thickness of sheeting;

E = modulus of elasticity of the material of the sheeting;

u = Poisson's ratio for the material;

q = dimension of one repeating corrugation (Fig.5.3); and

s = the flat width of one repeating cross section before forming.

By using the data given in Figs.5.2 - 6.4, the stiffness values for three different panel profiles are calculated and are listed in Table 5.1.

5.4 Application of the Simplified Formula

The critical buckling loads of many diaphragms are predicted by using Eq. 5.6 and the results are compared to test data in Table 5.1. The diaphragms chosen have been tested by Easley [28,29] and cover a wide

range of variables like the size of panels, thickness of sheeting, panel profile and material of sheeting. A total of fifteen specimens are considered to verify the simplified method. The first eight diaphragms were fabricated by using panels with rectangular profiles while diaphragms 9-12 had panels with trapezoidal corrugation. The last three diaphragms, 13-15, were manufactured by using panels with sinusoidal cross sections. These three panel profiles are designated as Type A, B and C in Table 5.1. Complete details of these diaphragms are reported by Easley [28,29].

5.5 Numerical Example

Equation 5.6 will be used to calculate the critical load of diaphragm No. 2 in Table 5.1.

Panel stiffnesses: $E = 10 \times 10^6$ psi;

$u = 0.3$;

Sheeting Thickness: $t = 0.016$ inch;

$s = 4.42$ inch;

$q = 3.48$ inch;

$I_y = 0.00124$ in.^{4}

Using Eq. 5.7, $D_y = \frac{EI_y}{q} = \frac{10\times10^6 \times 0.00124}{3.48} = 3580$ lb.inch

From Eq. 5.8, $D_x = \frac{Et^3}{12s} = \frac{10\times10^6 \times 0.016^3}{12 \times 4.42} = 2.65$ lb.inch

From Eq. 5.9, $D_{xy} = \frac{Et^3}{6(1+u)}\frac{s}{q} = \frac{10\times10^6 \times 0.016^3}{6(1+0.3)} \times \frac{4.42}{3.48} = 6.68$ lb.inch

Size of diaphragm: $a = 30$ inches; $b = 30$ inches.

Using Eq. 5.3, $m = \frac{a}{b}\left[\frac{D_y}{D_x}\right]^{1/4} = \frac{30}{30}\left[\frac{3580}{2.65}\right]^{1/4} = 6.06$

Taking the nearest integer for m as 6,

$$N_{cr} = \frac{4\pi^2 a}{mb^3} \cdot D_y = \frac{4 \times \pi^2 \times 30 \times 3580}{6 \times 30^3} = 26.2 \text{ lbs/inch.}$$

$N_{cr}(\text{test}) = 27.5$ lbs/inch

$$\frac{N_{cr}(\text{test})}{N_{cr}(\text{calc})} = \frac{27.5}{26.2} = 1.05 \text{ (see Table 5.1)}$$

5.6 Critical Load from Easley's Modified Formula

In addition to Eq. 5.1, Easley has also proposed another equation for calculating the critical load of shear diaphragms. This equation has been derived after making certain simplifications to Eq. 5.1. The modified formula is given as:

$$N_{cr} = \frac{36\, D_x^{1/4}\, D_y^{3/4}}{b^2} \qquad (5.10)$$

The critical buckling load of the diaphragm considered in the previous section may be calculated by using Eq. 5.10 as follows:

$D_x = 2.65$ lb.inch; $D_y = 3580$ lb.inch; $b = 30$ inch.

$$N_{cr} = \frac{36 \times 2.65^{1/4} \times 3580^{3/4}}{30^2} = 23.6 \text{ lbs/inch.}$$

Using Eq. 5.10, the critical loads of all the 15 diaphragms are also predicted and the results are given in Table 5.2. It is of interest to note

that the results from the proposed method are closer to the critical loads observed in tests than that of Easley's method.

5.7 Conclusions

The predicted values for the critical loads by using the simplified formula, agree well with the test results of several diaphragms. The modified equation proposed by Easley provides a conservative estimate of the critical load of diaphragms. However, in some cases, Easley's theory underestimates the shear capacity by as much as 30%. It can be easily seen from Table 5.2 that the simplified formula is suitable for both small size diaphragms and large diaphragms commonly found in buildings. The proposed formula, because of its simplicity, will be more useful for design purposes.

CHAPTER 6

BEHAVIOUR OF CLAD MULTISTORY FRAMES UNDER LATERAL LOADS

6.1 General

Provision of adequate lateral stiffness is important in the design of high rise structures. The structure must be stiff enough to avoid excessive drift under working load conditions. Excessive lateral deflection may cause cracking of plaster, dislocation of joints, misalignment of elevator shafts. Above all, the occupants of the building may be affected psychologically due to perceptible sway. Building codes usually specify the maximum allowable lateral deflection in terms of the 'Drift Index' defined as the ratio of the roof deflection to the building height. In the case of tall buildings a drift index between 0.003 to 0.002 is generally considered adequate [9]. The National Building Code of Canada [48] recommends a value of 0.002 as the limiting value for the drift index.

Plane frames of 25 to 30 stories designed on the basis of ultimate strength often do not have sufficient lateral stiffness; and it is necessary to add at least 30% more steel by weight to bring down the lateral deflection to an acceptable level. As an alternative to increasing the member sizes, light gage steel panels may be used to control the lateral deflection. This chapter is concerned with the lateral load response of multistory frames stiffened with corrugated steel claddings.

6.2 Structural Requirements of Steel Claddings

There are certain basic requirements which the claddings must satisfy in order to be considered as structural components in multistory frames. These requirements are listed below:

i. Adequacy of Shear Resistance: As shown in the previous chapters, the shear stiffness and strength of claddings depend primarily on the type of connections, the material of the sheeting and the type of profile. Cellular decks would seem to be the best choice due to its high shear and bending resistance. However, they are expensive to manufacture and difficult to transport. In contrast, decks with open profiles can be stacked together for easy transportation to the site. The possibility of profile distortion can be reduced by providing sufficient number of end fasteners.

ii. Adequacy of Out-of-Plane Bending Stiffness: The second structural requirement is the ability of the panels to withstand loads acting normal to the plane of the panels. Cold-formed steel panels possess considerable amount of bending stiffness because of the corrugated shape.

iii. Adequacy of Strength: The panels must possess high in-plane shear resistance to overall buckling. In addition to the possibility of overall shear buckling, the panels may fail due to failure of the connections. These types of failure have been discussed in detail in the previous chapters. The panels must be designed to avoid these failures.

6.3 Connection between the Frame and the Cladding

The cladding is composed of several corrugated steel sheets or panels connected to one another along the laps and to the four perimeter members. The connections may be of welds or screws. The direction of the corrugation is arbitrary; however, since the story height is usually less than the bay width, it would be more effective if the corrugation generator is placed vertical as shown in Fig.6.1. This arrangement would yield higher out-of-plane bending stiffness for the cladding. The perimeter members are pin-connected to each other in order to provide a state of pure shear in the cladding. The whole assembly of the cladding is connected to the girders and columns of the frame as indicated in Fig. 6.1. The connection between the cladding and the frame beam at the top should be designed so as to minimize the transfer of vertical forces between the two components and at the same time permit full transfer of lateral shear forces in the plane of the claddings. This could be achieved by connecting the frame beam and the cladding as shown in Fig. 6.2 (Ref. 9).

6.4 Analysis of Clad Multistory Frames

As already mentioned, there is a considerable amount of literature on the behaviour of shear diaphragms [3-6]. However, much less research activity has taken place with regard to the integrated behaviour of clad multistory frames. Miller [9] and Oppenheim [39] adopted the finite element technique and obtained the shear stiffness of the cladding. The method proposed by Dakhakhni [10] is based on the superposition of the applied lateral forces with the restraining

forces of the cladding to achieve the required compatibility of lateral deflections at each story level. All these approaches have their own limitations. Miller's approach will be too cumbersome and expensive because of the considerable amount of computer time as well as the time required for careful preparation of the input data. The methods of Dakhakhni [10] and Oppenheim [39] are approximate because of omission of the column axial deformation in the analysis. Further, all these methods assume that the stiffness of the cladding is the same at all story levels. The method proposed here does not have any of the limitations mentioned above.

6.4.1 Development of the Method

The practical method presented in this study is based on the conventional stiffness method of analysis [44-46].

with the following simplifying assumptions:

(i) It is assumed that the claddings do not interfere with the local bending of the framing members around the claddings. In other words, the panels are subjected only to loads in their own plane.

(ii) The joints at each floor level would drift the same amount laterally.

(iii) The perimeter members of the cladding are sufficiently stiff so that the cladding may be considered as connected to the frame at the four corners as shown in Fig. 6.1.

6.4.2 Stiffness Matrix of a Cladding

A typical element of width 'a' and height 'b' is shown in Fig. 6.3. The stiffness matrix, $[S_i]$, of the cladding may be derived from the shear stiffness, S, of the cladding for the following cases:

Case i. Axial deformation of columns neglected: The displacement coordinates for this case is shown in Fig. 6.4. The cladding is subjected to shear load in its plane. The stiffness matrix, $[S_i]$, can be derived by applying unit displacements at joints 1 and 2 and the resulting matrix will be of the form

$$[S_i] = S_i \begin{bmatrix} 1 & -1 \\ -1 & 1 \end{bmatrix} \qquad (6.1)$$

where S_i is the shear stiffness of one cladding at level i.

Case ii. Column axial deformation included: The effect of column shortening in calculating the lateral deflection of multistory frames is very significant especially in the case of slender frames. Omission of this effect could result in an error of up to 30% in deflection calculations. When axial deformations are included, the displacement coordinates of a cladding will be as shown in Fig. 6.5. The stiffness coefficients can be determined as before by applying unit displacements at each node as illustrated in Fig. 6.6. The resulting stiffness matrix of the cladding for this case is

$$[S_i] = S_i \begin{bmatrix} 1 & -1 & -b/a & b/a \\ -1 & 1 & b/a & -b/a \\ -b/a & b/a & b^2/a2 & -b^2/a2 \\ b/a & -b/a & -b^2/a2 & b^2/a2 \end{bmatrix} \qquad (6.2)$$

in which S_i = the shear stiffness of the cladding at level i and a, b = the dimensions of the cladding. It can be seen from the above expression that the stiffness matrix is affected by the axial deformation of the columns. When the last two columns and rows of matrix $[S_i]$ are omitted, Eq. 6.2 would reduce to Eq. 6.1.

6.5 Stiffness of the Overall Structure

A typical multistory frame with two bays is shown in Fig. 6.7. The frame has n stories and it is assumed that claddings are provided in the second bay throughout the height of the frame. The frame is subjected to lateral loads, P_i, at each floor level and the restraining forces developed by the claddings are represented by R_i. These restraining forces may be calculated from Eqs. 6.1 and 6.2 as explained in the following sections.

6.5.1 Column Axial Deformation Neglected

When the axial deformations of the columns are ignored, the stiffness matrix of one cladding is given by Eq. 6.1. It is of particular interest to note that Eq. 6.1 is identical with the stiffness matrix of a truss member or a spring of stiffness S_i. Thus, a cladding between two levels can be modelled by a horizontal spring, with the lateral displacement of the loose end of the spring coupled to that of the

lower level as shown in Fig. 6.8. Using this artifice, the overall stiffness matrix, $[K_c]$, of all the claddings may now easily be obtained as follows:

$$[K_c] = S_i \begin{bmatrix} 1 & -1 & & & & & \\ -1 & 2 & -1 & & & & \\ & -1 & 2 & -1 & & & \\ & & \cdot & \cdot & \cdot & & \\ & & & \cdot & \cdot & & \\ & & & \cdot & \cdot & & \\ & & & -1 & 2 & -1 & \\ & & & & -1 & 2 & \end{bmatrix} \qquad (6.3)$$

It is assumed in the above equation that the shear stiffnesses of the claddings are the same in all stories.

Knowing the value of $[K_c]$ from Eq. 6.3, the following relation can be written for the restraining forces, $[R]$, as:

$$\begin{bmatrix} R_1 \\ R_2 \\ R_3 \\ \cdot \\ \cdot \\ \cdot \\ R_n \end{bmatrix} = S_i \begin{bmatrix} 1 & -1 & & & \\ -1 & 2 & -1 & & \\ & -1 & 2 & -1 & \\ & & \cdot & & \\ & & & -1 & 2 \end{bmatrix} \begin{bmatrix} \Delta_1 \\ \Delta_2 \\ \Delta_3 \\ \cdot \\ \cdot \\ \cdot \\ \Delta_n \end{bmatrix} \qquad (6.4)$$

Equation 6.4 may also be written in matrix form as:

$$[R] = [K_c]\,[D] \qquad (6.5)$$

where [R] = the restraining forces at each story level: $[K_c]$ = the overall stiffness matrix of all the claddings given by Eq. 6.3; and [D] = the lateral displacements of the joints. Knowing the restraining forces and the applied loads at each joint of the frame, the net forces in the frame can be calculated as

$$[P]-[R] = [K_F]\,[D] \tag{6.6}$$

where $[K_F]$ is the lateral stiffness matrix of the bare frame. Substituting for [R] from Eq. 6.5, the following equation is obtained:

$$[P]-[K_c][D] = [K_F][D] \tag{6.7}$$

$$[P] = [\,[K_c] + [K_F]\,]\,[D] \tag{6.8}$$

or

$$[P] = [K_s][D] \tag{6.9}$$

where $[K_s]$ is the structure stiffness matrix of the integrated structure and is obtained by adding the overall stiffness of all the claddings and the bare frame.

6.5.2 Column Axial Deformation Included

The overall stiffness matrix of the integrated structure for this case can be derived as before. However, there is one major difference in that the overall stiffness matrix of all the claddings must be obtained from Eq. 6.2. Using Eq. 6.2, the stiffness matrices of all the claddings may be assembled and the resulting matrix can be represented as $[K'_c]$.

The overall structure stiffness matrix, $[K'_S]$, may again be obtained as before by adding $[K'_C]$ and $[K_F]$ as

$$[K'_S] = [K'_C] + [K_F] \qquad (6.10)$$

Once the structure stiffness matrix is obtained, the following equation may be written for the externally applied lateral forces as

$$[P] = [K'_S][D] \qquad (6.11)$$

Equations 6.9 and 6.11 may be solved by using standard computer programmes.

6.6 Computer Programme:

The proposed theory has been implemented after making necessary modifications to an existing frame analysis programme [58]. The programme has been written in Fortran and can be used for the analysis clad multistory frames. The programme can handle frames with any value of stiffness for the cladding along the height of the frame. The programme output produces the forces at the member ends, joint deflections and the shear forces in the claddings at each floor level. A typical clad frame with the numbering system for the joints and members is indicated in Fig. 6.9. A brief description of the input data and a typical output are given in Appendix A for the sake of reference.

6.7 Response of Clad Multistory Frames to Lateral Loads

In order to verify the accuracy of the proposed method and to study the behaviour of clad frames, three different multistory frames are chosen. These frames have been designed by a research group from

Lehigh University [52] and the frames have been analysed by Miller [9] and Dakhakhni [10]. A brief description of these frames is presented first and then the response of the frames under lateral loads will be discussed.

6.7.1 Description of 15-Story Frame

The first frame has 2 bays and 15 stories. The bay width is 30 feet and the story height is 12 feet. The overall dimension and member sizes are shown in Fig. 6.10. The frames are placed at 30' intervals. Assuming that the wind intensity is 20 psf, the wind load at each story level is calculated as 7.2 kips. It is assumed that cladding is provided in all the stories of the 2nd bay. The cladding is made from 18-gage corrugated sheets with 3-inch wide and 1½-inch deep profile.

6.7.2 Description of 24-Story Frame

The second frame in the series is also a 2 bay-frame with a bay width of 30 feet. The height of each story is 12 feet and the frames are spaced at 30-foot intervals in the building. The details of member sizes and the overall dimensions are given in Fig. 6.11. The frame is subjected to lateral loads of 7.2 kips at each story level. The frame is assumed to be stiffened with light gage steel panels in the 2nd bay throughout the height of the frame.

6.7.3 Details of 26-Story Frame

This frame is a 3-bay frame with 30-foot wide bays. The lateral loads acting at each floor level are indicated in Fig. 6.12. Also shown in

the figure are the details of member sizes and over-all dimensions of the frame. It is assumed that the frame is stiffened with cladding in the middle bay in all the 26 stories. This frame has been subject to detailed finite element analysis by Miller [9] and the details of the results are presented later in this chapter.

6.7.4 General Response of Clad Frames

The major objective of this section is to investigate the effect of cladding on the lateral deflection of multistory frames. The lateral deflection of a clad frame can be estimated by using the equation [Ref.10]

$$\Delta_c = \frac{1}{(r+1)} \Delta_b \qquad (6.12)$$

where Δ_b = the deflection of the bare frame subjected to the same loads as that of the clad frame; Δ_c = the maximum deflection of the clad frame. r = the ratio of the shear stiffness of the cladding to the shear stiffness of one story. The value of r may be obtained as

$$r = \frac{S_i}{\Sigma 12 \frac{EI_c}{L_c^3}} \qquad (6.13)$$

in which S_i = the shear stiffness of the cladding at story level, i; and I_c, L_c = the moment of inertia and the height of the column at the same story as that of the cladding. The summation should be carried out for all the columns in a given story. Equations 6.12 and 6.13 have been derived with the following assumptions:

i. The properties of the claddings and columns are the same throughout the height of the building.

ii. The beams have infinite bending rigidity; and

iii. The effect of axial deformations of the columns are ignored.

The responses of the frames described in the previous sections are predicted by using Eq. 6.12. In order to calculate the shear stiffness ratio, r, the column stiffness at 1/6 of the height from top has been used in Eq. 6.13. The frames are analysed for a wide range of cladding stiffnesses listed in Tables 6.1 to 6.3. The effect of cladding on the lateral deflection, on bending moments in the columns and beams and on axial forces in the columns are studied by using the proposed method.

Referring to Fig. 6.13, one of the curves is the graphical representation of Eq. 6.12 while the others show the variation of the ratio of maximum deflection of the clad frame to that in the bare frame with respect to r from the present analysis. There is a reduction of 32 to 35% in the lateral deflection for a shear stiffness ratio of 0.5 in the case of all the frames considered. For larger values of r, the deflection continues to reduce; but less rapidly and Eq. 6.12 tends to overestimate the effectiveness of the cladding.

The variation of maximum bending moments in the columns and beams are plotted in Fig. 6.14. The bending moments are reduced with increase in the shear stiffness ratio. The closeness of the curves for all the frames over a wide range of r indicates that the bending moment reduction depends mostly on the shear stiffness ratio.

The variation of maximum shear carried by the cladding in all the

frames is shown in Fig. 6.15. It is observed that the maximum shear in the cladding increases with the shear stiffness ratio.

Plotted in Figs. 6.16 and 6.17 are the variations of column axial forces. It can be seen that the axial forces are increased in the leeward columns (Fig. 6.16) while in the windward side columns they are decreased.

The results from the present analysis for all the three frames are also tabulated. (Tables 6.1 to 6.9). It is observed that while the provision of claddings reduces the shears, bending moments and lateral deflections, it tends to change the distribution of axial forces in the columns. Since the direction of the lateral load depends on the direction of wind, strengthening of all the columns in the lower stories may be necessary especially when claddings are used to control drift in multistory frames.

6.8 Comparison of Results

The results obtained from the present analysis could be compared with that obtained from other methods [9,10]. Miller [9] has analysed the 26-story frame shown in Fig. 6.12. The shear stiffness of the cladding was obtained from the finite element analysis [20]. The panel idealization used in the finite element technique is shown in Fig. 6.18. The marginal members and the frame members were idealized as linear, elastic beam elements. The corrugated sheeting was modelled as assemblage of orthotropic finite elements. The connections were modelled as linear, elastic springs whose spring constants were obtained from separate tests. More details about the finite element analysis of this cladding is reported in Reference 10.

6.8.1 Shear Stiffness of Cladding

The shear stiffness of the cladding should be known in order to employ the present technique. For the case of a single story, single bay clad frame of 12' height and 30' width, subjected to lateral load, the following results are reported [10] from finite element analysis:

Shear load in cladding = 76.8 kips (thickness of sheet 16 gage)
Corresponding shear deflection = 0.204 inch

From the above values, the shear stiffness may be calculated as $S = 76.8 \div 0.204 = 376.4$ kips/inch. Using this value of shear stiffness, the 26-story frame was analysed and the results are compared with those obtained by Miller [10] in Table 6.10. There is excellent agreement between the results. The lateral deflected shapes are also compared in Fig. 6.19. It is seen that the proposed simplified method predicts well the response of the 26-story frame stiffened with steel claddings.

6.8.2 Comparison of Results for 15 and 24-Story Frames

These two frames have been analysed and the deflected shapes are plotted in Figs. 6.20 and 6.21. The deflected shapes obtained by Dakhakhni are also shown for comparison. There is close agreement between the proposed method and Dakhakhni's approach.

Figure 6.22 shows the variation of cladding shear at each story level for two frames. The lateral deflections and the shear force in the claddings at each story level are also listed in Table 6.11.

6.9 Design Aspects

The structural system of a clad multistory frame is composed of linear and planar elements interconnected together in such a way that they would effectively resist the imposed loads and deformations. The planar members are the claddings fabricated from light gage steel panels and the linear elements are the beams and columns. The use of light gage steel panels has many advantages:

i. When properly connected to the frame, considerable amount of lateral stiffness could be achieved.

ii. Addition of the panels do not add much weight to the structure because of their light weight.

iii. Requirements such as sound and heat insulation could be easily installed when open corrugated panels are used as stiffening elements.

The main function of the cladding is to stiffen the frame or control the lateral deflection. The frame must be designed first to carry the wind and all superimposed loads. This could be done by using the existing methods outlined in Refs. 47 and 51. Next, the lateral deflection of the bare frame must be calculated. If the calculated deflection is less than the allowable value specified in the codes, then the design is complete. However, if the lateral deflection is more than the specified limit, then the frame should be stiffened by providing suitable claddings.

6.9.1 Design Example

The frame shown in Fig. 6.11 has been chosen to illustrate the design procedure. The frame has 24 stories and 2 bays and has been designed

[10] according to the strength requirements. However, at working load level (shown in Fig. 6.11) the lateral deflection of the bare frame is 11.14 inches. This deflection corresponds to a drift index of 0.0032. According to the National Building Code of Canada [48], the allowable drift index should be 0.002. The deflection at the top should be less than or equal to 6.91 inches to satisfy this requirement. This deflection is about 62% of the bare frame deflection. To reduce the deflection to this limit, the frame must be stiffened by providing steel claddings and the procedure for evaluating the required cladding stiffness is explained below.

Ratio of clad frame to bare frame deflection, $\alpha_1 = \frac{6.91}{11.14} = 0.62$. For this ratio of α_1, two values of r, one based on Eq. 6.12, and the other from the present theory may be obtained from Fig. 6.13. These values are respectively 0.612 and 0.713. Using the column shear stiffness as 253.16 kip/inch, the values of S may be obtained from Eq. 6.13 as 155.3 kip/inch and 184.8 kip/inch for the above values of r. (The column shear stiffness is calculated at 1/6 of the frame height and is given in Table 6.2.)

The 24 story frame was analysed by using the two cladding stiffnesses mentioned above and the deflected shapes are plotted in Fig. 6.23. The results for maximum lateral deflections are also compared below.

Comparison of Maximum Deflection (inches)

Design Value (Canadian Code)	Proposed Method	Dakhakhni's Method
6.91	6.94	5.36

It is clear that the method proposed in this study predicts the required

lateral deflection within 1% of the design value while the deflection from Dakhakhni's approach is lower than the design value by about 22%. This could be attributed to the omission of the effect of axial deformation of the columns in Dakhakhni's method.

6.10 Conclusions

By using the conventional stiffness approach, a simplified method is developed for the analysis of clad multistory frames. The present method has been used to predict the behaviour of three multistory frames subjected to lateral loads. The results obtained for the frames compare very closely with those from other approaches. Lateral load response of all the frames is presented in a generalized form and design curves are developed. By using the design curves, a simplified technique is suggested for choosing the correct cladding stiffness to limit the lateral deflection to any required value. The design procedure has been used to calculate the cladding stiffness for a two-bay frame whose lateral deflection is considered excessive. It is observed that the proposed technique is very efficient and the result for the lateral deflection is very close to the required value and that obtained from other existing methods.

CHAPTER 7

CONCLUSIONS AND RECOMMENDATIONS

7.1 Conclusions

The investigation reported in this study deals with the analysis of cold-formed steel shear diaphragms and the response of clad multistory frames to lateral loads. The present research has resulted in simplified methods for predicting the behaviour of shear diaphragms and of the integrated structure consisting of the frame and the claddings. The following major conclusions are made on the basis of the work covered in this investigation.

i. Based on an assumed deformation mode of the diaphragm, closed form expressions are derived for fastener forces and diaphragm flexibility. The proposed theory is applicable to both welded and screw connected diaphragms. The shear characteristics of several diaphragms having a wide range of variables are predicted using the present theory and the results are compared to test data. In most cases, excellent agreement between the theoretical results and test data has been obtained.

ii. It is observed that the shear behaviour of diaphragms depends strongly on the type and arrangement of fasteners. In general, welded diaphragms are stronger and stiffer than those with mechanical fasteners, for a given panel profile and size of diaphragm.

iii. The subject of shear buckling of metal diaphragms has been treated separately and a simplified formula has been proposed for predicting the elastic buckling load of shear diaphragms. The new expression for the buckling load has been derived after making certain simplifications to the formula proposed by Easley [29]. It has been observed that the critical buckling load depends mostly on the major bending stiffness of the panel while the twisting stiffness and minor bending stiffness have little influence on the critical loads of diaphragms used in practice.

iv. The elastic buckling loads obtained from the proposed simplified approach compare favourably with those observed in tests.

v. A practical method is presented for the analysis of clad multistory frames. The proposed artifice of replacing the claddings by equivalent elastic springs provides an easy tool for incorporating the stiffness of the claddings with the overall stiffness of the structure. It is observed that the results from the proposed method are in good agreement with those obtained from other methods proposed by El-Dakhakhani [10] and Miller [9].

vi. The results obtained from the proposed analysis for three clad multistory frames clearly indicate that cold-formed steel claddings are effective in controlling lateral deflection.

vii. It is also observed that the design curves developed in this study, because of their dimensionless nature, are highly suitable for the rapid

evaluation of the response of clad multistory frames subject to lateral loads. In particular, one could easily determine the required cladding stiffness from the design curves to keep the lateral drift within any specified value.

viii. Although the provision of cladding reduces the lateral deflections, bending moments and shear forces, axial forces in the leeward columns are found to increase in varying degrees depending upon the shear stiffness of the cladding.

7.2 Recommendations

i. The present study is limited to the case of shear diaphragms subjected to monotonically increasing static loads. However in reality buildings are subjected to both repeated and reversed loadings. Hence, the effects of these loadings on the response of shear diaphragms should be investigated.

ii. The theory proposed in this investigation is concerned with the analysis of simple diaphragm where there will be no openings or cuts. The present approach may be extended to evaluate the shear stiffness and strength of such diaphragms. In addition, tests on full-scale diaphragms with openings should be carried out to verify the accuracy of the theory.

iii. The equations developed in this work are limited to linear elastic behaviour of diaphragms. Theoretical investigation may be carried out on the non-linear behaviour of shear diaphragms. Of particular importance is the amount of ductility offered by the diaphragm.

iv. At present, no test data have been reported on clad multistory frames to verify the proposed theory. Thus, large-scale tests on clad frames would be useful in providing information on the behaviour of the connections between the claddings and the frame, mode of failure and the ultimate strength of the clad frame.

v. It is assumed in the analysis of clad frames that the claddings are effective only in resisting lateral loads in their plane. The most important aspect is the type of connection between the perimeter members of the cladding and the bounding members of the multistory frame. Hence, further experimental research is required to propose a suitable connection detail between the cladding and the frame.

vi. The practical method for clad frame analysis is limited to static loadings. However, buildings located in seismic zones will be subjected to dynamic loads. The present theory could readily be extended for such loading cases.

REFERENCES

1. "Complete line of metal building products", Engineering/Fabrication/ Erection, Report 5rms/WRL, Westeel-Rosco Ltd. Toronto.

2. Johnson, C.B., and Converse, J.F.;"Light Gage Steel Diaphragms in Building Construction", American Society of Civil Engineering Meeting, February 1950, Los Angeles, California, U.S.A.

3. Bryan, E.R., and El-Dakhakhni, W.M.; "Behaviour of Sheeted Portal Frame Sheds: Theory and Experiments", Proc. Inst. Civ. Engrs. Vol. 29, December 1964, pp. 743-778.

4. Bryan, E.R.; "Research into the Structural Behaviour of a Sheeted Building", Proc. Inst. Civ. Engrs. Vol. 48, January 1971, pp. 65-84.

5. Bryan, E.R., and El-Dakhakhni, W.M.; "Shear Flexibility and Strength of Corrugated Decks", Jour. Struct. Division, Proc. A.S.C.E., Vol. 94, No. ST 11, November 1968.

6. Luttrell, L.D.; "Strength and Behaviour of Light Gage Steel Shear Diaphragms", Cornell Engineering Research Bulletin, No. 67-1, July 1967.

7. Rathburn, J.C.; "Wind Forces on a Tall Building", Transactions of the American Society of Civil Engineers", Vol. 105, pp.1, 1940.

8. Wiss, J.F., and Curth, O.E.; "Wind Deflections of Tall Concrete Frame Buildings", Journal of the Structural Division, Proceedings of the American Society of Civil Engineering, Vol. 96, No. ST 7, p. 1461, July 1970.

9. Miller, C.J.; "Analysis of Multistory Frames with Light Gage Steel Panel Infills", Report No. 349, School of Civil and Environmental Engineering, Cornell University, August 1972.

10. El-Dakhakhani, W.M.; "Effect of Light-Gage Partitions on Multistory Buildings", Journal of the Structural Division, A.S.C.E., Proc., Vol. 103, No. ST-1, January 1977.

11. Nilson, A.H.; "Shear Diaphragms of Light Gage Steel", Journal of the Structural Division, ASCE Proceedings, Vol. 86, No. ST 11, November 1960.

12. American Iron and Steel Institute, "Design of Light Gage Steel Diaphragms", New York, 1967.

13. American Society for Testing Materials, "ASTM Standard for Testing of Light-Gage Steel Shear Diaphragms, 1976.

14. Apparao, T.V.S.R.; "Tests on Light Gage Steel Diaphragms", Report No. 328, Dept. of Structural Engineering, Cornell University, December 1966.

15. Easley, J.T.; "Strength and Stiffness of Corrugated Metal Shear Diaphragms", Journal of the Structural Division, A.S.C.E. Proc. Paper 12675, January 1977.

16. Easley, J.T.; "Tests of Light Gage Steel Shear Diaphragms", Report on CRES Project 85, Part 1, University of Kansas, Lawrence, Kansas, February 1967.

17. Easley, J.T.; "Tests of Light-Gage Steel Shear Diaphragms", Report on CRES Project 85, Part I, University of Kansas, Lawrence, Kansas, December 1967.

18. Chockalingam, S., Ha, H.K. and Fazio, P.P.; "Strength and Stiffness of Corrugated Metal Shear Diaphragms", Discussion in Journal of the Structural Division, A.S.C.E. Proc. January 1978.

19. Chockalingam, S., Fazio, P.P. and Ha, H.K.;"Strength of Light Gage Steel Corrugated Diaphragms", Proceedings of the Fourth International Specialty Conference on Cold-Formed Steel Structures, University of Missouri, Rolla, Missouri, June 1978.

20. Ammar, A.R. and Nilson, A.H.; "Analysis of Light Gage Steel Shear Diaphragms", Reports 350 and 351, Dept. of Structural Engineering, Cornell University, Ithaca, New York, July 1973.

21. Ha, H.K.; "Corrugated Shear Diaphragms", Journal of the Structural Division, A.S.C.E. (Appearing in March 1979).

22. Bryan, E.R., and Jackson, P.; "The Shear Behaviour of Corrugated Steel Sheeting", Thin Walled Steel Structures, Crosby, Lockwood, London, 1969.

23. Davies, J.M.; "The Design of Shear Diaphragms of Corrugated Steel Sheeting", Report Reference No. 74/50, University of Salford, Dept. of Civil Engg., September 1974.

24. Davies, J.M.; "Simplified Diaphragm Analysis", Journal of the Structural Division, A.S.C.E., July 1977.

25. "Seismic Design for Buildings", Departments of the Army, the Navy and the Air Force of U.S.A., March 1966.

26. Canadian Sheet Steel Building Institute, "Diaphragm Action of Cellular Steel Floor and Roof Deck Construction", CSSBI, Mississauga, Ontario, December 1972.

27. Bergmann, V.S., and Reissner, H.; "Neuere-Probleme ausder Flugzeugstatik", Zeitschrift Flugtech und Mororluftsch, Vol. 20, 1929.

28. Easley, J.T., and McFarland, D.; "Buckling of Light Gage Corrugated Metal Shear Diaphragms", Journal of the Structural Division, A.S.C.E., Vol. 95, No. ST-7, July 1969.

29. Easley, J.T.; "Buckling Formulas for Corrugated Metal Shear Diaphragms", Journal of the Structural Division, A.S.C.E., Vol. 101, No. ST-7, July 1975.

30. Hlavacek, V.; "Shear Instability of Orthotropic Panels", Acta Technica CSAV, Prague, Czechoslovakia, No. 1, 1968.

31. Ellifritt, D. and Luttrell, L.D.; "Strength and Stiffness of Steel Deck Shear Diaphragms", First Specialty Conference in Cold-Formed Steel Structures, University of Missouri, Rolla, Missouri, U.S.A. November 24-25, 1975.

32. Amos, A.K.; "An Investigation of Elastic Buckling in Corrugated Plates under Shearing Stresses", Doctoral Dissertation, Civil Engineering Dept., Princeton University, 1966.

33. Libove, C. and Lin, C.; "Theoretical Study of Corrugated Plates: Shearing of a Trapezoidally Corrugated Plate with Trough Lines Held Straight", Syracuse University Research Institute, Dept. of Mechanical and Aerospace Engineering, Report No. MAE 1833-T May 1970.

34. McKenzie, K.I.; "The Shear Stiffness of Corrugated Web", R.A.E. Report No. Structures 275, June 1962.

35. Horne, M.R., and Raslan, R.A.S.; "An Energy Solution to the Shear Deformation of Corrugated Plates", Publication of the International Association for Bridge and Structural Engineering, Vol. 31-1, 1971.

36. Baehre, t.dr.; "Sheet Metal Panels for Use in Building Construction", Current Research Projects in Sweden, Proceedings of the Third Specialty Conference on Cold-Formed Steel Structures, University of Missouri, Rolla, Missouri, U.S.A., November 24-25, 1975.

37. "Research Needs in Structural Engineering for the Decade 1966-1975", Journal of the Structural Division, Proceedings of the A.S.C.E., Vol. 92, No. ST-5, October 1966.

38. El-Dakhakhani, W.M., and Daniels, J.H.; "Integrated Structural Behavior of Buildings", ASCE National Structural Engineering Meeting, Ohio, April 24-28, 1972.

39. Oppenheim, I.J.; "Control of Lateral Deflexions in Planar Frames Using Structural Partitions", Proceedings of the Institution of Civil Engineers, London, England, Vol. 55, June 1973.

40. El-Dakhakhani, W.M.; "Shear of Light Partitions in Tall Buildings", Journal of the Structural Division, A.S.C.E., Vol. 102, No. St-7, Proc. Paper 12257, July 1976.

41. Levelt, H.L. and Fung, C.; "Report on Steel Deck Diaphragms", Research and Development Dept., Westeel-Rosco Ltd., Toronto, May 1969.

42. Bryan, E.R.; "The Stressed Skin Design of Steel Buildings", Crosby Lockwood Staples, London, 1973.

43. "European Recommendations for the Stressed Skin Design of Steel Structures", Constrado, ECCS-XVII-77-1E, March 1977.

44. Ha, H.K., Fazio, P. and Chockalingam, S.; "Effect of Light-Gage Partitions on Multistory Buildings", Discussion in the Journal of the Structural Division, A.S.C.E., August 1977.

45. Ha, H.K., Fazio, P. and Chockalingam, S.; "The Analysis and Design of Multistory Frames with Light Gage Corrugated Panels", Report No. CBS 66, March 1977.

46. Ha, H.K.; "Lateral Load Response of Multistory Frames Stiffened with Corrugated Panels", International Symposium on Building Systems, Vanderbilt University (appearing in March 1979).

47. Plastic Design in Steel, A Guide and Commentary, A.S.C.E., 1971.

48. National Building Code of Canada, 1975.

49. Gere, J.M., and Weaver, J.; Analysis of Framed Structures. Van Norstrand Reinhold, New York, 1965.

50. Ha, H.K.; "Computer Program for the Analysis of Plane Frames", Report No. CBS, Concordia University, Montreal. (To be published)

51. Beedle, L.S. et al., "Plastic Design in Structural Steel", Lecture Notes, Lehigh University, Bethlehem, Pa.;and American Institute of Steel Construction, New York, Sept. 1955.

52. Daniels, J.H.; "Effective Column Length and Frame Stability", American Iron and Steel Institute Project 174, Lehigh University

APPENDIX A

A.1 Preparation of Input Data

In all the input data cards, ten-column fields are used for each item of information. The following guidelines are given to prepare the data cards for clad frame analysis [50].

Set	Number of Cards	Details of Information
A	1	Blank card to start a problem
B	1	NCC, NCOM, NSPR, NLAT, NAXIAL, NCLAD
C	NCC	comments or headings (50 characters/card)
D	1	NRJ, NRM, NJFIX, MPIN, NLC, ELAS, NBAY, NSTOR

Note: NCC = Number of comment cards

NCOM = Number of load combinations (maximum 12)

NSPR = Number of spring supports

NLAT > o (for rigid floors, ie. equal lateral displacements for all joints in the same level)

NAXIAL > o Axial deformations of all columns are ignored (applicable only when NBAY > o)

NCLAD = Number of shear diaphragms; (applicable only when NBAY > o and NLAT > o)

NRJ = Number of joints

NRM = Number of members

NJFIX = Number of restrained joints

MPIN = Number of members with pinned ends

NLC = Number of loading cases

ELAS = Modulus of elasticity

NBAY = Number of bays

NSTOR = Number of stories

E Variable I,J,K,ND(1), ND(2), ND(3)

Notes: I = first joint of sequence

J = last joint of sequence

K = increment for generation of joint number

(J& K may be zero if there is no generation)

ND(1)=0; if x-displacement is restrained

ND(2)=0; if y-displacement is restrained

ND(3)=0; if rotation of joint is restrained

ND(I)=1 if the i^{th} direction of the joint is free to displace

ND(I)=L>1 if the i^{th} displacement of the joint is the same as the i^{th} displacement of joint L.

F* Variable List of member end condition:I, J, K, KL, KG

Notes: I = first member of sequence

J = last member of sequence

K = increment for generation of sequence

KE = 1 if the lesser numbered joint is pinned; otherwise = 0

KG = 1 if the greater numbered joint is pinned, otherwise = 0

Set F is not required if MPIN = 0 in Set D.

G.1 1 NBAY, (BL(I), I = 1, NBAY)

Notes: NBAY = number of bays

BL(I) = length of bay I, continuing from left to right

1 NSTOR, (SL(I), I = 1, NSTOR)

Notes: NSTOR = number of stories;

SL(I) = height of story i, continuing from bottom

Set G.1 not required if NBAY is zero in card D.

G.2 Variable Cladding information:NC1, NC2, K, NS, NB, GP

Notes: NC1 = first diaphragm of sequence

NC2 = last diaphragm of sequence

K = increment number of diaphragm

NS = story number of first diaphragm

NB = bay number of first diaphragm

GP = shear stiffness for all diaphragms generated in this sequence

If NS < o the story number of the next diaphragm of sequence is increased by 1

If NB < o the bay number of the next diaphragm of sequence is increased by 1

G.3 NRJ JT, X, Y

Notes: JT = joint number

X,Y = coordinates of joint

Joint numbers must be in sequence starting from 1 to the last joint. Set G.3 is required only if NBAY in card D is zero.

H.1 Variable I,J,K,A,T,DL,BL,AS

Notes: I = first member of sequence

J = last member of sequence

K = increment of member number

A = area of member

T = moment of inertia

DL = length of rigid arm at lesser joint number

BL = length of rigid arm at greater joint number

AS = effective shear area

Set H.1 is required only if NBAY is not zero in card D.

H.2 NRM MN, JNL, JNG, A, T, DL, BL, AS

Notes: MN = member number

JNL = lesser numbered joint

JNG = greater numbered joint

A,T,DL,BL,AS same as in set H.1

Set H.2 is required only if NBAY = 0 in card D.

I NSPR JN, NDIR, S

Notes: JN = joint number where spring support is attached

NDIR= 1 :along x-direction
= 2 :along y-direction
= 3 :torsional spring

S = spring stiffness

Set I is not required if NSPR = 0 in card B.

J.1 1 NLJ, NLM

Notes: NLJ = number of loaded joints

NLM = number of loaded members

J.2 Variable J1, J2, K, FX, FY, FZ:

Notes: J1 = first joint in sequence

J2 = last joint in sequence

K = increment

FX, FY, FZ : Joint forces

J.3 Variable I,J,K,W

Notes: I = first member of sequence

J = last member of sequence

K = member number increment

W = load intensity of uniform load over complete length of member W is positive if it creates clockwise moment about lesser joint number

*For uniform loading on members of orthogonal frame. Not required if NLM = 0 on card J1 or if NBAY = 0 on card D.

J.4 NLM NM, W, PB, XP, PA, XPS, CM, XM

Notes: NM = Number of loaded member

W = uniform load intensity over whole length

PB = concentrated load normal to beam. Positive if tends to rotate beam clockwise about lesser joint number

PA = concentrated load along beam. Positive from lesser joint to greater joint number

XP = distance along beam axis to concentrated load. Measured from lesser joint number.

XPS = 0

CM1 = concentrated moment. Same sign convention as above

XM = distance to CM measured from lesser joint number..

If XPS ≠ 0 PA & PB are specified along global X and Y axes respectively. And XPS = distante along X-axis from lesser joint number to PA & PB

General Comments for Card J

* Member load must be in sequence starting with the lowest member number. Only one card may be used for loads on one member.
* Repeat sets J1 to J4 included, for each load case. That is NLC times.

K NCOM (N, WT(I), I = 1,NLC)

Notes: N = combination sequence number

WT(I)= weight attached to load case I

This set is not required if NCOM = 0 in card B.

A.2 A typical output for a clad multistory frame is given in this section.

NALYSI FOR A TWO BAY CLADDED FRAME
XAMPLE.NO.2 El-Dakhakhni's paper ASCE,January 1977

YOUNG MODULUS	29000.
NUMBER OF JOINTS	75
NUMBER OF MEMBERS	120
NUMBER OF LOAD CASES	1

JOINT INFORMATION
LIST OF RESTRAINED JOINTS

1	0	0	0
2	0	0	0
3	0	0	0

CLADDING PROPERTIES

NO	STOREY	BAY	STIFFNESS
1	1	2	126.400
2	2	2	126.400
3	3	2	126.400
4	4	2	126.400
5	5	2	126.400
6	6	2	126.400
7	7	2	126.400
8	8	2	126.400
9	9	2	126.400
10	10	2	126.400
11	11	2	126.400
12	12	2	126.400
13	13	2	126.400
14	14	2	126.400
15	15	2	126.400
16	16	2	126.400
17	17	2	126.400
18	18	2	126.400
19	19	2	126.400
20	20	2	126.400
21	21	2	126.400
22	22	2	126.400
23	23	2	126.400
24	24	2	126.400

JOINT				X	Y
1	0	0	0	0.00	0.00
2	0	0	0	360.00	0.00
3	0	0	0	720.00	0.00
4	1	0	2	0.00	144.00
5	1	0	3	360.00	144.00
6	1	0	4	720.00	144.00
7	5	0	6	0.00	288.00
8	5	0	7	360.00	288.00
9	5	0	8	720.00	288.00
10	9	0	10	0.00	432.00
11	9	0	11	360.00	432.00
12	9	0	12	720.00	432.00
13	13	0	14	0.00	576.00
14	13	0	15	360.00	576.00
15	13	0	16	720.00	576.00
16	17	0	18	0.00	720.00
17	17	0	19	360.00	720.00
18	17	0	20	720.00	720.00
19	21	0	22	0.00	864.00
20	21	0	23	360.00	864.00
21	21	0	24	720.00	864.00
22	25	0	26	0.00	1008.00
23	25	0	27	360.00	1008.00
24	25	0	28	720.00	1008.00

CONCORDIA UNIVERSITY COMPUTER CENTER

25	29	0	30	0.00	1152.00
26	29	0	31	360.00	1152.00
27	29	0	32	720.00	1152.00
28	33	0	34	0.00	1296.00
29	33	0	35	360.00	1296.00
30	33	0	36	720.00	1296.00
31	37	0	39	0.00	1440.00
32	37	0	39	360.00	1440.00
33	37	0	40	720.00	1440.00
34	41	0	42	0.00	1584.00
35	41	0	43	360.00	1584.00
36	41	0	44	720.00	1584.00
37	45	0	46	0.00	1728.00
38	45	0	47	360.00	1728.00
39	45	0	48	720.00	1728.00
40	49	0	51	0.00	1872.00
41	49	0	51	360.00	1872.00
42	49	0	52	720.00	1872.00
43	53	0	54	0.00	2016.00
44	53	0	55	360.00	2016.00
45	53	0	56	720.00	2016.00
46	57	0	58	0.00	2160.00
47	57	0	59	360.00	2160.00
48	57	0	60	720.00	2160.00
49	61	0	62	0.00	2304.00
50	61	0	63	360.00	2304.00
51	61	0	64	720.00	2304.00
52	65	0	66	0.00	2448.00
53	65	0	67	360.00	2448.00
54	65	0	68	720.00	2448.00
55	69	0	70	0.00	2592.00
56	69	0	71	360.00	2592.00
57	69	0	72	720.00	2592.00
58	73	0	74	0.00	2736.00
59	73	0	75	360.00	2736.00
60	73	0	76	720.00	2736.00
61	77	0	78	0.00	2880.00
62	77	0	79	360.00	2880.00
63	77	0	80	720.00	2880.00
64	81	0	82	0.00	3024.00
65	81	0	83	360.00	3024.00
66	81	0	84	720.00	3024.00
67	85	0	86	0.00	3168.00
68	85	0	87	360.00	3168.00
69	85	0	88	720.00	3168.00
70	89	0	90	0.00	3312.00
71	89	0	91	360.00	3312.00
72	89	0	92	720.00	3312.00
73	93	0	94	0.00	3456.00
74	93	0	95	360.00	3456.00
75	93	0	96	720.00	3456.00

50	50	53	27.900	1060.000	0.000	0.000	0.000
51	51	64	20.000	724.000	0.000	0.000	0.000
62	62	65	20.000	724.000	0.000	0.000	0.000
63	63	65	20.000	724.000	0.000	0.000	0.000
64	64	67	20.000	724.000	0.000	0.000	0.000
65	65	68	20.000	724.000	0.000	0.000	0.000
66	66	69	20.000	724.000	0.000	0.000	0.000
67	67	70	17.700	344.000	0.000	0.000	0.000
68	68	71	11.500	210.000	0.000	0.000	0.000
69	69	72	17.700	344.000	0.000	0.000	0.000
70	70	73	17.700	344.000	0.000	0.000	0.000
71	71	74	11.500	210.000	0.000	0.000	0.000
72	72	75	17.700	344.000	0.000	0.000	0.000
73	4	5	31.800	4470.000	0.000	0.000	0.000
74	5	6	31.900	4470.000	0.000	0.000	0.000
75	7	8	31.900	4470.000	0.000	0.000	0.000
76	8	9	31.800	4470.000	0.000	0.000	0.000
77	10	11	31.800	4470.000	0.000	0.000	0.000
78	11	12	31.900	4470.000	0.000	0.000	0.000
79	13	14	29.100	4000.000	0.000	0.000	0.000
80	14	15	29.100	4000.000	0.000	0.000	0.000
81	16	17	29.100	4000.000	0.000	0.000	0.000
82	17	18	29.100	4000.000	0.000	0.000	0.000
83	19	20	29.100	4000.000	0.000	0.000	0.000
84	20	21	29.100	4000.000	0.000	0.000	0.000
85	22	23	29.100	4000.000	0.000	0.000	0.000
86	23	24	29.100	4000.000	0.000	0.000	0.000
87	25	26	27.700	3270.000	0.000	0.000	0.000
88	26	27	27.700	3270.000	0.000	0.000	0.000
89	28	29	27.700	3270.000	0.000	0.000	0.000
90	29	30	27.700	3270.000	0.000	0.000	0.000
91	31	32	27.700	3270.000	0.000	0.000	0.000
92	32	33	27.700	3270.000	0.000	0.000	0.000
93	34	35	24.800	2930.000	0.000	0.000	0.000
94	35	36	24.800	2830.000	0.000	0.000	0.000
95	37	38	24.800	2930.000	0.000	0.000	0.000
96	38	39	24.900	2930.000	0.000	0.000	0.000
97	40	41	24.700	2370.000	0.000	0.000	0.000
98	41	42	24.700	2370.000	0.000	0.000	0.000
99	43	44	24.700	2370.000	0.000	0.000	0.000
100	44	45	24.700	2370.000	0.000	0.000	0.000
101	46	47	22.400	2100.000	0.000	0.000	0.000
102	47	48	22.400	2100.000	0.000	0.000	0.000
103	49	50	22.400	2100.000	0.000	0.000	0.000
104	50	51	22.400	2100.000	0.000	0.000	0.000
105	52	53	22.400	2100.000	0.000	0.000	0.000
106	53	54	22.400	2100.000	0.000	0.000	0.000
107	55	56	20.000	1820.000	0.000	0.000	0.000
108	56	57	20.000	1820.000	0.000	0.000	0.000
109	58	59	20.000	1820.000	0.000	0.000	0.000
110	59	60	20.000	1820.000	0.000	0.000	0.000
111	61	62	19.000	1540.000	0.000	0.000	0.000
112	62	63	19.000	1540.000	0.000	0.000	0.000
113	64	65	16.200	1140.000	0.000	0.000	0.000
114	65	66	16.200	1140.000	0.000	0.000	0.000
115	67	68	16.200	1140.000	0.000	0.000	0.000
116	68	69	16.200	1140.000	0.000	0.000	0.000
117	70	71	16.200	1140.000	0.000	0.000	0.000
118	71	72	16.200	1140.000	0.000	0.000	0.000
119	73	74	13.000	843.000	0.000	0.000	0.000
120	74	75	13.000	843.000	0.000	0.000	0.000

EMBER INFORMATION

NO	LJT	GJT	AREA	I			
1	1	4	109.000	5450.000	0.000	0.000	0.000
2	2	5	125.000	6610.000	0.000	0.000	0.000
3	3	6	109.000	5450.000	0.000	0.000	0.000
4	4	7	109.000	5451.000	0.000	0.000	0.000
5	5	8	125.000	6610.000	0.000	0.000	0.000
6	6	9	109.000	5450.000	0.000	0.000	0.000
7	7	10	101.000	4910.000	0.000	0.000	0.000
8	9	11	109.000	5450.000	0.000	0.000	0.000
9	9	12	101.000	4910.000	0.000	0.000	0.000
10	10	13	101.000	4910.000	0.000	0.000	0.000
11	11	14	109.000	5450.000	0.000	0.000	0.000
12	12	15	101.000	4910.000	0.000	0.000	0.000
13	13	16	92.300	4400.000	0.000	0.000	0.000
14	14	17	101.000	4910.000	0.000	0.000	0.000
15	15	18	92.300	4400.000	0.000	0.000	0.000
16	15	19	92.300	4400.000	0.000	0.000	0.000
17	17	20	101.000	4910.000	0.000	0.000	0.000
18	18	21	92.300	4400.000	0.000	0.000	0.000
19	19	22	84.400	3910.000	0.000	0.000	0.000
20	20	23	92.300	4400.000	0.000	0.000	0.000
21	21	24	84.400	3910.000	0.000	0.000	0.000
22	22	25	84.400	3910.000	0.000	0.000	0.000
23	23	26	92.300	4400.000	0.000	0.000	0.000
24	24	27	84.400	3910.000	0.000	0.000	0.000
25	25	28	72.300	3230.000	0.000	0.000	0.000
26	26	29	84.400	3910.000	0.000	0.000	0.000
27	27	30	72.300	3230.000	0.000	0.000	0.000
28	28	31	72.300	3230.000	0.000	0.000	0.000
29	29	32	84.400	3910.000	0.000	0.000	0.000
30	30	33	72.300	3230.000	0.000	0.000	0.000
31	31	34	62.100	2670.000	0.000	0.000	0.000
32	32	35	69.700	3060.000	0.000	0.000	0.000
33	33	36	62.100	2670.000	0.000	0.000	0.000
34	34	37	62.100	2670.000	0.000	0.000	0.000
35	35	38	69.700	3060.000	0.000	0.000	0.000
36	36	39	62.100	2670.000	0.000	0.000	0.000
37	37	40	54.100	2270.000	0.000	0.000	0.000
38	38	41	62.100	2670.000	0.000	0.000	0.000
39	39	42	54.100	2270.000	0.000	0.000	0.000
40	40	43	54.100	2270.000	0.000	0.000	0.000
41	41	44	62.100	2670.000	0.000	0.000	0.000
42	42	45	54.100	2270.000	0.000	0.000	0.000
43	43	46	44.100	1790.000	0.000	0.000	0.000
44	44	47	51.700	2150.000	0.000	0.000	0.000
45	45	48	44.100	1790.000	0.000	0.000	0.000
46	46	49	44.100	1790.000	0.000	0.000	0.000
47	47	50	51.700	2150.000	0.000	0.000	0.000
48	48	51	44.100	1790.000	0.000	0.000	0.000
49	49	52	37.300	1480.000	0.000	0.000	0.000
50	50	53	41.400	1670.000	0.000	0.000	0.000
51	51	54	37.300	1480.000	0.000	0.000	0.000
52	52	55	37.300	1480.000	0.000	0.000	0.000
53	53	56	41.400	1670.000	0.000	0.000	0.000
54	54	57	37.300	1480.000	0.000	0.000	0.000
55	55	58	27.000	1060.000	0.000	0.000	0.000
56	56	59	32.700	1270.000	0.000	0.000	0.000
57	57	61	27.000	1060.000	0.000	0.000	0.000
58	58	62	32.700	1270.000	0.000	0.000	0.000
59	59	63	32.700	1270.000	0.000	0.000	0.000

CONCORDIA UNIVERSITY

HALF BAND WIDTH 4

LOAD CASE NO. 1

NO. OF JOINTS LOADED 24
NO. OF MEMBERS LOADED 0
****

JT	FX	FY	MT
4	7.2000	0.0000	0.0000
7	7.2000	0.0000	0.0000
10	7.2000	0.0000	0.0000
13	7.2000	0.0000	0.0000
16	7.2000	0.0000	0.0000
19	7.2000	0.0000	0.0000
22	7.2000	0.0000	0.0000
25	7.2000	0.0000	0.0000
28	7.2000	0.0000	0.0000
31	7.2000	0.0000	0.0000
34	7.2000	0.0000	0.0000
37	7.2000	0.0000	0.0000
40	7.2000	0.0000	0.0000
43	7.2000	0.0000	0.0000
46	7.2000	0.0000	0.0000
49	7.2000	0.0000	0.0000
52	7.2000	0.0000	0.0000
55	7.2000	0.0000	0.0000
58	7.2000	0.0000	0.0000
61	7.2000	0.0000	0.0000
64	7.2000	0.0000	0.0000
67	7.2000	0.0000	0.0000
70	7.2000	0.0000	0.0000
73	7.2000	0.0000	0.0000
TOTAL 24	172.8	0.0	0.0

JOINT DEFLECTIONS

1	0.	0.	0.
2	0.	0.	0.
3	0.	0.	0.
4	1.9490E-01	0.	-1.7712E-03
5	1.9490E-01	0.	-1.5759E-03
6	1.9490E-01	0.	-1.7712E-03
7	5.1718E-01	0.	-2.0097E-03
8	5.1718E-01	0.	-1.7923E-03
9	5.1718E-01	0.	-2.0097E-03
10	8.5900E-01	0.	-2.0107E-03
11	8.5900E-01	0.	-1.7465E-03
12	8.5900E-01	0.	-2.0107E-03

COLUMBIA UNIVERSITY COMPUTER CENTER

14	1.1980E+00	0.	-1.7937E-03
15	1.1980E+00	0.	-2.0305E-03
16	1.5359E+00	0.	-1.3551E-03
17	1.5359E+00	0.	-1.7035E-03
18	1.5359E+00	0.	-1.9553E-03
19	1.9592E+00	0.	-1.4626E-03
20	1.9592E+00	0.	-1.6216E-03
21	1.8582E+00	0.	-1.9506E-03
22	2.1715E+00	0.	-1.7888E-03
23	2.1715E+00	0.	-1.5349E-03
24	2.1715E+00	0.	-1.7888E-03
25	2.4805E+00	0.	-1.8545E-03
26	2.4805E+00	0.	-1.6478E-03
27	2.4805E+00	0.	-1.8545E-03
28	2.7927E+00	0.	-1.7630E-03
29	2.7927E+00	0.	-1.5667E-03
30	2.7927E+00	0.	-1.7630E-03
31	3.0874E+00	0.	-1.5741E-03
32	3.0874E+00	0.	-1.4524E-03
33	3.0874E+00	0.	-1.6741E-03
34	3.3819E+00	0.	-1.5798E-03
35	3.3819E+00	0.	-1.4566E-03
36	3.3819E+00	0.	-1.6788E-03
37	3.6640E+00	0.	-1.5425E-03
38	3.6640E+00	0.	-1.3595E-03
39	3.6640E+00	0.	-1.5425E-03
40	3.9418E+00	0.	-1.5819E-03
41	3.9418E+00	0.	-1.3998E-03
42	3.9418E+00	0.	-1.5819E-03
43	4.2054E+00	0.	-1.4679E-03
44	4.2054E+00	0.	-1.2652E-03
45	4.2054E+00	0.	-1.4679E-03
46	4.4609E+00	0.	-1.3966E-03
47	4.4609E+00	0.	-1.2171E-03
48	4.4609E+00	0.	-1.3966E-03
49	4.6949E+00	0.	-1.2609E-03
50	4.6949E+00	0.	-1.0639E-03
51	4.6949E+00	0.	-1.2609E-03
52	4.9117E+00	0.	-1.1154E-03
53	4.9117E+00	0.	-9.1247E-04
54	4.9117E+00	0.	-1.1154E-03
55	5.1045E+00	0.	-1.0276E-03
56	5.1045E+00	0.	-8.5635E-04
57	5.1045E+00	0.	-1.0276E-03
58	5.2835E+00	0.	-8.5691E-04
59	5.2835E+00	0.	-7.0475E-04
60	5.2835E+00	0.	-8.5691E-04
61	5.4347E+00	0.	-7.6675E-04
62	5.4347E+00	0.	-6.0402E-04
63	5.4347E+00	0.	-7.6675E-04
64	5.5749E+00	0.	-5.4077E-04
65	5.5749E+00	0.	-5.2041E-04
66	5.5749E+00	0.	-6.4073E-04
67	5.6927E+00	0.	-4.9147E-04
68	5.6927E+00	0.	-3.1258E-04
69	5.6927E+00	0.	-4.9147E-04
70	5.7675E+00	0.	-2.3805E-04
71	5.7675E+00	0.	-3.3163E-05
72	5.7675E+00	0.	-2.3805E-04
73	5.8104E+00	0.	-1.4242E-04
74	5.8104E+00	0.	-4.1862E-05
75	5.8104E+00	0.	-1.4242E-04

FORCES AT MEMBER ENDS

NO	LJT	GJT						
1	1	4	0.	4.2737E+01	5.025+E+03	0.	-4. 737E+01	1.1774 +03
2	2	5	0.	6.2570E+01	5.6069E+03	0.	-6. 570E+01	2.4032E+03
3	3	6	0.	4.2737E+01	5.0254E+03	0.	-4. 737E+01	1.1774E+03
4	4	7	0.	3.1732E+01	2.5599E+03	0.	-3. 732E+01	2.0277E+03
5	5	8	0.	5.1240E+01	4.6952E+03	0.	-6. 240E+01	4.1291E+03
6	6	9	0.	3.1732E+01	2.5508E+03	0.	-3. 732E+01	2.0273E+03
7	7	10	0.	2.3959E+01	2.1541E+03	0.	-2. 959E+01	2.1591E+03
8	8	11	0.	5.5276E+01	3.9206E+03	0.	-5. 276E+01	4.0301E+03
9	9	12	0.	2.3959E+01	2.1581E+03	0.	-2. 959E+01	2.1561E+03
10	10	13	0.	2.7474E+01	1.9977E+03	0.	-2. 474E+01	1.3548E+03
11	11	14	0.	5.3405E+01	3.4970E+03	0.	-5. 405E+01	3.7934E+03
12	12	15	0.	2.7474E+01	1.9977E+03	0.	-2. 474E+01	1.3595E+03
13	13	16	0.	2.6125E+01	1.8144E+03	0.	-2. 125E+01	1.3477E+03
14	14	17	0.	4.9036E+01	3.4473E+03	0.	-4. 036E+01	3.3179E+03
15	15	18	0.	2.6125E+01	1.8144E+03	0.	-2. 125E+01	1.3477E+03
16	16	19	0.	2.4418E+01	1.6741E+03	0.	-2. 418E+01	1.3420E+03
17	17	20	0.	4.7218E+01	3.3129E+03	0.	-4. 218E+01	3.4866E+03
18	18	21	0.	2.4419E+01	1.6741E+03	0.	-2. 419E+01	1.3420E+03
19	19	22	0.	2.3022E+01	1.6011E+03	0.	-2. 022E+01	1.7141E+03
20	20	23	0.	4.3958E+01	3.0916E+03	0.	-4. 958E+01	3.2743E+03
21	21	24	0.	2.3022E+01	1.6011E+03	0.	-2. 022E+01	1.7141E+03
22	22	25	0.	2.1271E+01	1.5933E+03	0.	-2. 271E+01	1.4738E+03
23	23	26	0.	4.0400E+01	3.0341E+03	0.	-4. 400E+01	2.9411E+03
24	24	27	0.	2.1271E+01	1.5933E+03	0.	-2. 271E+01	1.4738E+03
25	25	28	0.	1.9471E+01	1.3426E+03	0.	-1. 471E+01	1.4615E+03
26	26	29	0.	3.6797E+01	2.5855E+03	0.	-3. 797E+01	2.7133E+03
27	27	30	0.	1.9471E+01	1.3426E+03	0.	-1. 471E+01	1.4615E+03
28	28	31	0.	1.7769E+01	1.2215E+03	0.	-1. 776E+01	1.3371E+03
29	29	32	0.	3.5216E+01	2.4454E+03	0.	-3. 216E+01	2.6252E+03
30	30	33	0.	1.7769E+01	1.2215E+03	0.	-1. 769E+01	1.3371E+03
31	31	34	0.	1.6524E+01	1.1922E+03	0.	-1. 524E+01	1.1872E+03
32	32	35	0.	3.0526E+01	2.2002E+03	0.	-3. 526E+01	2.1355E+03
33	33	36	0.	1.6524E+01	1.1922E+03	0.	-1. 524E+01	1.1872E+03
34	34	37	0.	1.4716E+01	1.0078E+03	0.	-1. 716E+01	1.1114E+03
35	35	38	0.	2.8509E+01	1.9918E+03	0.	-2. 509E+01	2.2135E+03
36	36	39	0.	1.4716E+01	1.0078E+03	0.	-1. 716E+01	1.1114E+03
37	37	40	0.	1.3212E+01	9.5103E+02	0.	-1. 212E+01	9.5151E+02
38	38	41	0.	2.4865E+01	1.8071E+03	0.	-2. 865E+01	1.7734E+03
39	39	42	0.	1.3212E+01	9.5103E+02	0.	-1. 212E+01	9.5151E+02
40	40	43	0.	1.1658E+01	7.8723E+02	0.	-1. 659E+01	9.9151E+02
41	41	44	0.	2.2558E+01	1.5573E+03	0.	-2. 559E+01	1.6912E+03
42	42	45	0.	1.1658E+01	7.8723E+02	0.	-1. 659E+01	8.9151E+02
43	43	46	0.	1.0254E+01	7.1259E+02	0.	-1. 254E+01	7.9400E+02
44	44	47	0.	1.9210E+01	1.3623E+03	0.	-1. 210E+01	1.4039E+03
45	45	48	0.	1.0254E+01	7.1259E+02	0.	-1. 254E+01	7.9400E+02
46	46	49	0.	8.3129E+00	5.9281E+02	0.	-8. 129E+00	6.9665E+02
47	47	50	0.	1.7389E+01	1.1882E+03	0.	-1. 389E+01	1.3159E+03
48	48	51	0.	8.9129E+00	5.9281E+02	0.	-8. 129E+00	6.9665E+02
49	49	52	0.	7.8872E+00	5.2451E+02	0.	-7. 872E+00	6.1125E+02
50	50	53	0.	1.4420E+01	9.8530E+02	0.	-1. 420E+01	1.0912E+03
51	51	54	0.	7.8872E+00	5.2451E+02	0.	-7. 872E+00	6.1125E+02
52	52	55	0.	6.6439E+00	4.5221E+02	0.	-6. 439E+00	5.3451E+02
53	53	56	0.	1.2740E+01	8.3964E+02	0.	-1. 740E+01	1.0819E+03
54	54	57	0.	6.6439E+00	4.5221E+02	0.	-6. 439E+00	5.3451E+02
55	55	58	0.	5.3536E+00	3.4923E+02	0.	-5. 596E+00	4.2256E+02
56	56	59	0.	8.9554E+00	6.7095E+02	0.	-9. 554E+00	7.4831E+02
57	57	60	0.	5.3536E+00	3.4923E+02	0.	-5. 596E+00	4.2256E+02
58	58	61	0.	4.2379E+00	2.8610E+02	0.	-4. 379E+00	3.2416E+02
59	59	62	0.	8.0205E+00	5.9046E+02	0.	-8. 205E+00	6.3239E+02
60	60	63	0.	4.2379E+00	2.8610E+02	0.	-4. 379E+00	3.2416E+02
61	61	64	0.	3.2778E+00	2.2641E+02	0.	-3. 778E+00	2.5133E+02

CONCORDIA UNIVERSITY LIBRARIES

62	62	65	0.	5.0005E+00	3.4794E+02	1.	-5.0057E+00	3.7222E+02
63	63	66	0.	3.0379E+00	2.0618E+02	1.	-3.3795E+00	2.3127E+02
64	64	67	0.	1.9703E+00	1.1437E+02	0.	-1.7097E+00	1.5944E+02
65	65	69	1.	4.0341E+00	2.6015E+02	1.	-4.3415E+00	3.2176E+02
66	66	69	0.	1.9703E+00	1.1437E+02	0.	-1.7097E+00	1.5944E+02
67	67	71	1.	1.1436E+00	5.3595E+01	0.	-1.4057E+00	3.5804E+01
68	68	71	0.	1.3797E+00	8.9556E+01	1.	-1.7875E+00	1.0837E+02
69	69	72	0.	1.1496E+00	6.8644E+01	1.	-1.4965E+00	9.5888E+01
70	70	73	1.	4.7615E-01	2.4194E+01	1.	-4.6157E-01	4.4372E+01
71	71	74	0.	8.2831E-01	5.7935E+01	1.	-8.4914E-01	6.1424E+01
72	72	75	0.	4.7615E-01	2.4194E+01	1.	-4.6157E-01	4.4372E+01
73	4	5	0.	-2.0105E+01	-3.6882E+03	0.	2.1051E+01	-3.5497E+03
74	5	6	0.	-2.0105E+01	-3.5497E+03	1.	2.1051E+01	-3.6882E+03
75	7	8	0.	-2.2817E+01	-4.1854E+03	1.	2.3817E+01	-4.0238E+03
76	8	9	0.	-2.2817E+01	-4.0238E+03	1.	2.3817E+01	-4.1854E+03
77	10	11	0.	-2.2548E+01	-4.1534E+03	0.	2.5497E+01	-3.9675E+03
78	11	12	0.	-2.2548E+01	-3.9675E+03	1.	2.5497E+01	-4.1534E+03
79	13	14	0.	-2.0537E+01	-3.7730E+03	1.	2.5375E+01	-3.9234E+03
80	14	15	0.	-2.0537E+01	-3.6204E+03	0.	2.5375E+01	-3.7730E+03
81	16	17	0.	-1.9681E+01	-3.6218E+03	0.	1.6815E+01	-3.4234E+03
82	17	18	0.	-1.7691E+01	-3.4634E+03	1.	1.5815E+01	-3.5219E+03
83	19	20	0.	-1.9701E+01	-3.4431E+03	0.	1.7015E+01	-3.2891E+03
84	20	21	0.	-1.9701E+01	-3.2891E+03	1.	1.7015E+01	-3.4431E+03
85	22	23	0.	-1.7871E+01	-3.2973E+03	0.	1.8715E+01	-3.1352E+03
86	23	24	0.	-1.7871E+01	-3.1352E+03	1.	1.8715E+01	-3.2973E+03
87	25	26	0.	-1.5376E+01	-2.9222E+03	1.	1.3765E+01	-2.7133E+03
88	26	27	0.	-1.5376E+01	-2.7133E+03	0.	1.3765E+01	-2.9222E+03
89	28	29	0.	-1.4618E+01	-2.6830E+03	0.	1.6185E+01	-2.5795E+03
90	29	30	0.	-1.4618E+01	-2.5795E+03	1.	1.6195E+01	-2.6830E+03
91	31	32	0.	-1.3726E+01	-2.5294E+03	1.	1.7295E+01	-2.4127E+03
92	32	33	0.	-1.3726E+01	-2.4127E+03	0.	1.7285E+01	-2.5294E+03
93	34	35	0.	-1.1913E+01	-2.1951E+03	0.	1.9135E+01	-2.0937E+03
94	35	36	0.	-1.1913E+01	-2.0937E+03	0.	1.9135E+01	-2.1951E+03
95	37	39	1.	-1.1174E+01	-2.0624E+03	1.	1.1745E+01	-1.9613E+03
96	38	39	0.	-1.1174E+01	-1.9613E+03	1.	1.1745E+01	-2.0624E+03
97	40	41	0.	-9.4558E+00	-1.7387E+03	0.	9.5585E+00	-1.8651E+03
98	41	42	0.	-9.4558E+00	-1.6651E+03	0.	9.5685E+00	-1.7347E+03
99	43	44	0.	-9.6967E+00	-1.6041E+03	0.	9.9675E+00	-1.7207E+03
100	44	45	0.	-9.6967E+00	-1.5267E+03	0.	9.9675E+00	-1.8041E+03
101	46	47	0.	-7.3692E+00	-1.3569E+03	0.	7.6925E+00	-1.2961E+03
102	47	48	0.	-7.3692E+00	-1.2961E+03	0.	7.6925E+00	-1.3569E+03
103	49	50	0.	-6.5714E+00	-1.2152E+03	0.	6.7145E+00	-1.1595E+03
104	50	51	0.	-6.5714E+00	-1.1595E+03	0.	6.7145E+00	-1.2152E+03
105	52	53	0.	-5.7174E+00	-1.0635E+03	0.	5.1745E+00	-1.0448E+03
106	53	54	0.	-5.7174E+00	-9.0480E+02	0.	5.1745E+00	-1.0635E+03
107	55	56	0.	-4.6035E+00	-8.5375E+02	0.	4.0395E+00	-9.0352E+02
108	56	57	0.	-4.6035E+00	-9.0352E+02	0.	4.0395E+00	-8.5375E+02
109	58	59	0.	-3.8140E+00	-7.0965E+02	0.	3.1405E+00	-6.6439E+02
110	59	60	0.	-3.8140E+00	-6.6439E+02	0.	3.1405E+00	-7.0965E+02
111	61	62	0.	-2.8342E+00	-5.3034E+02	0.	2.3425E+00	-4.8997E+02
112	62	63	0.	-2.8342E+00	-4.8997E+02	0.	2.3425E+00	-5.3034E+02
113	64	65	0.	-1.9334E+00	-3.4564E+02	0.	1.3845E+00	-3.1613E+02
114	65	66	0.	-1.9334E+00	-3.1613E+02	0.	1.3845E+00	-3.4564E+02
115	67	69	0.	-1.2313E+00	-2.3999E+02	0.	1.3135E+00	-2.0515E+02
116	68	69	0.	-1.2313E+00	-2.0515E+02	0.	1.3135E+00	-2.3999E+02
117	70	71	0.	-5.6815E-01	-1.2109E+02	0.	5.8155E-01	-8.3433E+01
118	71	72	0.	-5.6815E-01	-8.3433E+01	0.	5.8155E-01	-1.2109E+02
119	73	74	0.	-2.0857E-01	-4.4372E+01	0.	2.3575E-01	-1.3714E+02
120	74	75	0.	-2.0857E-01	-1.3714E+01	0.	2.4575E-01	-4.4372E+01

SHEAR FORCES IN CLADDINGS

1	2.4636E+01	-2.4636E+01	-9.8544E+00	9.8544E+00
2	4.0736E+01	-4.0736E+01	-1.6294E+01	1.6294E+01
3	4.3206E+01	-4.3206E+01	-1.7282E+01	1.7282E+01
4	4.2846E+01	-4.2846E+01	-1.7138E+01	1.7138E+01
5	4.2713E+01	-4.2713E+01	-1.7085E+01	1.7085E+01
6	4.0746E+01	-4.0746E+01	-1.6298E+01	1.6298E+01
7	3.9598E+01	-3.9598E+01	-1.5839E+01	1.5839E+01
8	3.9058E+01	-3.9058E+01	-1.5623E+01	1.5623E+01
9	3.9461E+01	-3.9461E+01	-1.5784E+01	1.5784E+01
10	3.7247E+01	-3.7247E+01	-1.4899E+01	1.4899E+01
11	3.7226E+01	-3.7226E+01	-1.4891E+01	1.4891E+01
12	3.5659E+01	-3.5658E+01	-1.4263E+01	1.4263E+01
13	3.5111E+01	-3.5111E+01	-1.4044E+01	1.4044E+01
14	3.3326E+01	-3.3326E+01	-1.3330E+01	1.3330E+01
15	3.2282E+01	-3.2282E+01	-1.2913E+01	1.2913E+01
16	2.9585E+01	-2.9585E+01	-1.1834E+01	1.1834E+01
17	2.7406E+01	-2.7406E+01	-1.0962E+01	1.0962E+01
18	2.4372E+01	-2.4372E+01	-9.7487E+00	9.7487E+00
19	2.2625E+01	-2.2625E+01	-9.0502E+00	9.0502E+00
20	1.9104E+01	-1.9104E+01	-7.6415E+00	7.6415E+00
21	1.7724E+01	-1.7724E+01	-7.0896E+00	7.0896E+00
22	1.3624E+01	-1.3624E+01	-5.4496E+00	5.4496E+00
23	1.0722E+01	-1.0722E+01	-4.2889E+00	4.2889E+00
24	5.4188E+00	-5.4188E+00	-2.1675E+00	2.1675E+00

TABLE 1. GAGE NUMBER AND THICKNESS OF SHEET STEEL

Gage Number	Thickness in inch	
	Galvanized	Uncoated
8	0.168	0.1644
9	0.1532	0.1495
10	0.1382	0.1345
11	0.1233	0.1196
12	0.1084	0.1046
13	0.0934	0.0897
14	0.0785	0.0747
15	0.0710	0.0673
16	0.0635	0.0598
17	0.0575	0.0538
18	0.0516	0.0478
19	0.0456	0.0418
20	0.0396	0.0359
21	0.0366	0.0329
22	0.0336	0.0299
23	0.0306	0.0269
24	0.0276	0.0239
25	0.0247	0.0209
26	0.0217	0.0179
27	0.0202	0.0164
28	0.0187	0.0149
29	0.0172	0.0135
30	0.0157	0.0120

TABLE 3.1 - COMPARISON OF RESULTS

Specimen Identification	Predicted values of shear deflection Δ, in inches		Measured value of shear deflection Δ, in inches	$\frac{\Delta_{(test)}}{\Delta_{(calc)}}$
	Proposed Method	Finite Element Method		
57-2	0.061	-	0.060	1.00
58-5	0.145	-	0.157	1.08
A_1	0.011	0.010	0.010	0.91
A_2	0.029	0.038	0.035	1.18
C_1	0.0039	0.0046	0.0033	0.86
C_2	0.0135	0.0140	0.0137	1.02

TABLE 4.1 - Results for Welded Diaphragms

No.	Specimen Identification	Name of Investigator	Diaphragm Size (a x b) in feet	Calculated Value of N_u in lbs/ft.	Measured Value of N_u in lbs/ft.	$\frac{N_{u(test)}}{N_{u(calc)}}$
1	3	Westeel-Rosco, Ltd. [41]	36 x 8	1048	963	0.92
2	1-C	Nilson [11]	30 x 12	3053	3230	1.06
3	59-4	"	30 x 15	2929	3190	1.08
4	58-6	"	30 x 30	2821	2670	0.91
5	57-2	"	30 x 12	3053	3220	1.05
6	58-5	"	30 x 30	2821	2670	0.94
7	59-2	"	30 x 22	2540	2380	0.93
8	58-4	"	30 x 30	2821	2290	0.81
9	58-8	"	30 x 22	3004	2910	0.96
10	58-2a	"	30 x 30	2821	2730	0.96
11	9	"	30 x 12	2565	2080	0.81
12	58-2	"	30 x 30	2821	2130	0.76
13	59-6	"	12 x 10	3481	3580	1.02
14	59-10	"	12 x 10	3481	3330	0.95
15	59-7	"	12 x 10	2925	2320	0.79
16	59-3	"	30 x 15	1717	1650	0.96
17	59-1	"	30 x 30	1506	1490	0.99
18	59-12	"	12 x 10	2225	2630	1.18
19	5	"	30 x 12	-170	1460	1.24

TABLE 4.2 - Results for Screw Connected Diaphragms

No.	Specimen Identification	Name of Investigator	Diaphragm Size (a x b) in feet	Calculated Value of N_u in lbs/ft.	Measured Value of N_u in lbs/ft.	$\frac{N_{u(test)}}{N_{u(calc)}}$
1	A1	Davies [23]	12.80 x 12.40	2330	-	-
2	A2	"	"	2177	2330	1.07
3	B1	"	"	2114	2056	0.97
4	B2	"	"	2015	1371	0.65
5	B3	"	"	1705	1097	0.64
6	C1	"	23.62 x 12.13	3496	-	-
7	C2	"	"	2803	-	-
8	6AP	Luttrell [6]	10 x 12	297	307	1.03
9	6A-P2	"	10 x 12	297	341	1.14
10	3C-11	"	2 x 2.33	833	815	0.97
11	SC-1	"	10 x 12	341	417	1.21
12	4P	"	10 x 12	386	467	1.20

TABLE 4.3 - Comparison of Results for Seam Forces[a]

No.	Specimen Identification	Force in the Seam Fasteners in lbs. Proposed Method	Davies' Approach	Finite Element Method
1	A1	374	365	369
2	A2	401	396	396
3	B1	414	365	383
4	B2	431	396	409
5	B3	427	401	414
6	C1	205	178	196
7	C2	240	209	227

[a] Seam forces are calculated for an applied load of 4450 lbs.

TABLE 5.1- Predicted and Measured Values of Critical Loads (N_{cr})

Specimen Identification	Type of Profile	Investigator	Size of specimen in inches a	b	Panel Stiffness in lb.in. D_y	D_x	D_{xy}	N_{cr}(calc) in lbs/in.	N_{cr}(test) in lbs/in.	$\frac{N_{cr}(test)}{N_{cr}(calc)}$
1	Type A		30	30	2070	2.92	6.05	18.2	21.0	1.15
2	Type B		30	30	3580	2.65	6.68	26.2	27.5	1.05
3	Type A	Easley [29]	30	30	5150	2.38	7.42	33.5	35.0	1.04
4	Type A		26	34	2750	2.90	6.12	14.69	17.5	1.19
5	Type A		26	34	5260	2.40	7.40	27.50	26.5	0.96
6	Type A		34	26	2600	2.83	6.26	28.36	30.0	1.06
7	Type A		35	26	3090	2.73	6.47	29.41	32.0	1.08
8	Type A		34	26	3580	2.65	6.67	34.17	35.0	1.02
9	Type B		180	163	135000	14.9	31.3	20.3	21.5	1.06
10	Type B		180	163	153000	21.8	45.9	25.0	25.0	1.00
11	Type B	Easley and McFarland [28]	108	163	135000	14.9	31.3	22.5	22.2	1.01
12	Type B		108	163	153000	21.8	45.9	25.1	25.0	1.00
13	Type C		96	115	23400	33.4	59.0	14.9	14.5	0.97
14	Type C		96	115	26700	49.5	87.4	17.0	18.0	1.06
15	Type C		96	115	31200	106.2	198.2	26.0	32.0	1.23

TABLE 5.2 - Comparison of Results for Critical Loads

Specimen Number	Diaphragm size in inches	Critical Load from Easley's Method in lbs/inch	Critical Load from Proposed Method in lbs/inch	Critical Load from test in lbs/inch
1	30 x 30	16.0	18.2	21.0
2	30 x 30	23.6	26.2	27.5
3	30 x 30	31.1	33.5	25.0
4	26 x 34	13.3	14.7	17.5
5	26 x 34	23.9	27.5	26.5
6	34 x 26	25.1	28.4	30.0
7	34 x 26	28.4	29.4	32.0
8	34 x 26	31.4	34.2	35.0
9	180 x 163	18.7	20.3	21.5
10	180 x 163	22.6	25.0	25.0
11	180 x 163	18.7	22.5	22.2
12	108 x 163	22.6	25.0	25.0
13	96 x 115	12.4	14.9	14.5
14	96 x 115	15.0	17.0	18.0
15	96 x 115	20.4	26.0	32.0

TABLE 6.1

Variation of Maximum Lateral Deflection and Shear in Cladding
(15 Story Frame)

No	Shear Stiffness of Cladding S in Kip/inch	Shear Stiffness ratio r*	$\frac{1}{1+r}$	Δ_c inch	$\frac{\Delta_c}{\Delta_b}$	V_c in Kips	$\frac{V_c}{V_t}$
1	0 (bare frame)	0	1	5.86	-	-	-
2	14.7	0.10	0.91	5.29	0.90	6.30	0.08
3	36.7	0.25	0.80	4.67	0.80	13.95	0.17
4	86.8	0.59	0.63	3.81	0.65	26.66	0.28
5	126.4	0.86	0.54	3.38	0.58	34.54	0.34
6	173.5	1.18	0.46	3.02	0.52	41.96	0.42
7	275.0	1.87	0.35	2.52	0.43	53.20	0.53

* $r = \frac{S}{\Sigma \frac{12 EI_c}{L_c^3}}$ where S = shear stiffness of cladding

I_c and L_c are the moment of inertia and height of the column around 1/6 of the frame height [10]; E = Youngs modulus of the material. $\Sigma \frac{12 EI_c}{L_c^3}$ = 147 Kip/inch;

Δ_c = maximum deflection of clad frame

Δ_b = maximum deflection of bare frame = 5.86 inch;

V_c = maximum shear force in cladding and V_T = total story shear.

V_t = story shear

TABLE 6.2

Variation of Max. Lateral Deflection and Shear in Cladding
(24 Story Frame)

No.	Shear Stiffness of Cladding S in Kip/inch	Shear Stiffness ratio r	$\frac{1}{(1+r)}$	Δ_c inch	$\frac{\Delta_c}{\Delta_b}$	V_c in kips	$\frac{V_c}{V_t}$
1	0	0.0	1.00	11.14	1.00	0	0
2	25.32	0.10	0.91	9.93	0.89	10.98	0.08
3	63.30	0.25	0.80	8.79	0.79	24.14	0.17
4	86.75	0.34	0.75	8.29	0.74	31.47	0.21
5	126.4	0.50	0.67	7.63	0.68	41.55	0.27
6	173.5	0.69	0.59	7.06	0.63	51.24	0.34
7	252.8	1.00	0.50	6.39	0.57	63.85	0.40
8	347.0	1.37	0.42	5.86	0.53	76.05	0.48
9	375.0	1.48	0.40	5.73	0.51	79.05	0.50

$\Sigma \frac{12\ EI_c}{L_c^3}$ = 253.16 kip/inch calculated @ 1/6 of the frame height

TABLE 6.3

Variation of Max. Lateral Deflection and Shear in Cladding
(26 Story Frame)

No.	Shear Stiffness of Cladding S in Kip/inch	Shear Stiffness ratio r	$\frac{1}{(1+r)}$	Δ_c inch	$\frac{\Delta_c}{\Delta_b}$	V_c in kips	$\frac{V_c}{V_t}$
1	0	0	1	10.08	1.0	0	0.0
2	41.5	0.11	0.87	8.47	0.84	15.8	0.09
3	83.0	0.23	0.81	7.56	0.75	28.5	0.16
4	166.0	0.46	0.69	6.49	0.64	47.7	0.28
5	249.0	0.68	0.59	5.85	0.58	61.3	0.36
6	332.0	0.91	0.52	5.42	0.54	71.3	0.42
7	376.4	1.03	0.49	5.24	0.52	75.6	0.44
8	415.0	1.14	0.47	5.11	0.51	79.4	0.45
9	500.0	1.37	0.42	4.86	0.48	86.9	0.48
10	551.0	1.51	0.39	4.73	0.46	90.7	0.51
11	728.0	2.00	0.33	4.41	0.44	101.0	0.57

$$\Sigma \frac{12\, EI_c}{L^3} = 364 \text{ kip/inch calculated @ 1/6 frame height}$$

TABLE 6.4

Variation of Max. Bending Moments in Beams and Columns.
(15 Story Frame)

No.	Shear Stiffness of Cladding S in Kip/inch	Shear Stiffness ratio r	Max. Moment in Beams kip/inch	$\frac{M_c}{M_b}$	Max. Moment in Columns kip/inch	$\frac{M'_c}{M'_b}$
1	0	0	3357	1.00	4779	1.00
2	14.7	0.10	3155	0.94	4605	0.96
3	36.7	0.25	2923	0.87	4373	0.92
4	86.8	0.59	2495	0.74	3941	0.82
5	126.4	0.86	2241	0.67	3664	0.77
6	173.5	1.18	2004	0.60	3389	0.71
7	275.0	1.87	1643	0.49	2931	0.61

Note: M_c = Max. moment in beams of clad frame

M'_c = Max. moment in columns of clad frame

M_b = Max. moment in beams of bare frame

M'_b = Max. moment in columns of clad frame

TABLE 6.5

Variation of Max. Bending Moments in Beams and Columns
(24 Story Frame)

No.	Shear Stiffness of Cladding S in Kip/inch	Shear Stiffness ratio r	Max. Moment in Beams kip/inch	$\frac{M_c}{M_b}$	Max. Moment in Columns kip/inch	$\frac{M'_c}{M'_b}$
1	0	0	5725	1.00	8018	1.00
2	25.32	0.10	5378	0.94	7692	0.96
3	63.30	0.25	4936	0.86	7261	0.91
4	86.75	0.34	4702	0.82	7023	0.88
5	126.40	0.50	4361	0.76	6661	0.83
6	173.50	0.69	4024	0.70	6285	0.78
7	252.8	1.00	3580	0.63	5753	0.72
8	347.0	1.37	3188	0.56	5240	0.65
9	375.0	1.48	3092	0.54	5107	0.64

TABLE 6.6

Variation of Max. Bending Moments in Beams and Columns
(26 Story Frame)

No.	Shear Stiffness of Cladding S in kip/inch	Shear Stiffness ratio r	Max. Moment in Beams kip/inch	$\frac{M_c}{M_b}$	Max. Moment in Columns kip/inch	$\frac{M'_c}{M'_b}$
1	0	0	3983	1.00	7014	1.00
2	41.5	0.11	3652	0.92	6634	0.95
3	83.0	0.23	3378	0.85	6306	0.90
4	166.0	0.46	2952	0.74	5759	0.82
5	249.0	0.68	2636	0.66	5318	0.76
6	332.0	0.91	2393	0.60	4951	0.71
7	376.4	1.03	2285	0.57	4778	0.68
8	415.0	1.14	2200	0.55	4639	0.66
9	500.0	1.37	2040	0.51	4364	0.62
10	551.0	1.51	1958	0.49	4216	0.60
11	728.0	2.00	1732	0.43	3779	0.54

TABLE 6.7

Variation of Column Axial Forces
(15 Story Frame)

No.	Shear Stiffness of Cladding S in kip/inch	Shear Stiffness ratio r	Windward Side		Leeward Side	
			Axial force in kips	$\frac{F_c}{F_b}$	Axial force in kips	$\frac{F'_c}{F'_b}$
1	0	0	156	1.0	156	1.0
2	14.7	0.10	145	0.93	168	1.08
3	36.7	0.25	131	0.84	181	1.16
4	86.8	0.59	111	0.71	201	1.29
5	126.4	0.86	100	0.64	211	1.35
6	173.5	1.18	91	0.58	220	1.41
7	275.0	1.87	78	0.50	233	1.49

Note: F_c, F'_c = Max. axial force in windward and leeward columns of clad frame

F_b, F'_b = Max. axial force in windward and leeward columns of bare frame.

TABLE 6.8

Variation of Max. Axial Forces in Columns
(24 Story Frame)

No.	Shear Stiffness of Cladding S in kip/inch	Shear Stiffness ratio r	Windward Side		Leeward Side	
			Axial force in kips	$\frac{F_c}{F_b}$	Axial force in kips	$\frac{F_c}{F_b}$
1	0	0	404	1.00	404	1.00
2	25.32	0.10	375	0.93	433	1.07
3	63.30	0.25	344	0.85	464	1.15
4	86.75	0.34	328	0.81	479	1.19
5	126.4	0.50	308	0.76	499	1.24
6	173.5	0.69	289	0.72	517	1.28
7	252.8	1.00	266	0.66	541	1.34
8	347.0	1.37	246	0.61	559	1.38
9	375.0	1.48	242	0.60	564	1.40

TABLE 6.9

Variation of Axial Forces in Columns
(26 Story Frame)

No.	Shear Stiffness of Cladding S in kip/inch	Shear Stiffness ratio r	Exterior Column		Interior Column	
			Axial force in kips	$\frac{F_c}{F_b}$	Axial force in kips	$\frac{F_c}{F_b}$
1	0.0	0.0	303	1.00	20	1.00
2	41.5	0.11	274	0.90	107	5.48
3	83.0	0.23	254	0.84	167	8.56
4	166.0	0.46	227	0.75	247	12.66
5	249.0	0.68	209	0.69	300	15.38
6	332.0	0.91	197	0.65	337	17.30
7	376.4	1.03	192	0.63	354	18.2
8	415.0	1.14	187	0.62	366	18.8
9	500.0	1.37	179	0.59	389	20.0
10	551.0	1.50	176	0.58	400	20.5
11	728.0	2.00	166	0.54	430	22.0

TABLE 6.10

Comparison Between the Proposed Method and

Miller's Approach for Clad Frame

	Bare Frame		Clad Frame*	
	Proposed Method	Miller's Approach	Proposed Method	Miller's Approach
Axial ** Force	19.98 kips	19.98 kips	264.11 kips	272 kips
Bending ** Moment	328-334 ft.kips	324-328 ft.kips	167-168 ft.kips	166-169 ft.kips
Max. Lateral ** Deflection	10.08 inch	10.09 inch	5.25 inch	5.28 inch

* cladding stiffness = 376.4 kips per inch

** values are for the interior column between 3rd and 4th story level

TABLE 6.11

Lateral Deflection and Shear Force in Cladding
(Shear Stiffness of Cladding - 126.4 kip/inch)

	24 Story Frame		15 Story Frame	
Story Level	Lateral Deflection in inches	Shear in Cladding in kips	Lateral Deflection in inches	Shear in Cladding in kips
1	0.19	24.6	0.17	21.5
2	0.52	40.7	0.45	35.2
3	0.86	43.2	0.73	35.4
4	1.19	42.8	1.00	35.1
5	1.54	42.7	1.27	33.3
6	1.86	40.7	1.53	32.3
7	2.17	39.6	1.76	29.6
8	2.48	39.1	1.98	27.4
9	2.79	39.5	2.17	24.4
10	3.08	37.2	2.35	22.6
11	3.38	37.2	2.50	19.1
12	3.66	35.7	2.64	17.7
13	3.94	35.1	2.75	13.6
14	4.20	33.3	2.83	10.7
15	4.46	32.3	2.87	5.4
16	4.69	29.6		
17	4.91	27.4		
18	5.10	24.4		
19	5.28	22.6		
20	5.43	19.1		
21	5.57	17.7		
22	5.68	13.6		
23	5.76	10.7		
24	5.81	5.4		

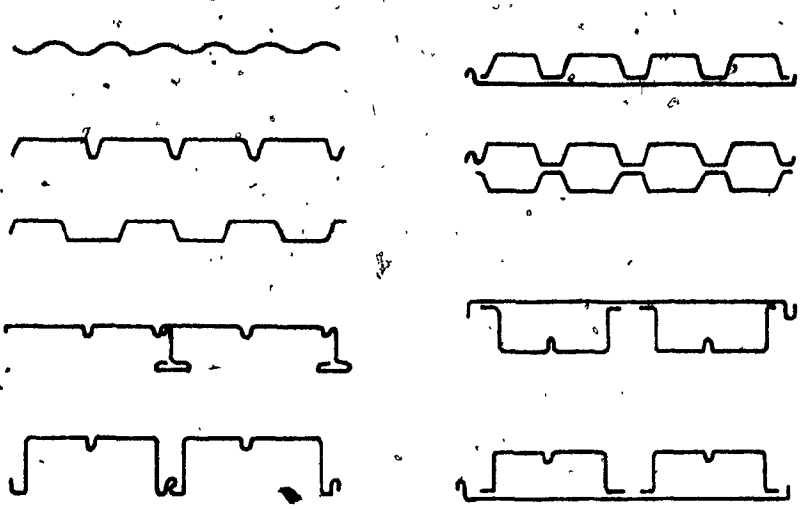

Fig. 1.1 Types of Light Gage Steel Panels.

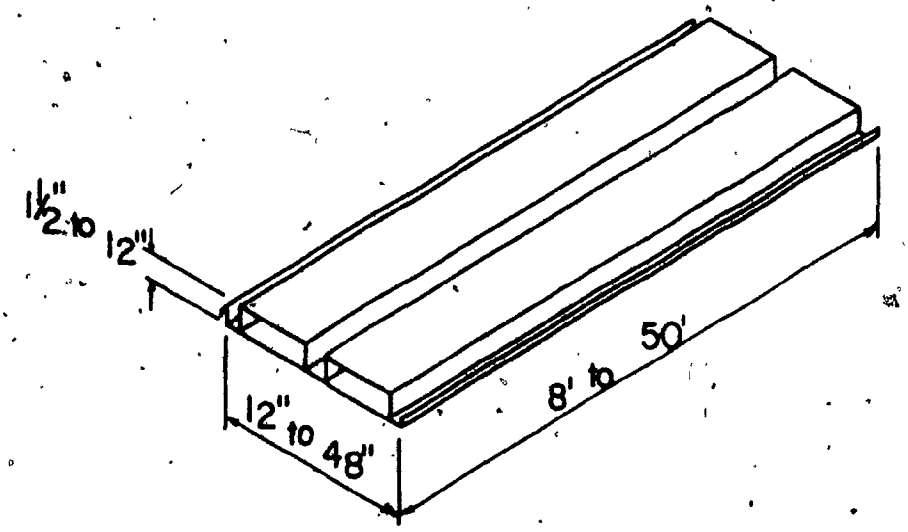

Fig. 1.2. Nominal Dimensions of Panels.

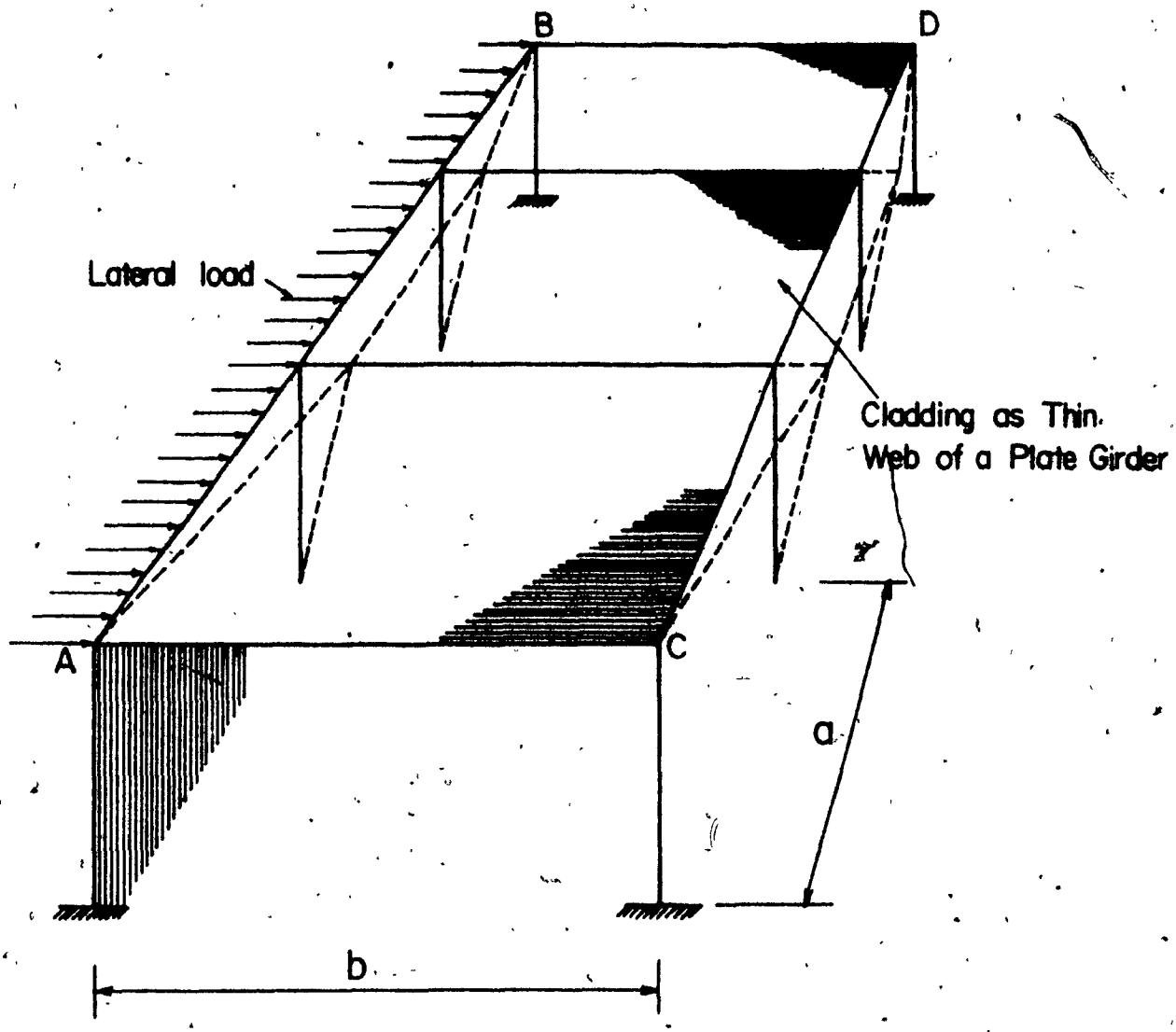

Fig.1.3. Lateral Load in a Typical Building.

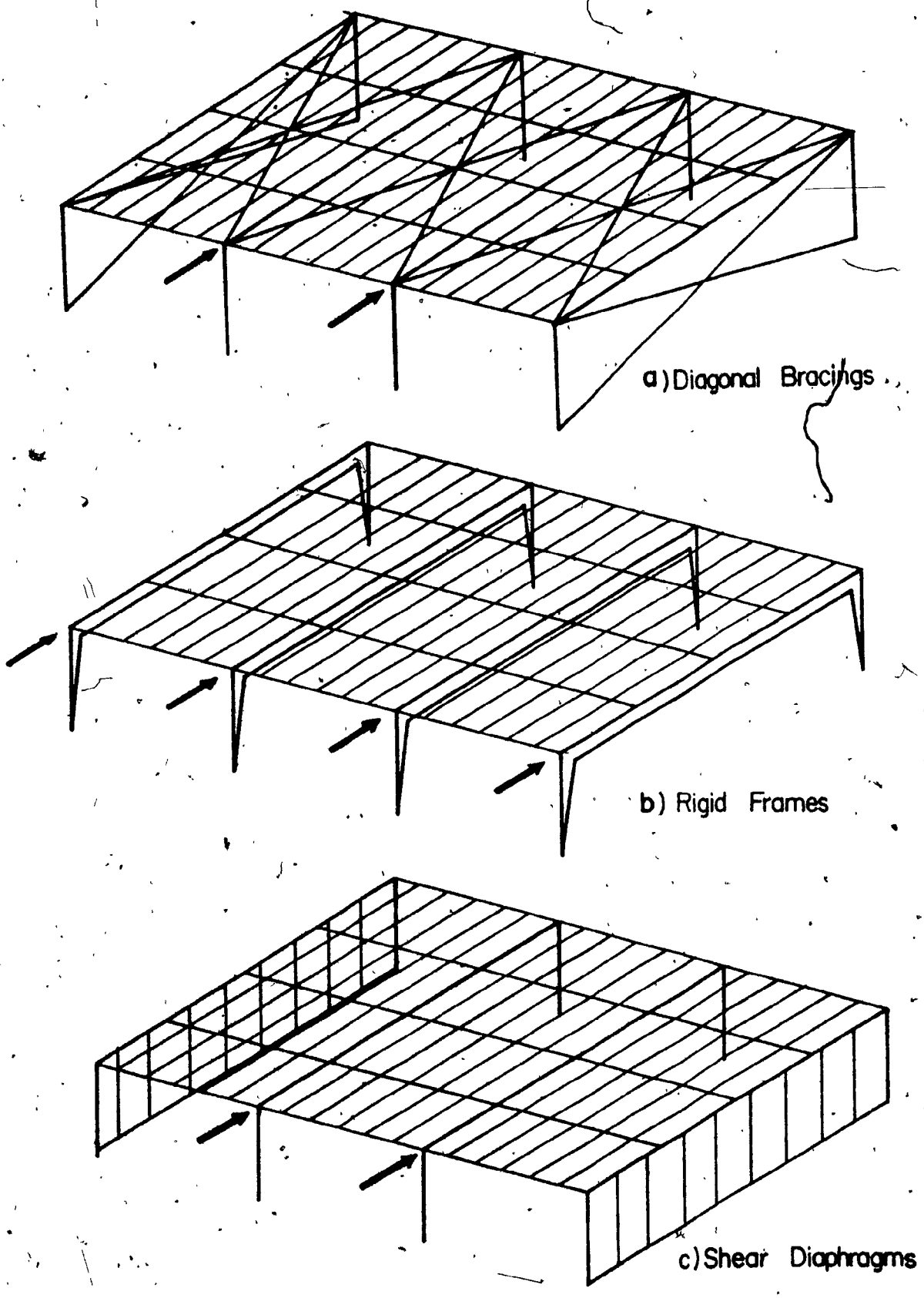

Fig. I.4. Design Methods for Resisting Lateral Forces.

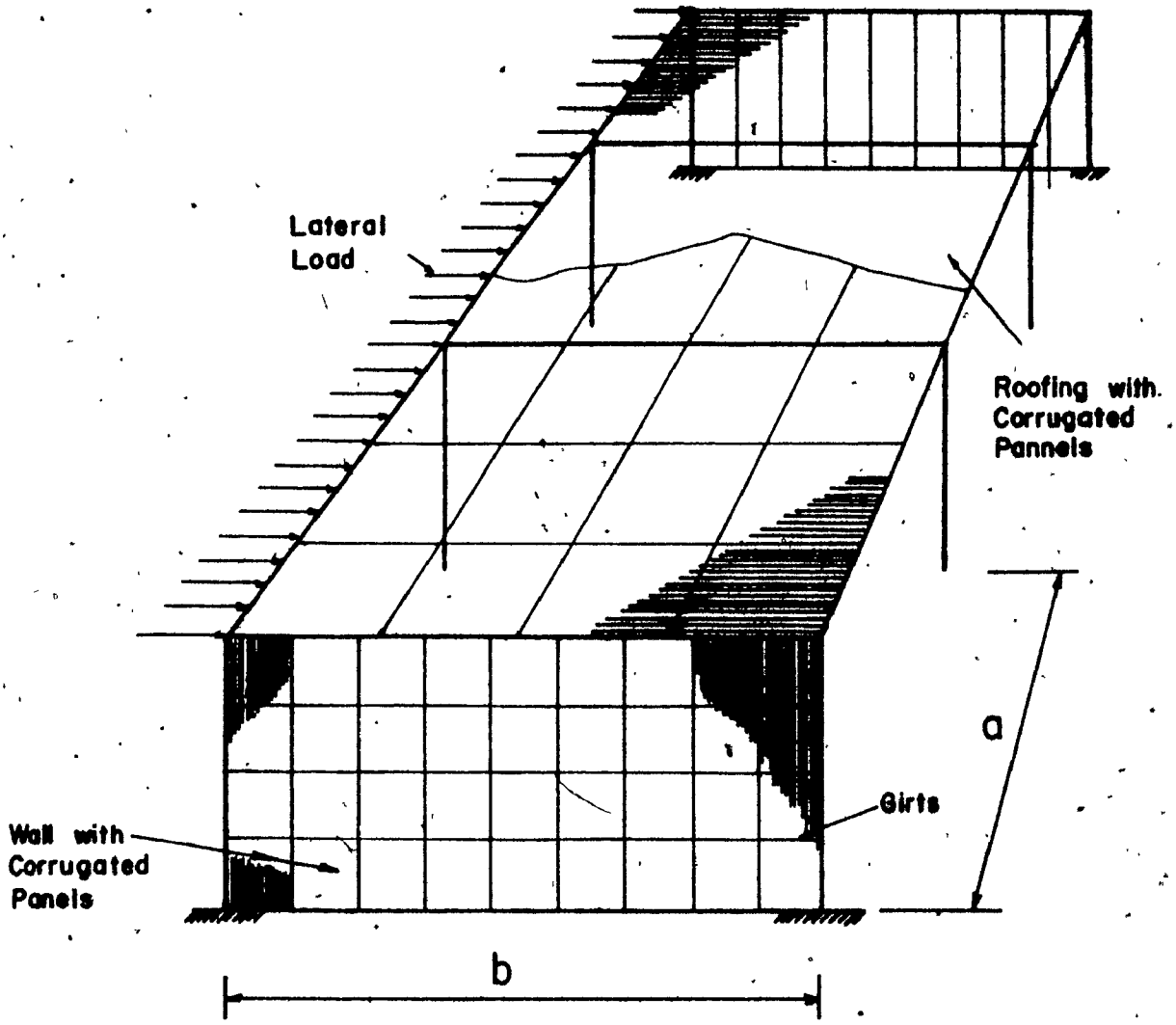

Fig. 1.5 Panels Spanning Between Girts in walls.

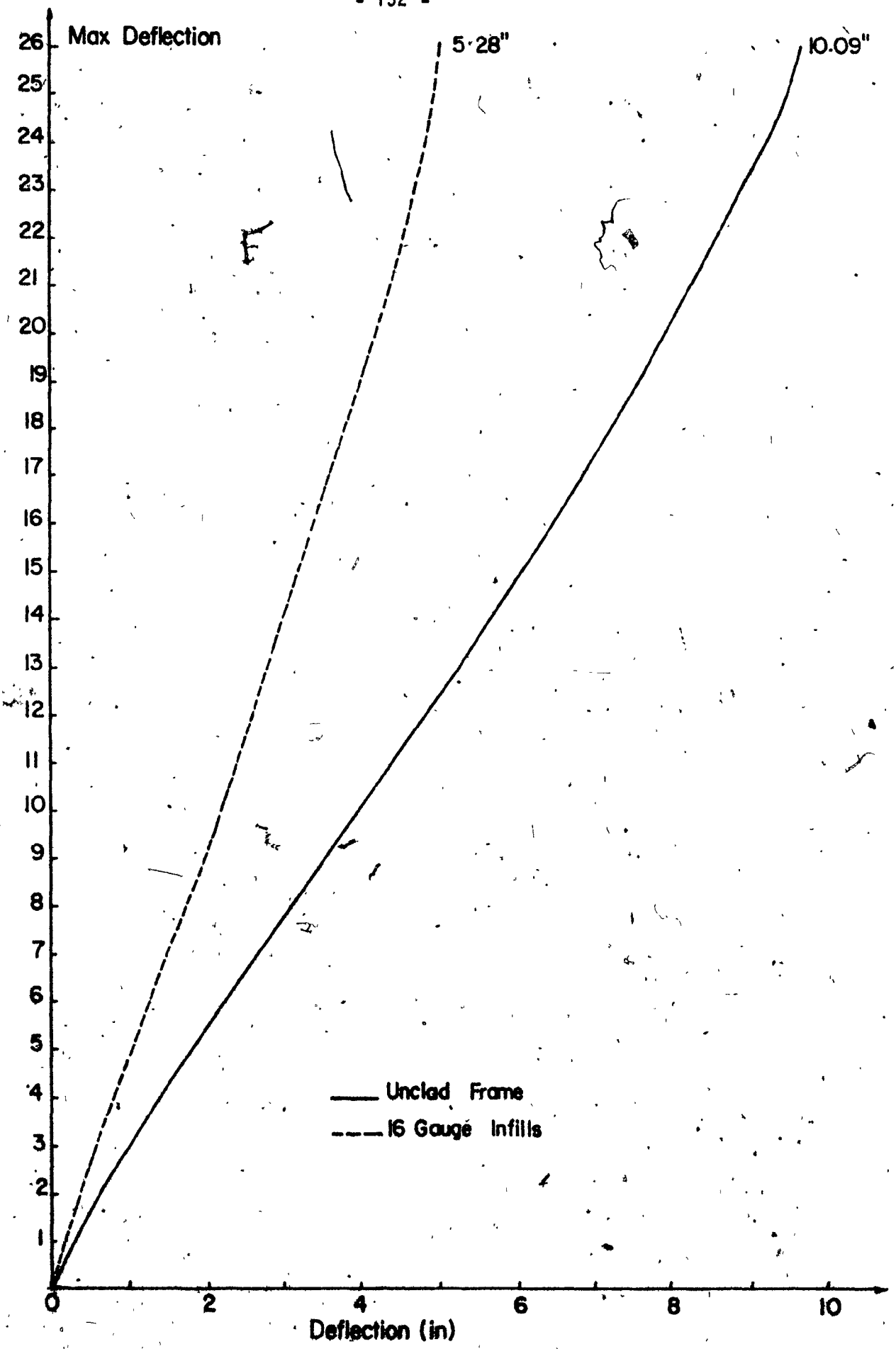

Fig. I.6. Deflected Shapes for 26 Story Frame. (REF. 9)

Loading:
wind load: 7.2 kips
at each story level.

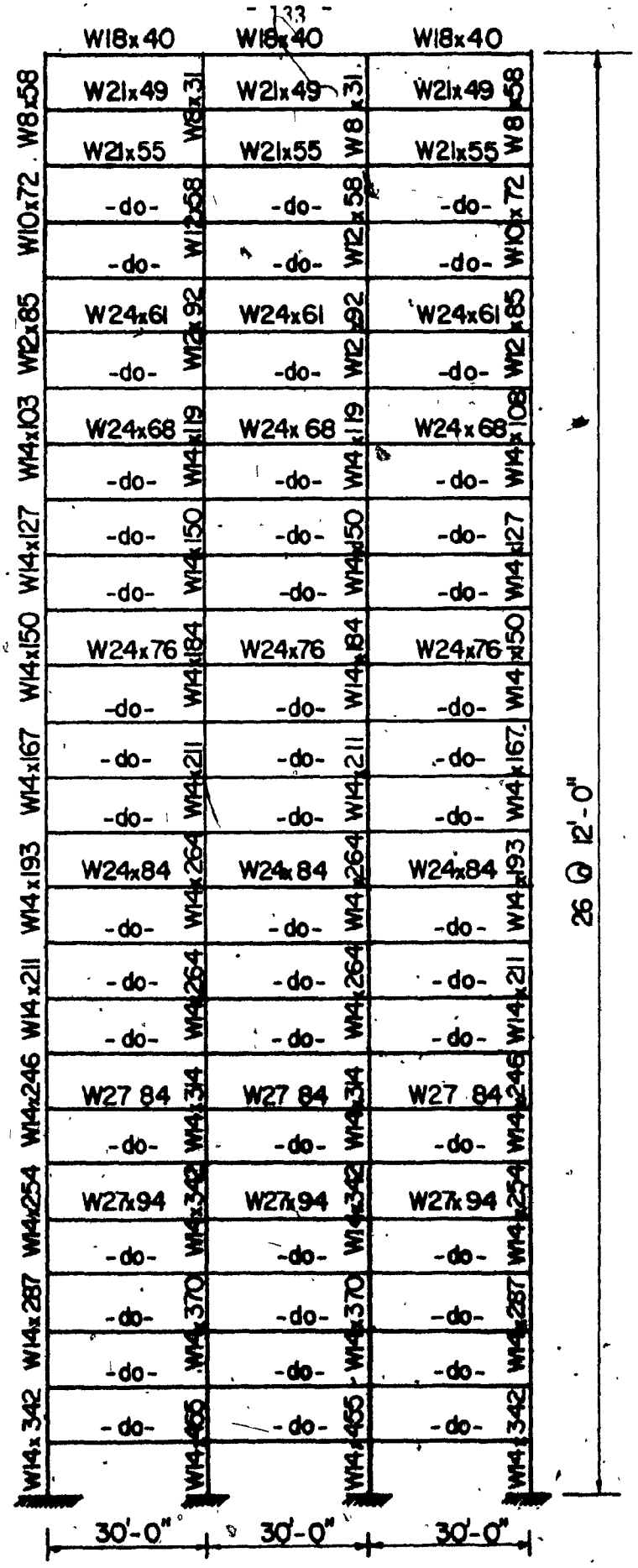

Fig. 1.7. Twenty-Six Story Frame. (REF. 9)

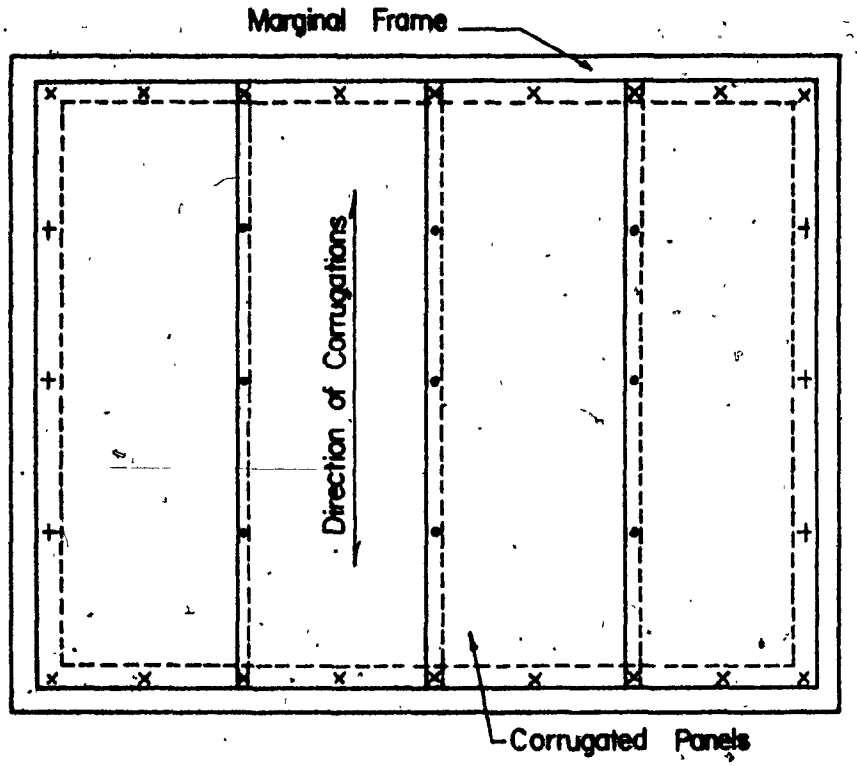

× = End connector (Sheet-purlin fasteners)

+ = Edge connector (Side fasteners)

● = Seam connector (Seam fasteners or Side lap fasteners)

Fig 1.8. Components Of A Typical Cladding.

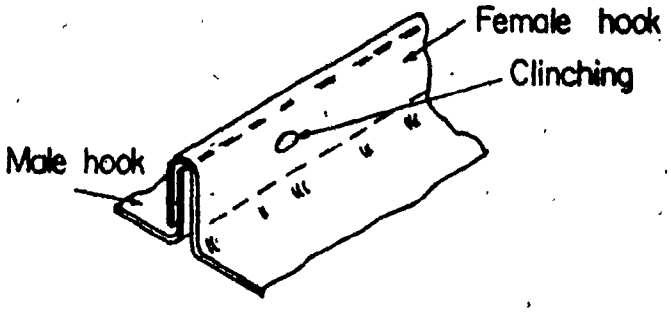

(a) Button Punch (Mechanical clinching)

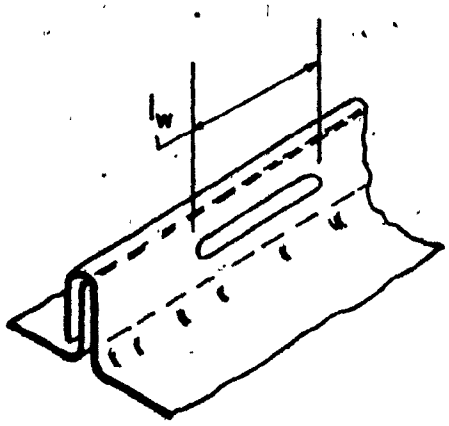

(b) Seam weld engage the square end. (l_w = length of weld)

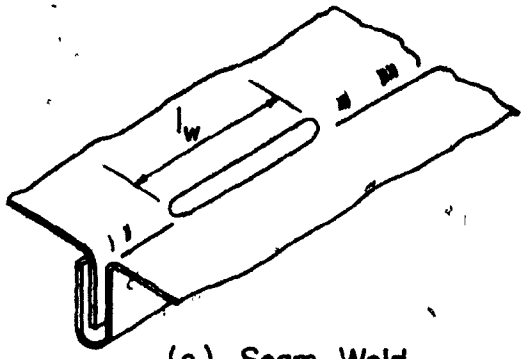

(c) Seam Weld

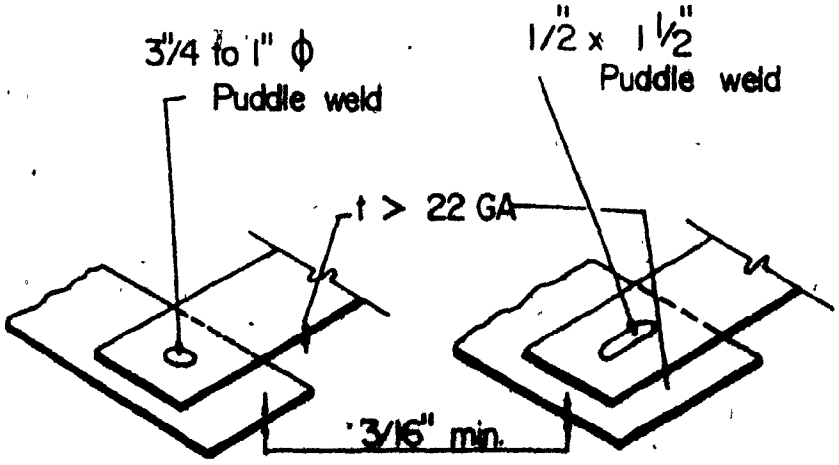

(d) Typical welded connections

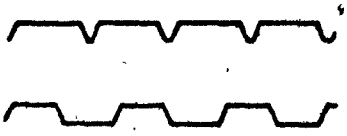

Fig. 1.9. Typical Connections and Panel Shapes.

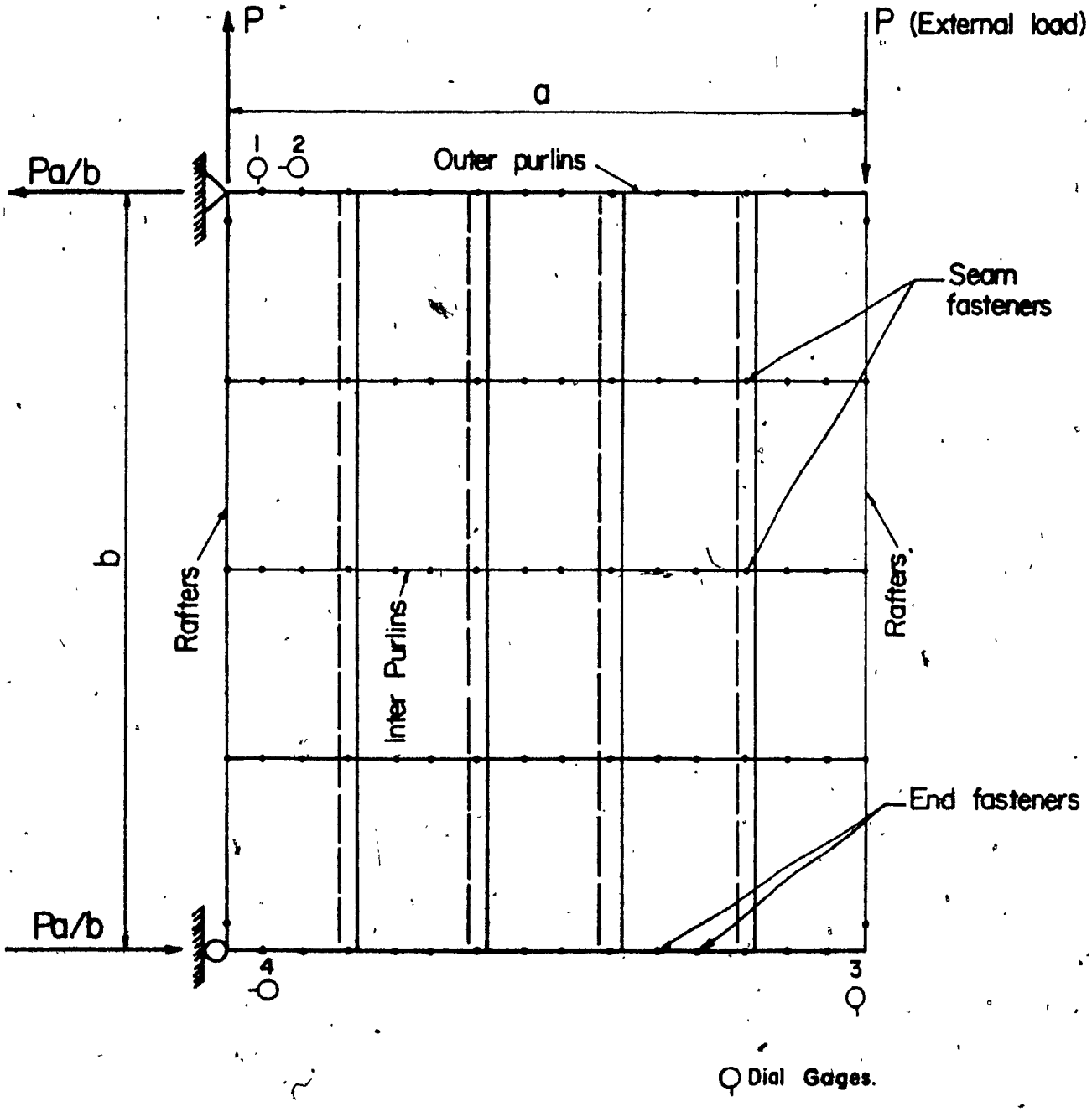

Fig 1.10. Arrangement of Panels in Typical Shear Diaphragm.

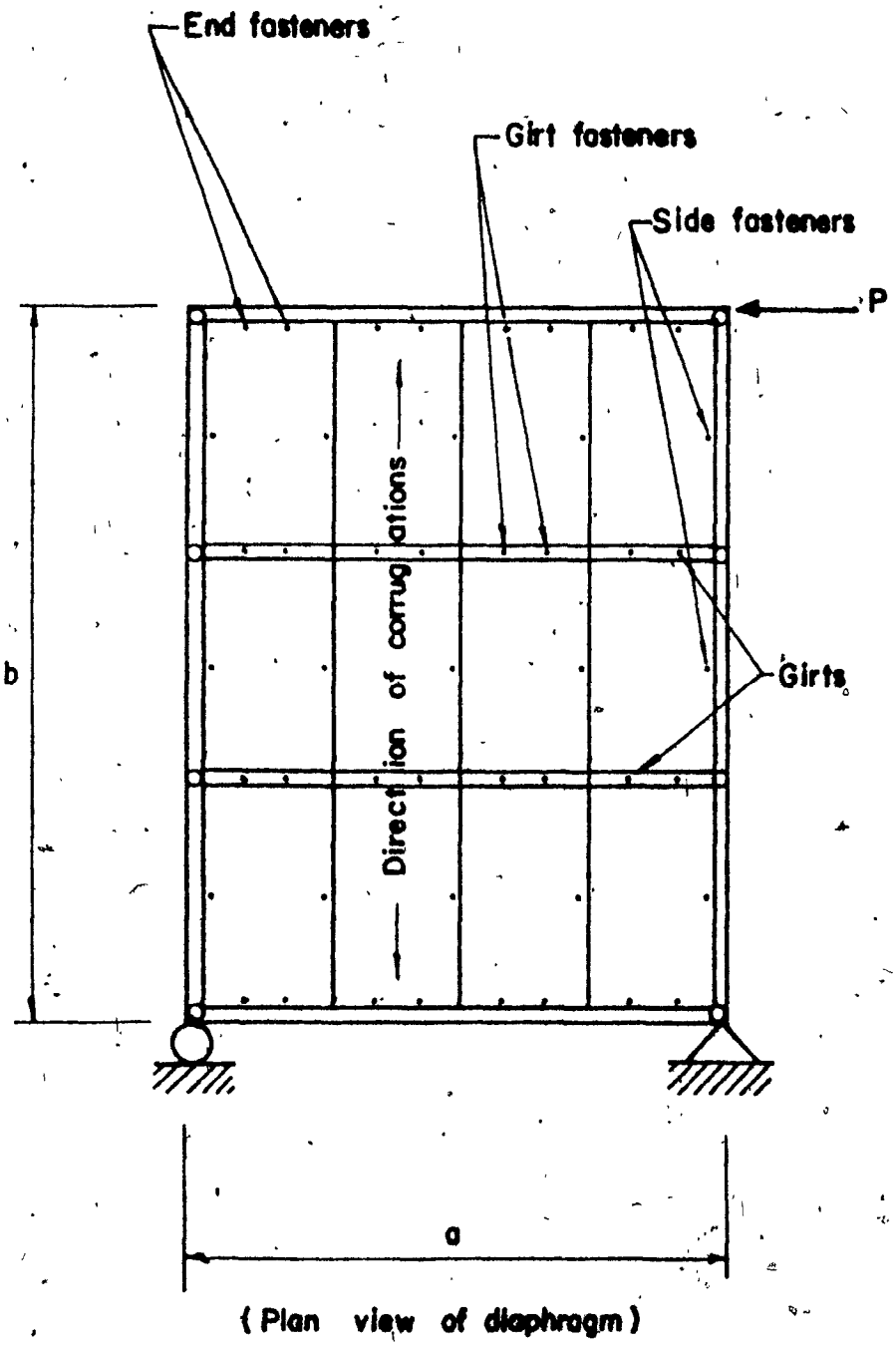

Fig. 3.1. Details of Diaphragm Panels and Fasteners.

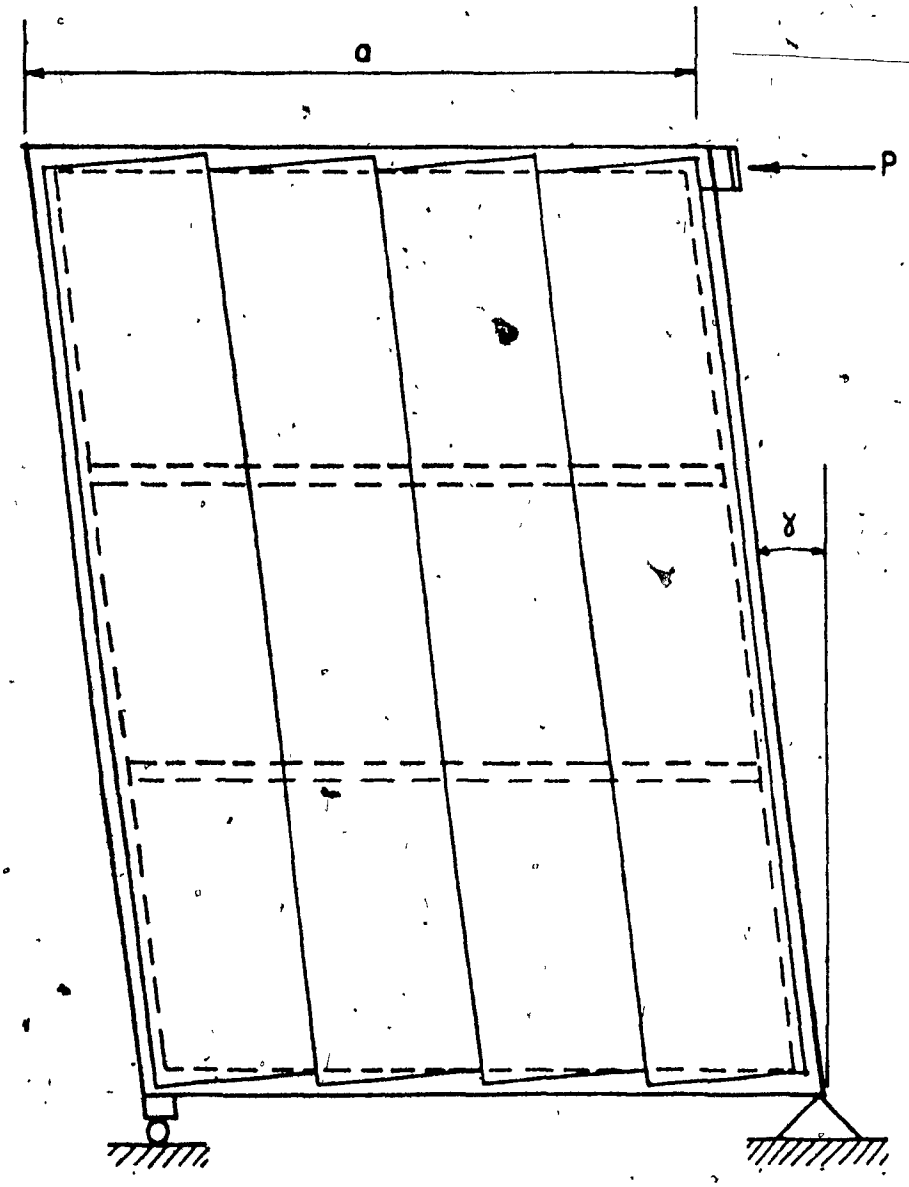

(Plan view of diaphragm)

Fig. 3.2. Deformed Shape of Diaphragm.

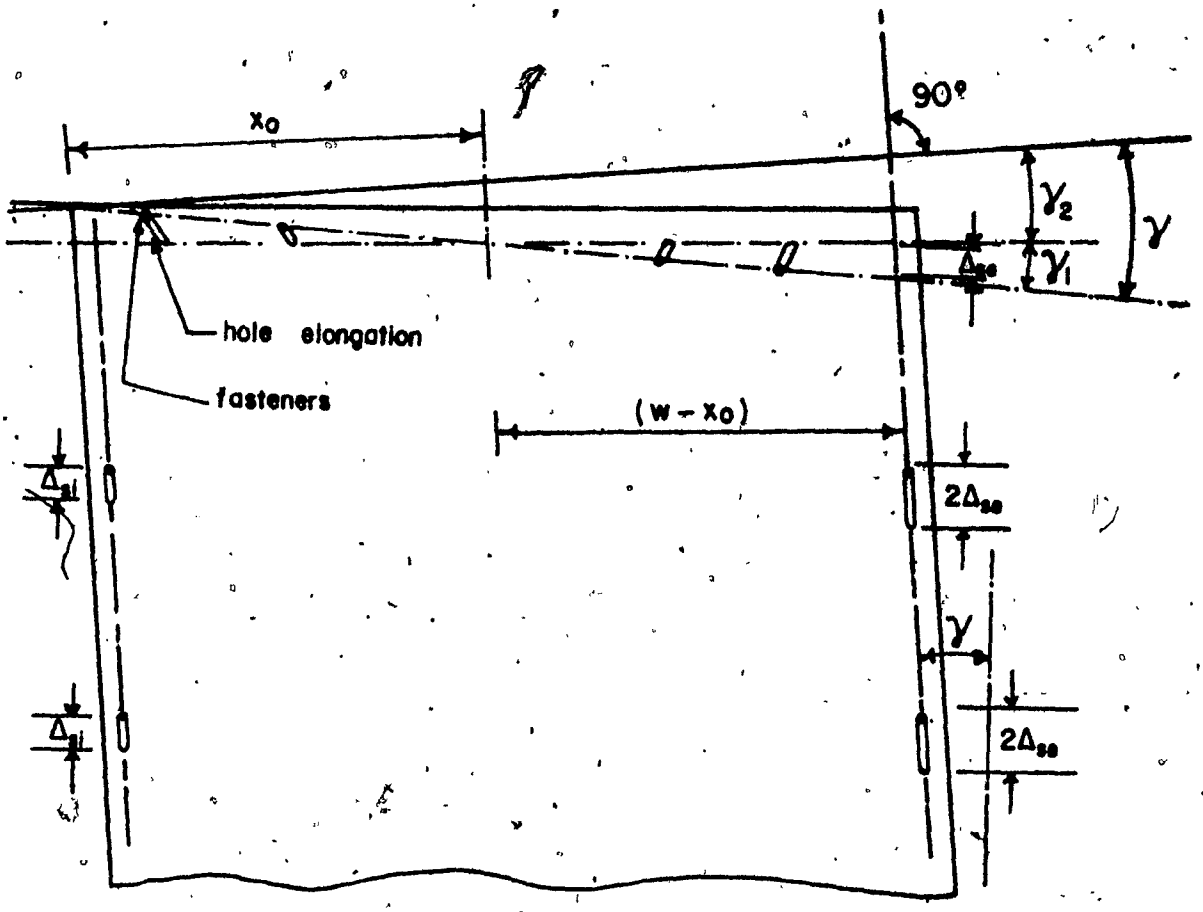

Fig. 3.3 Deformation of an end panel and fasteners (Ref. 15)

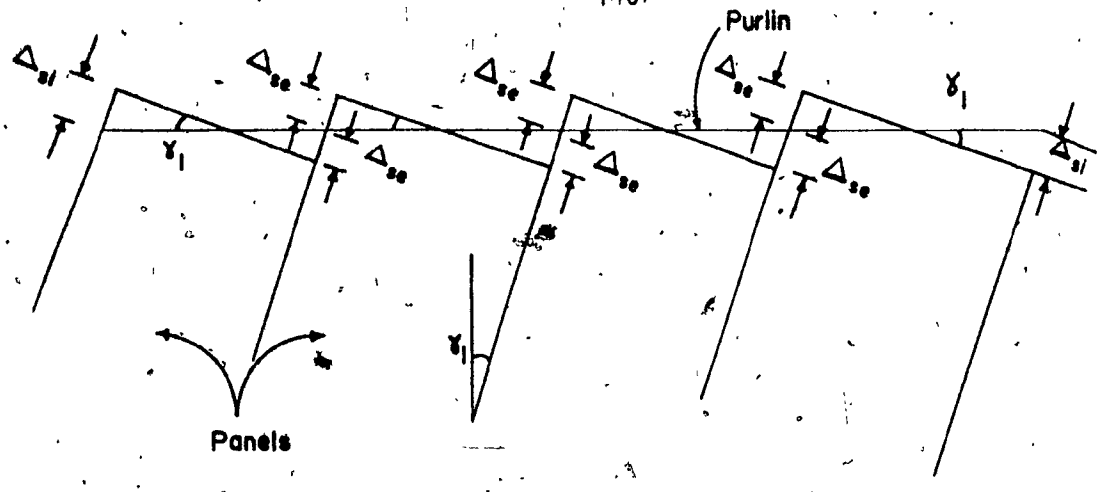

Fig. 3.4 Deformation Due to Fasteners.

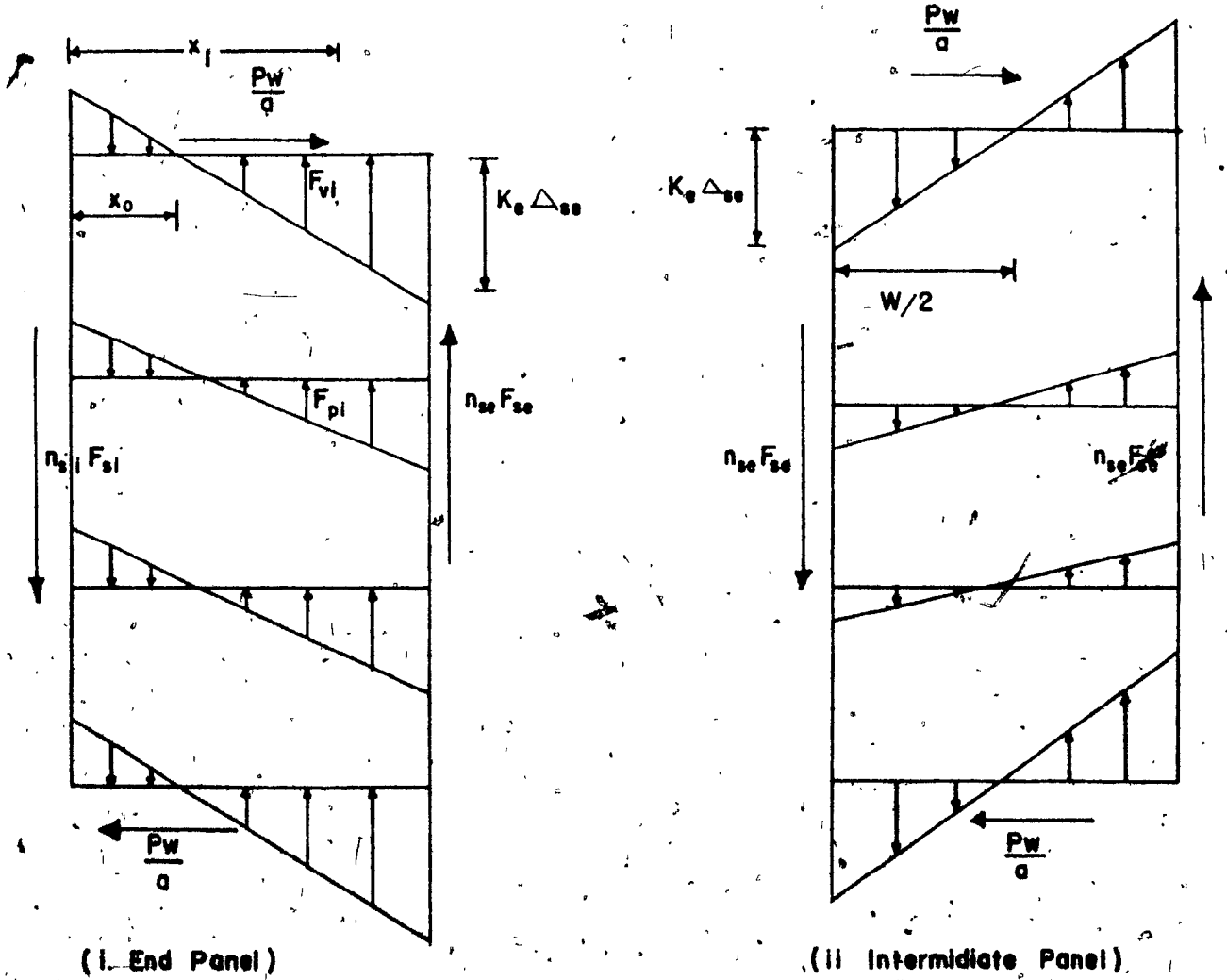

Fig. 3.5 Free-body Diagrams of Diaphragm Panels.

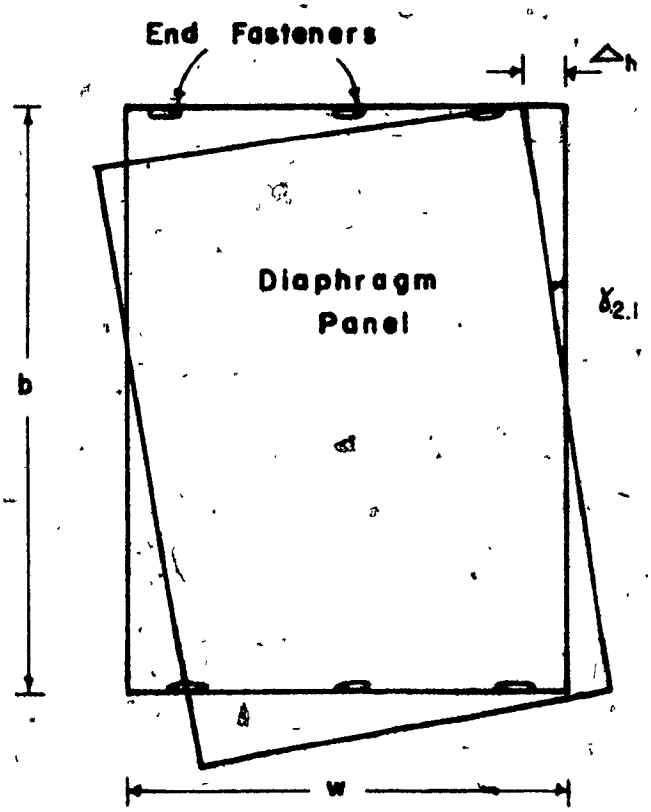

Fig. 3.6 Horizontal Deformation of End Panel

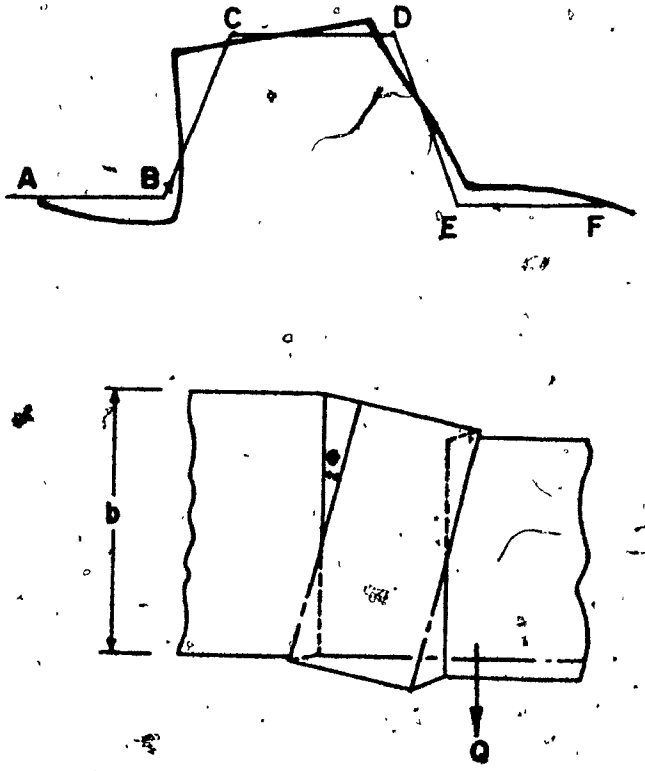

Fig. 3.7 Bending of Corrugation Profile (Ref. 42)

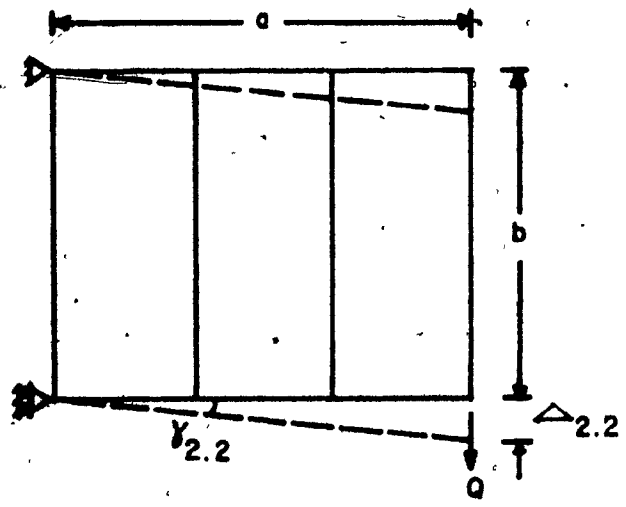

Fig. 3.8. Load Parallel to Corrugation

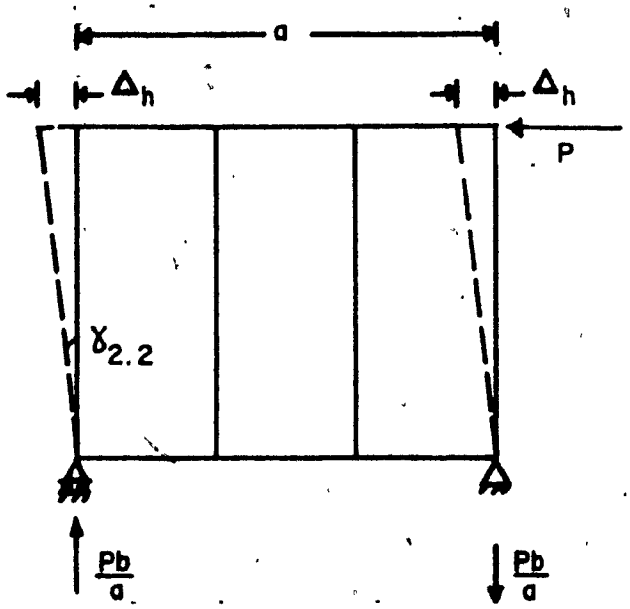

Fig. 3.9. Line Loading.

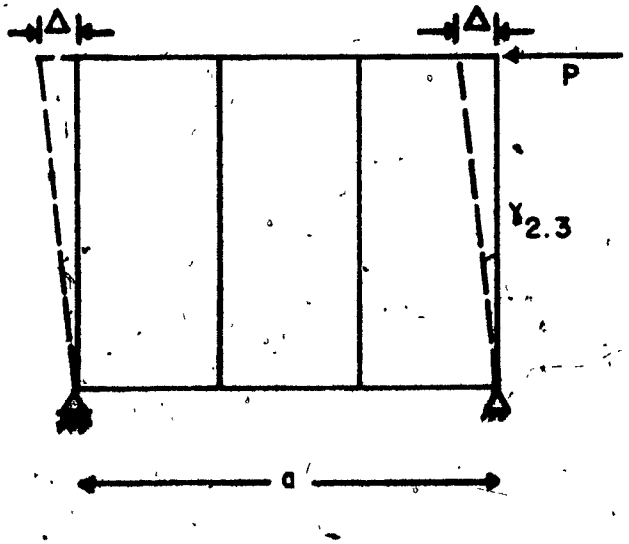

Fig. 3.10. Deflection Due to Shear Strain from Sheeting.

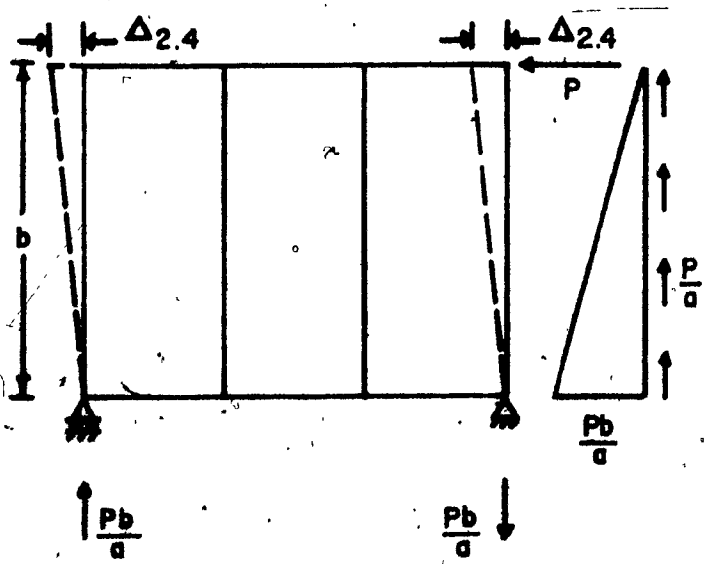

Fig. 3.11. Shear Deformation from Axial Force in Edge Members.

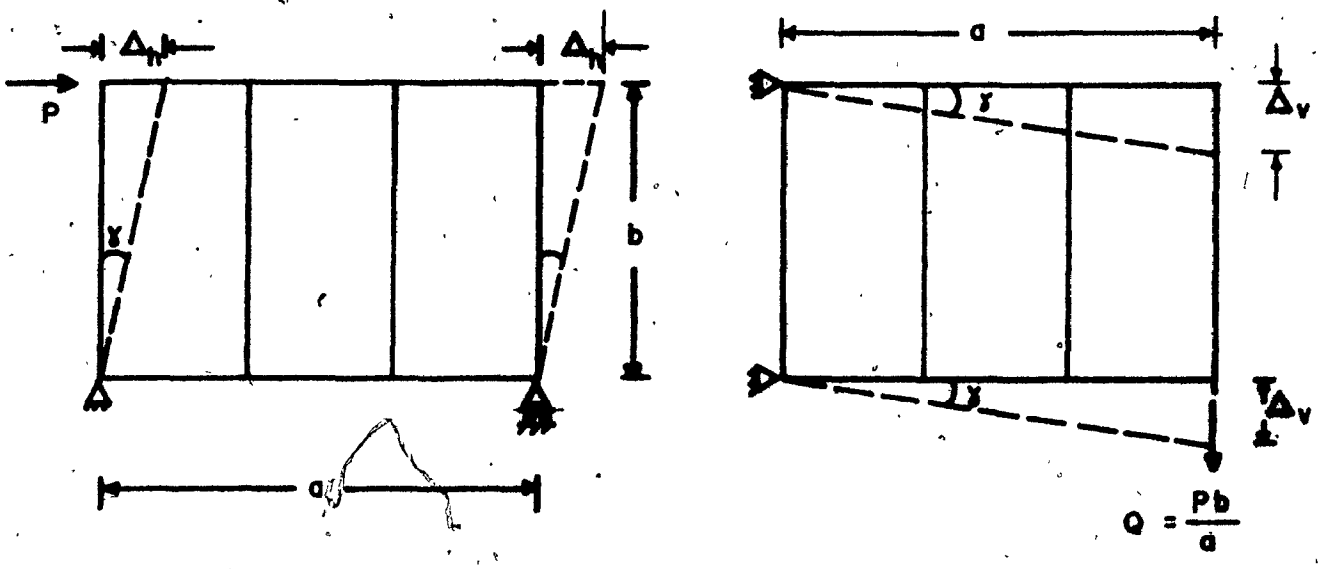

Fig. 3.12. Panel Orientation Relative to Load.

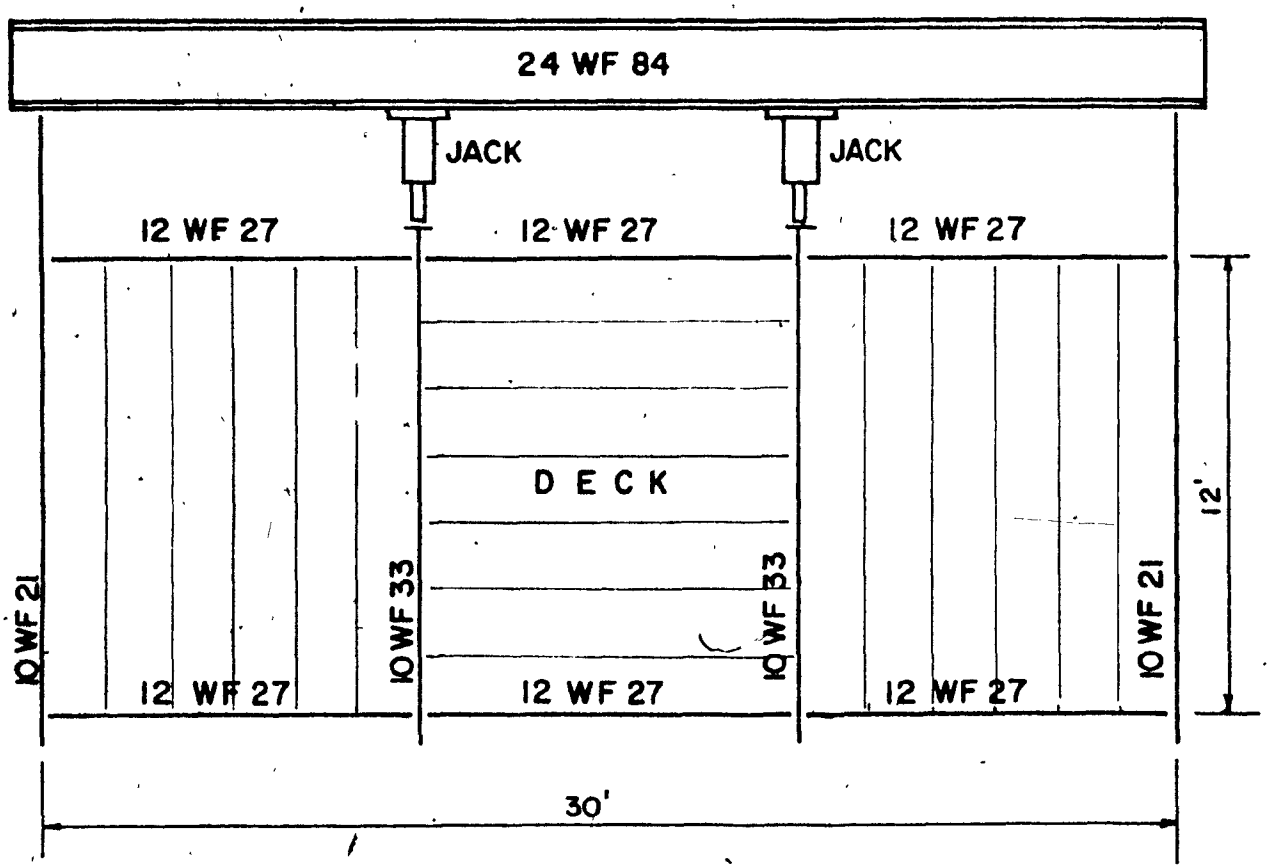

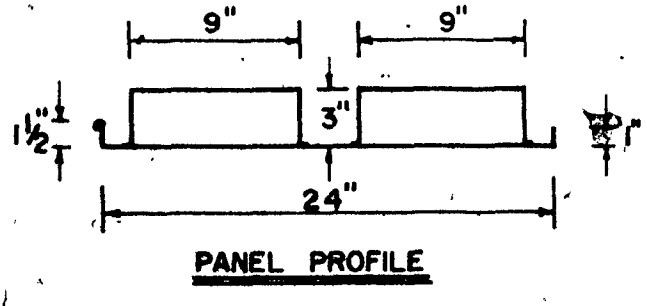

Fig. 3.13 Welded Diaphragm 12'-0" x 30'-0" (Ref. 11)

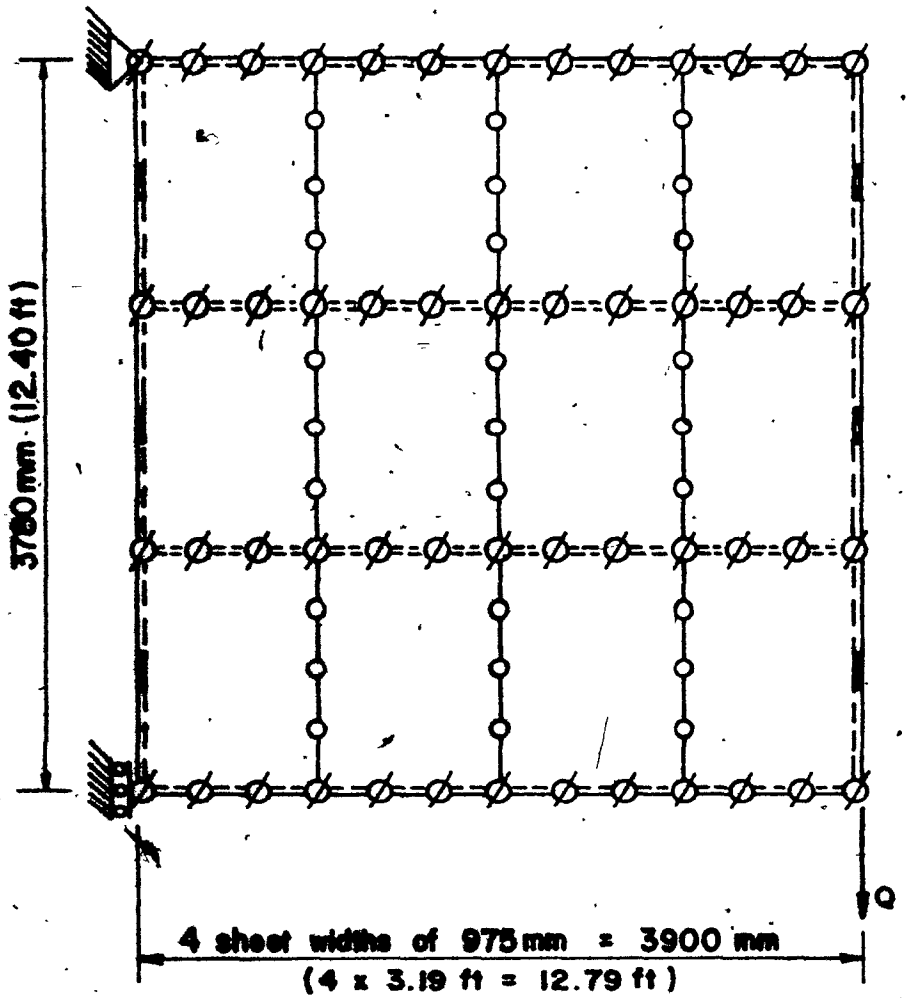

sheet / purlin fasteners thus ⌀
s = 0.35mm/kN (6.125x10^{-5} in/lb)
F_p = 4.08 kN (900 lbs)
seam fasteners thus ○
s_s = 0.35mm/kN (6.125x10^{-5} in/lb)
F_s = 1.70 kN (382 lbs)
shear connectors thus ▯
s_{cs} = 0.117 mm/kN (2.04x10^{-5} in/lb)
F_{cs} = 12.24 kN (2750 lbs)
Z purlins thus ====
A = 49.4 mm^2(0.76 in^2) I_y = 20000 mm^4(0.048 in^4)
rafters thus ▮▮▮▮
A = 23.20 mm^2 (3.59 in^2) I_y = 3420000 mm^4(8.21 in^4)

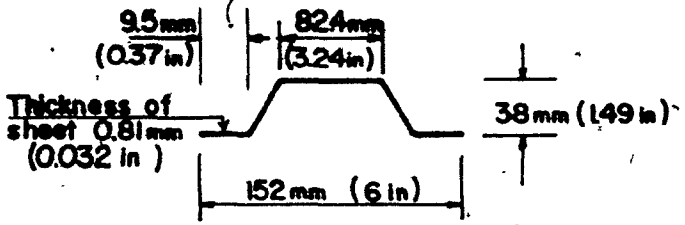

Panel shape

Fig. 3.14. Details of Diaphragm A2 with Mechanical Fasteners (alternate corrugations fastened)
(Ref. 23)

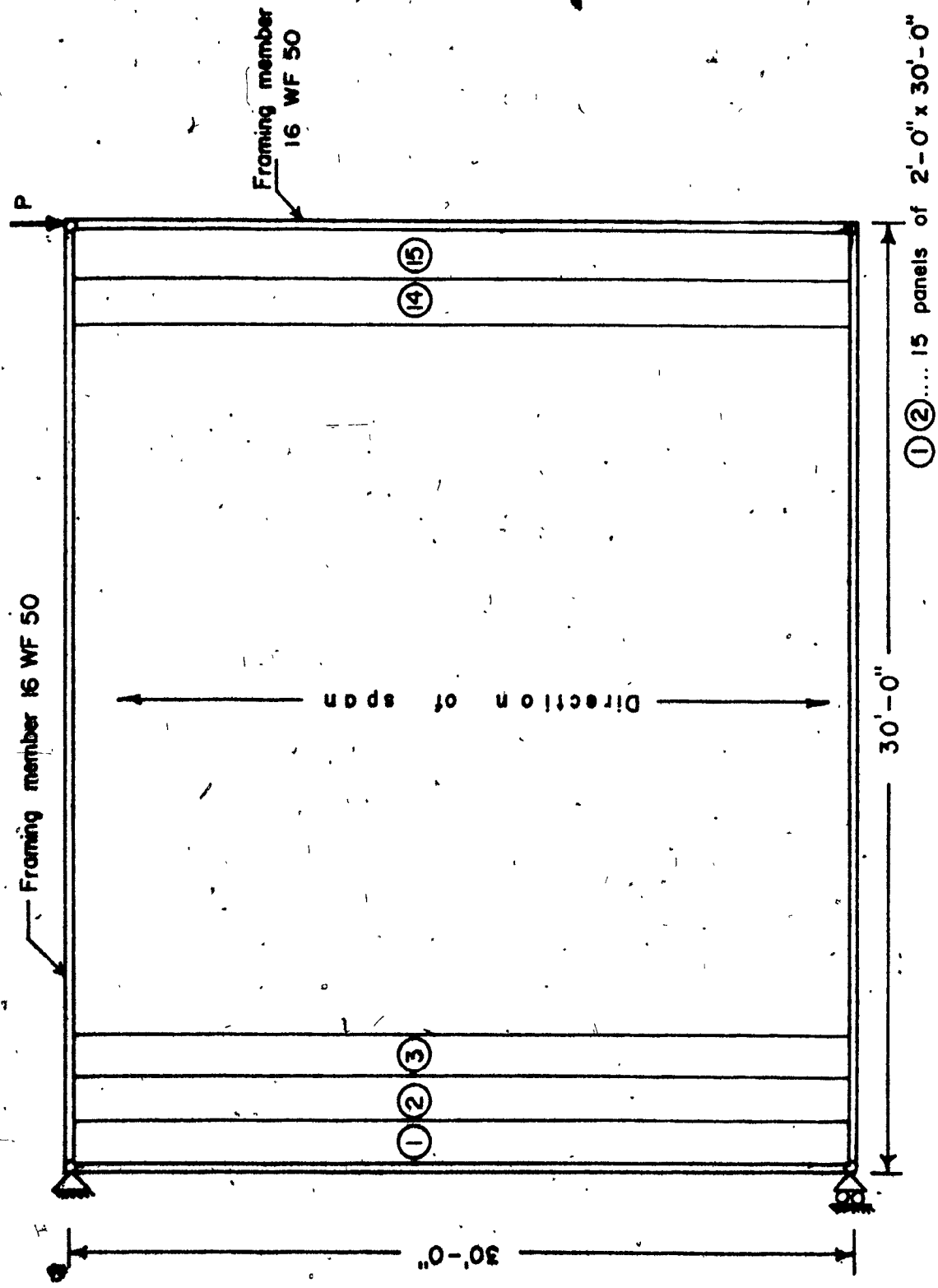

Fig. 3.15 Welded Diaphragm 30'-0" x 30'-0" — Cantilever Test (Ref. 11)

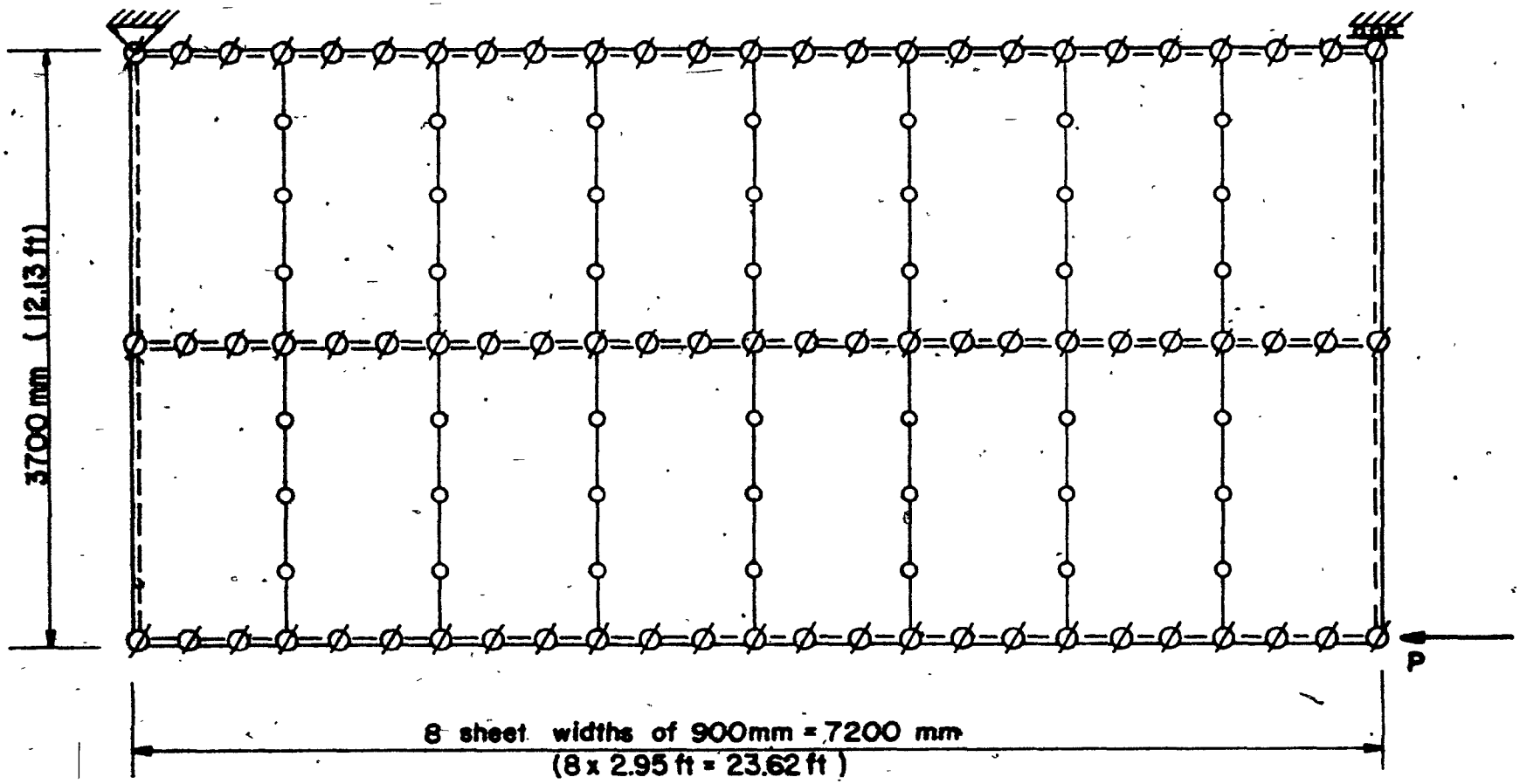

sheet/purlin fasteners ⌀, $s = 0.12$ mm/kN (2.1×10^{-5} in/lb), $F_p = 4.86$ kN (1092 lbs), seam fasteners o, $s_s = 0.35$ mm/kN (6.12×10^{-5} in/lb), $F_s = 2.02$ kN (454 lbs). Main and secondary supporting members were trusses. Assumed properties $A = 996$ mm^2 (1.54 in^2) $I_y = 520000$ mm^4 (1.25 in^4).

Fig. 3.16 Dimensions and Details of Panel C2 (alternate corrugations fastened)
(Ref: 23)

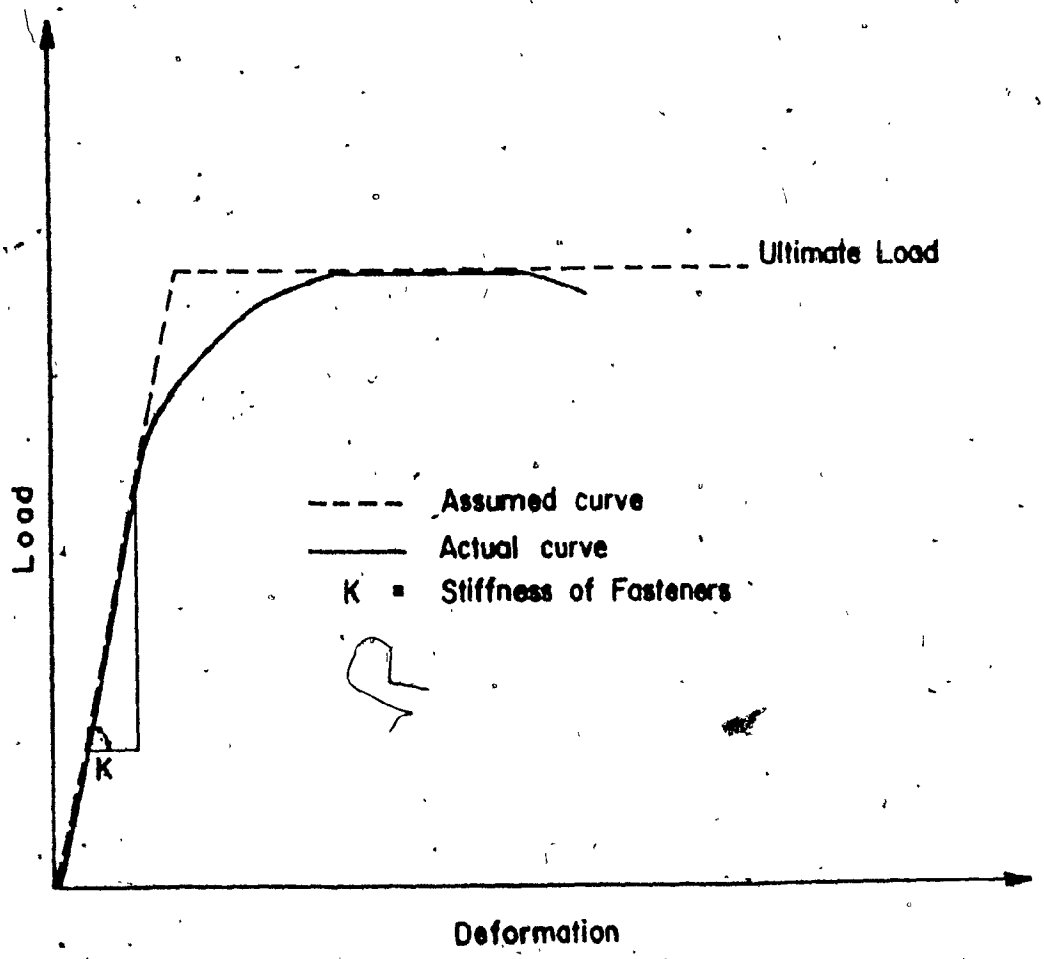

Fig. 4.1 Assumed Load – Deformation Curve for Fasteners.

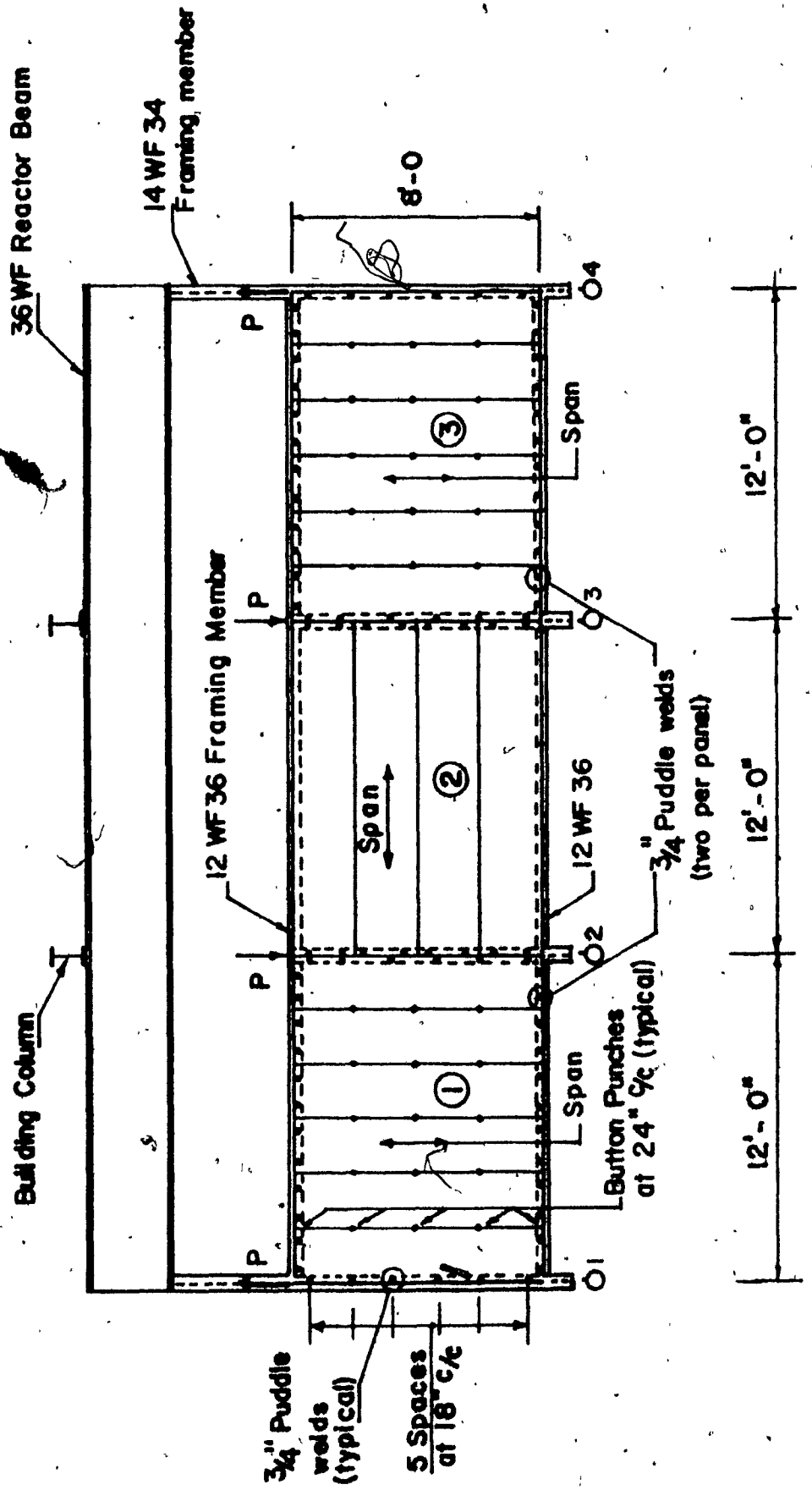

Fig. 4.2 Simple Beam Testing Arrangement and Layout of Diaphragm Panel (Ref. 41)

(PLAN VIEW of DIAPHRAGM)

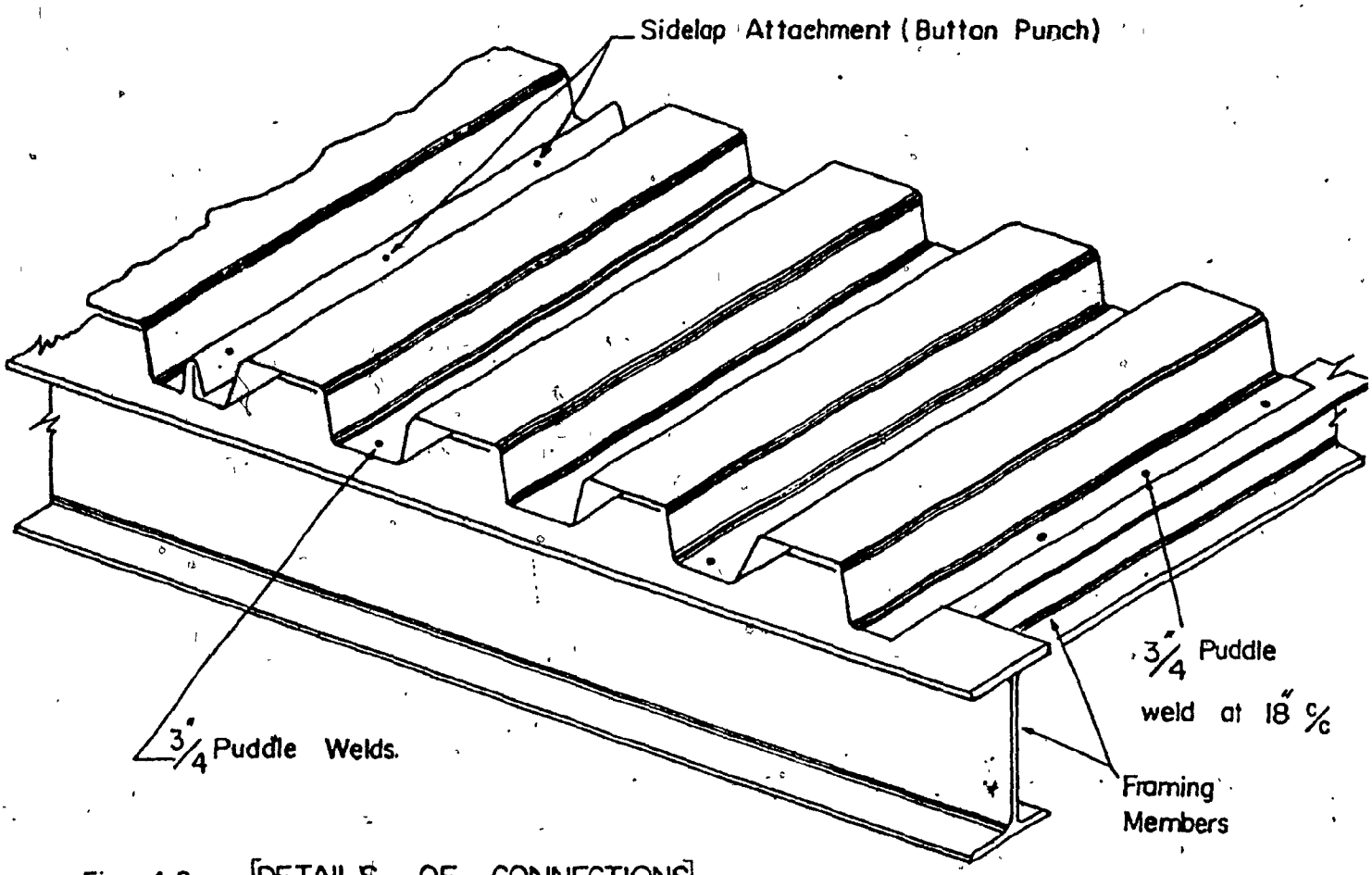

Fig. 4.2 a [DETAILS OF CONNECTIONS]

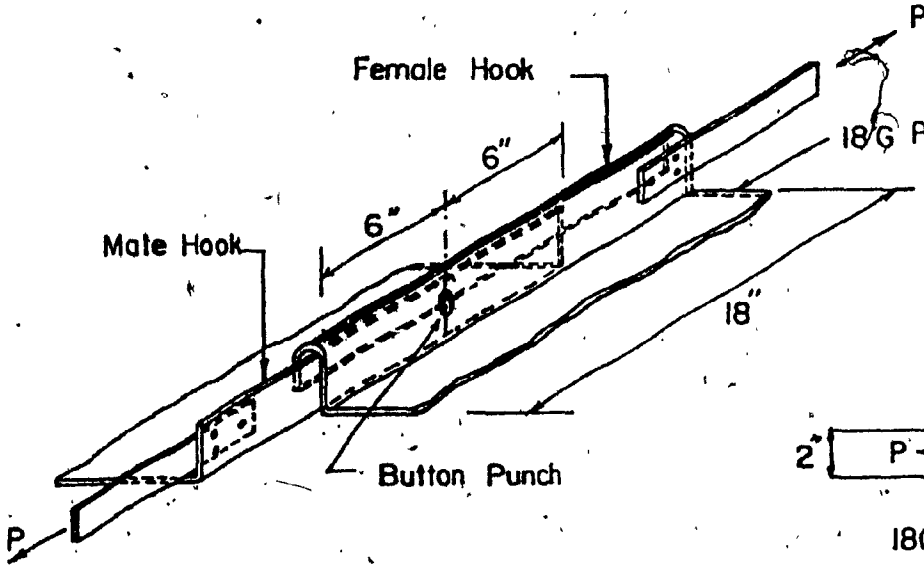

FIG. 4.3 TEST SPECIMEN FOR BUTTON PUNCH (MECHANICAL CLINCHING)

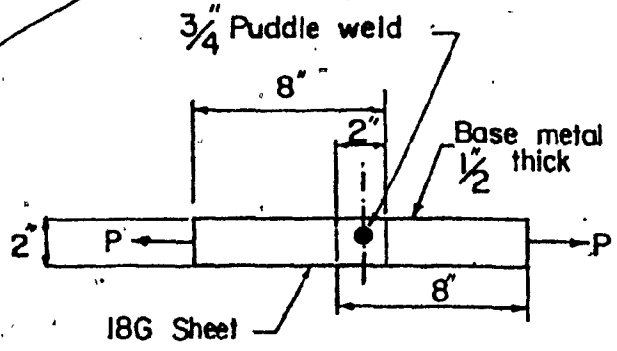

FIG. 4.8 TEST SPECIMEN FOR WELDED CONNECTION

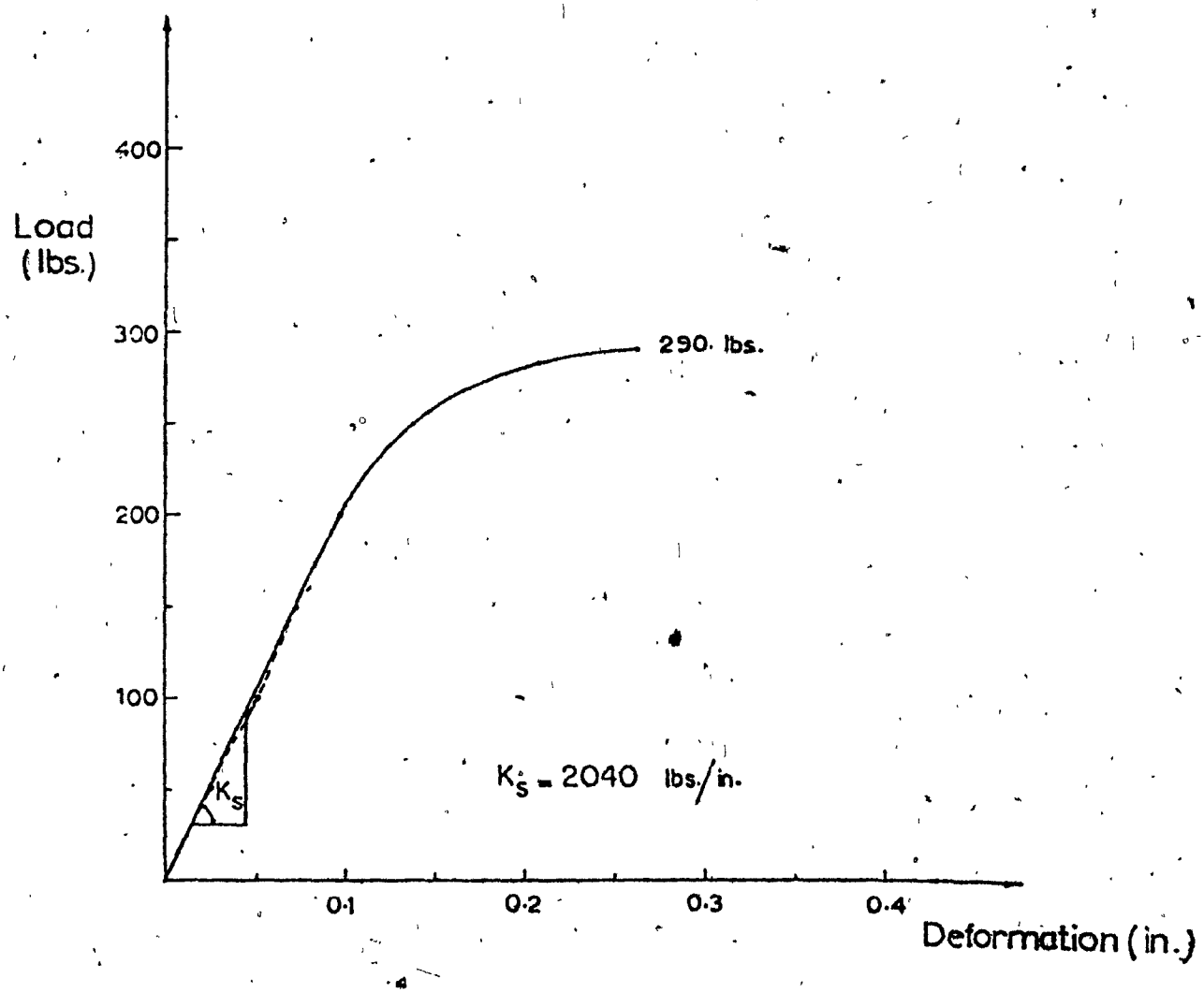

Fig. 4.4 Typical Load-Deformation Curve For Mechanical Clinch (Button Punch)
P_u = 290. lbs. — 18 Gage — One Clinch

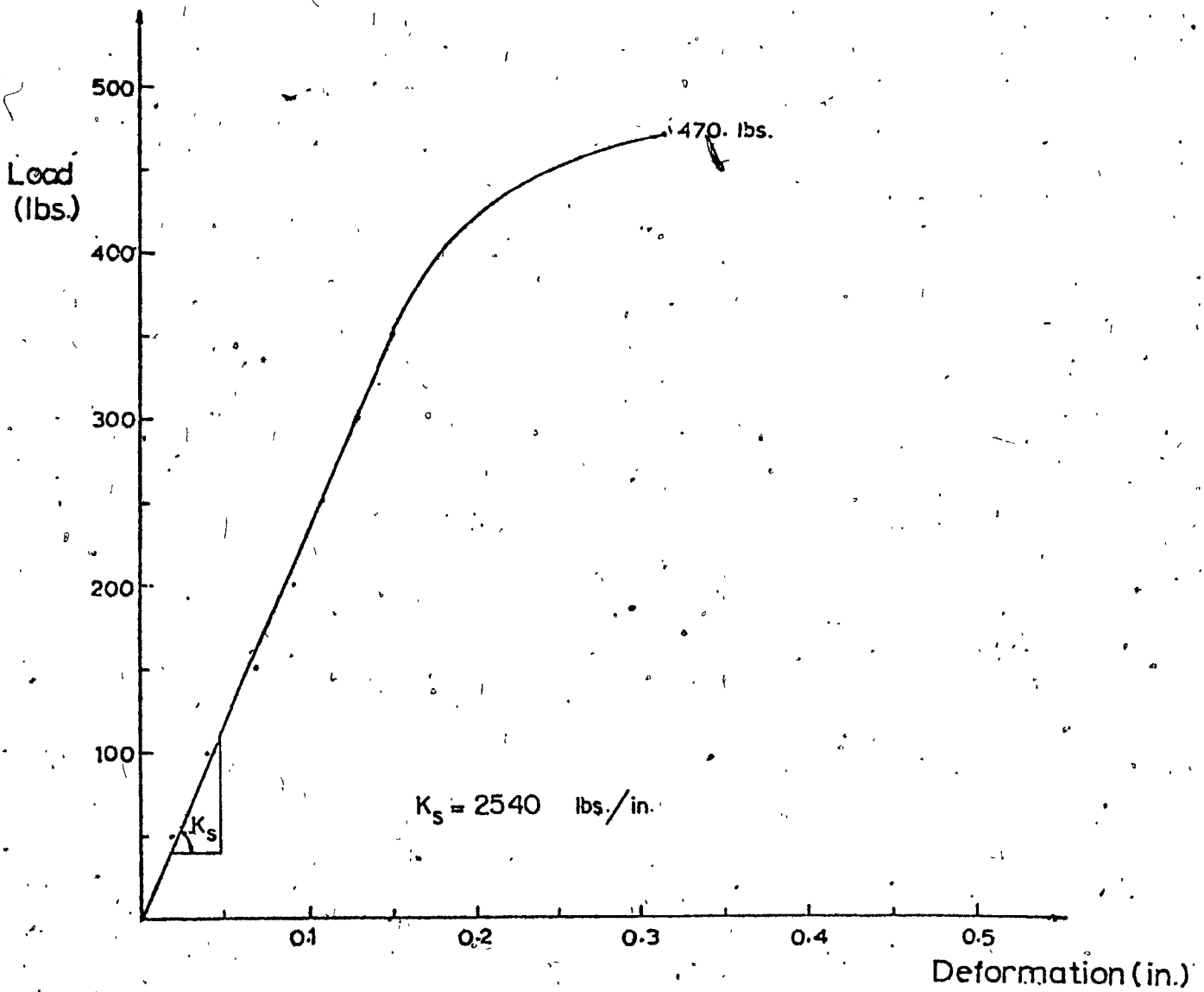

Fig. 4.5 Typical Load - Deformation Curve For Mechanical Clinch (Button Punch)
P_u = 470. lbs. - 18 Gage - One Clinch

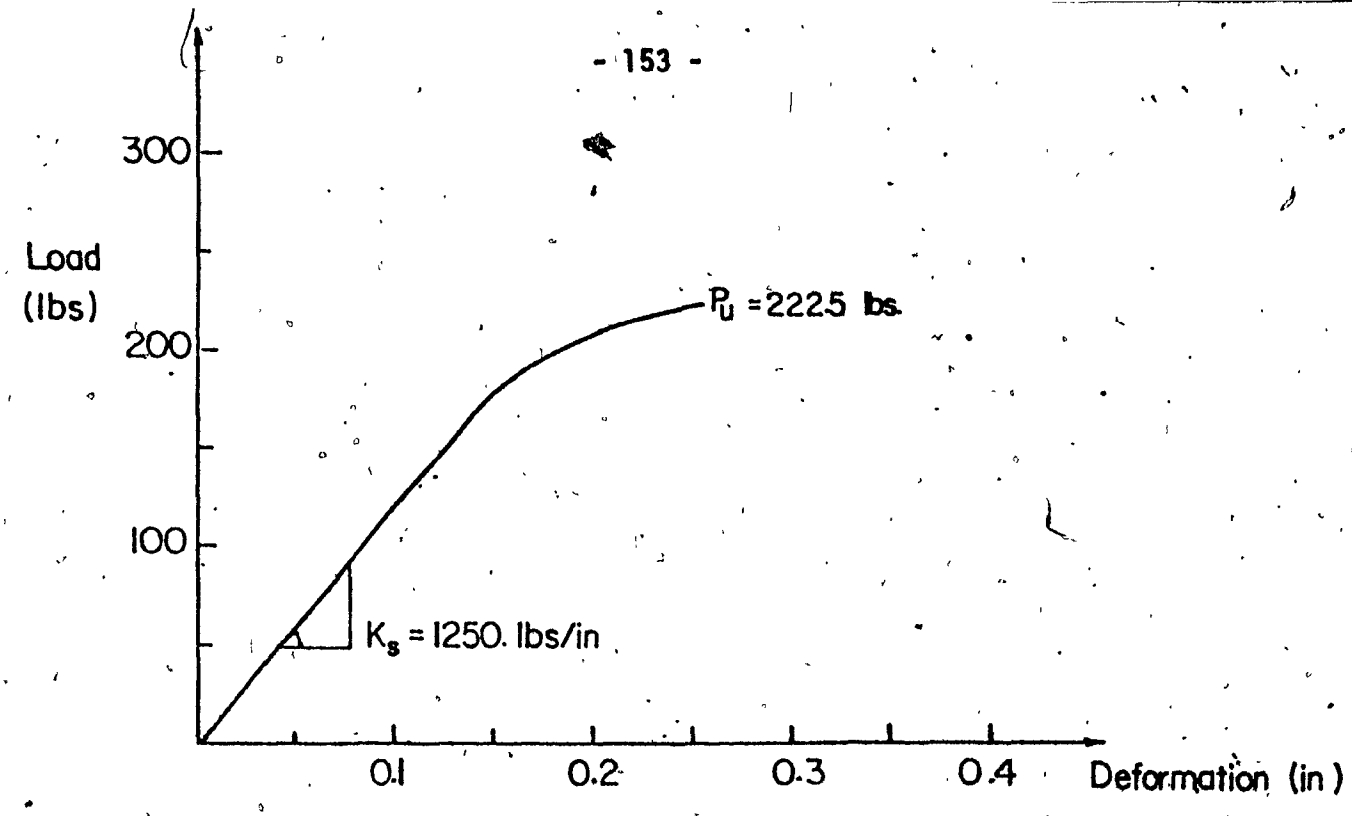

Fig. 4.6 Load Deformation Curve for Button Punch (22 Gage)

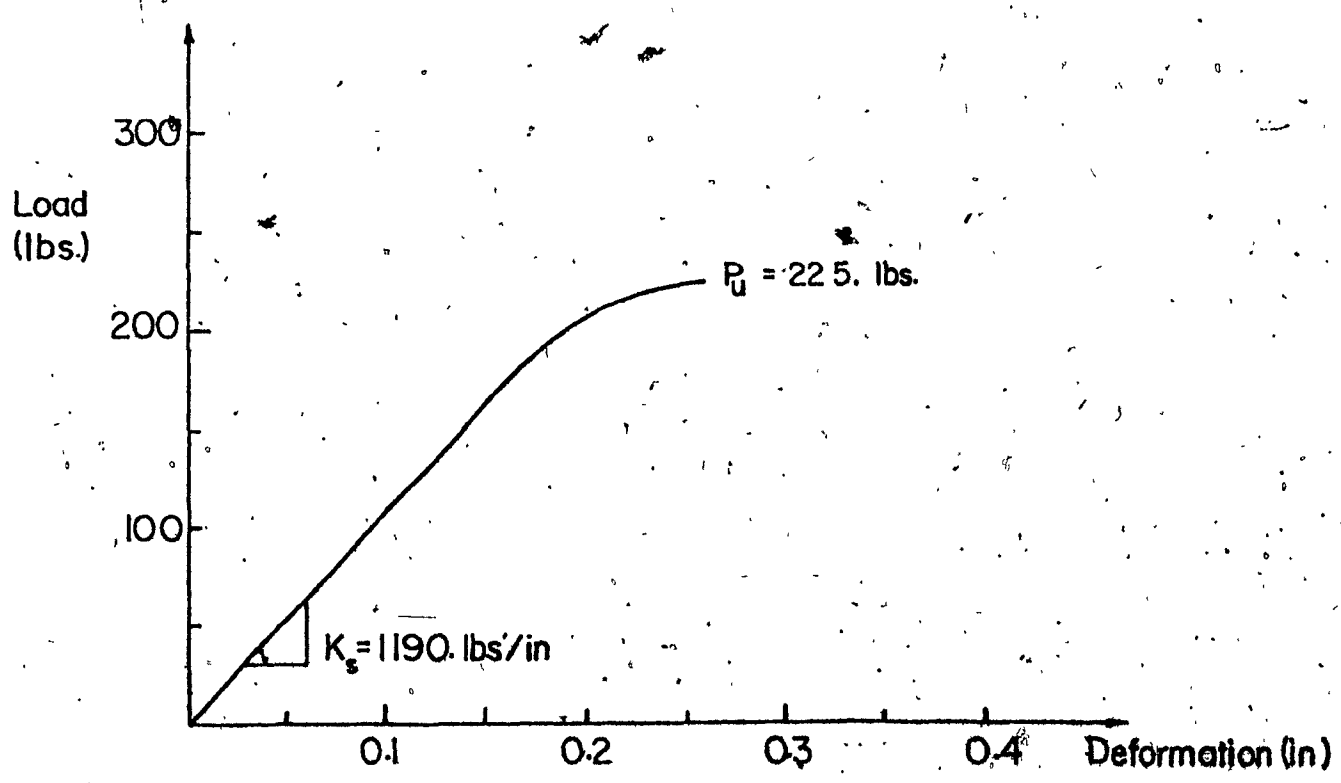

Fig. 4.7 Load Deformation Curve for Button Punch (22 Gage)

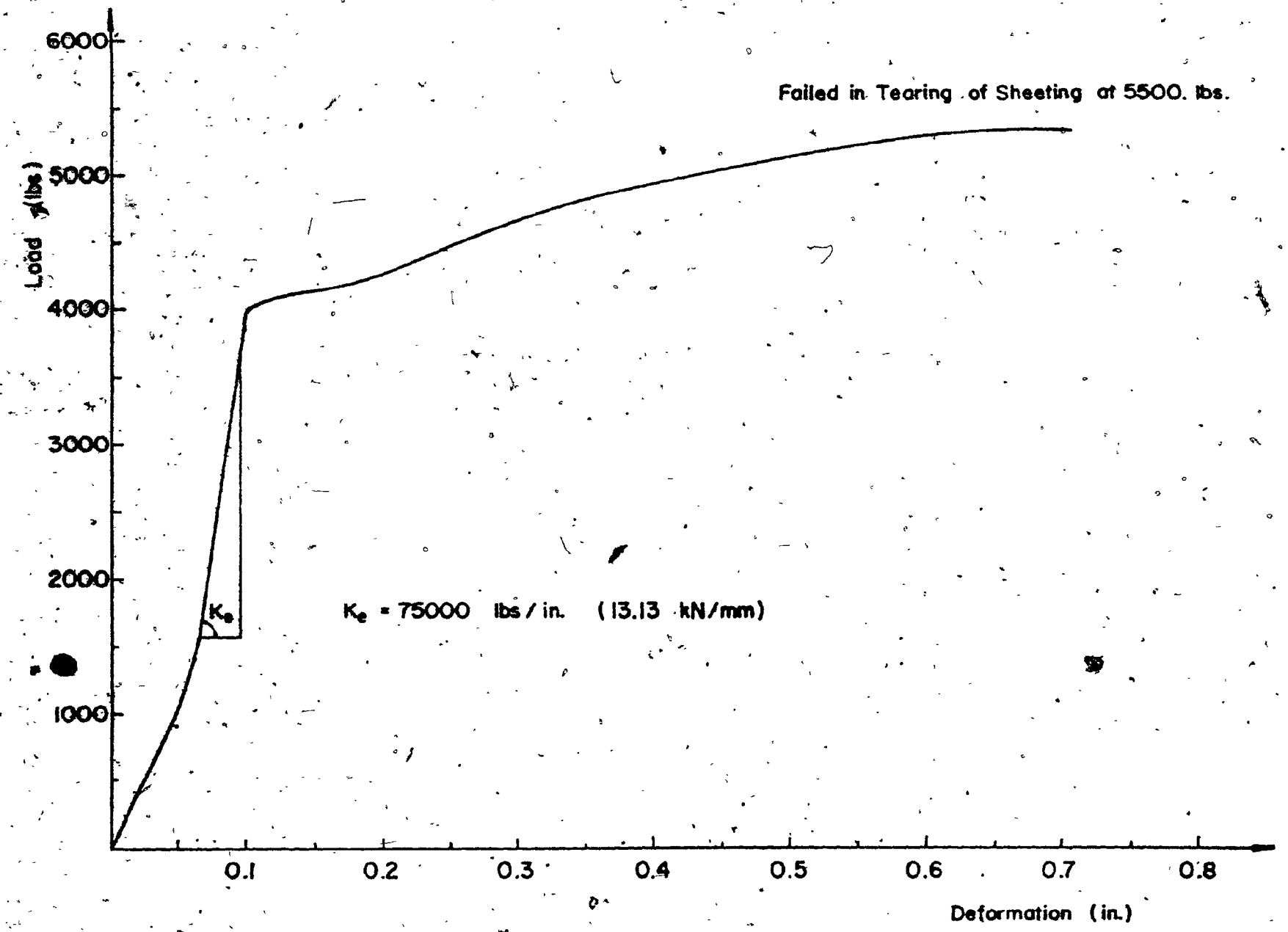

Fig. 4.9 Load Deformation Curve for Welded Connections (18 Gage)

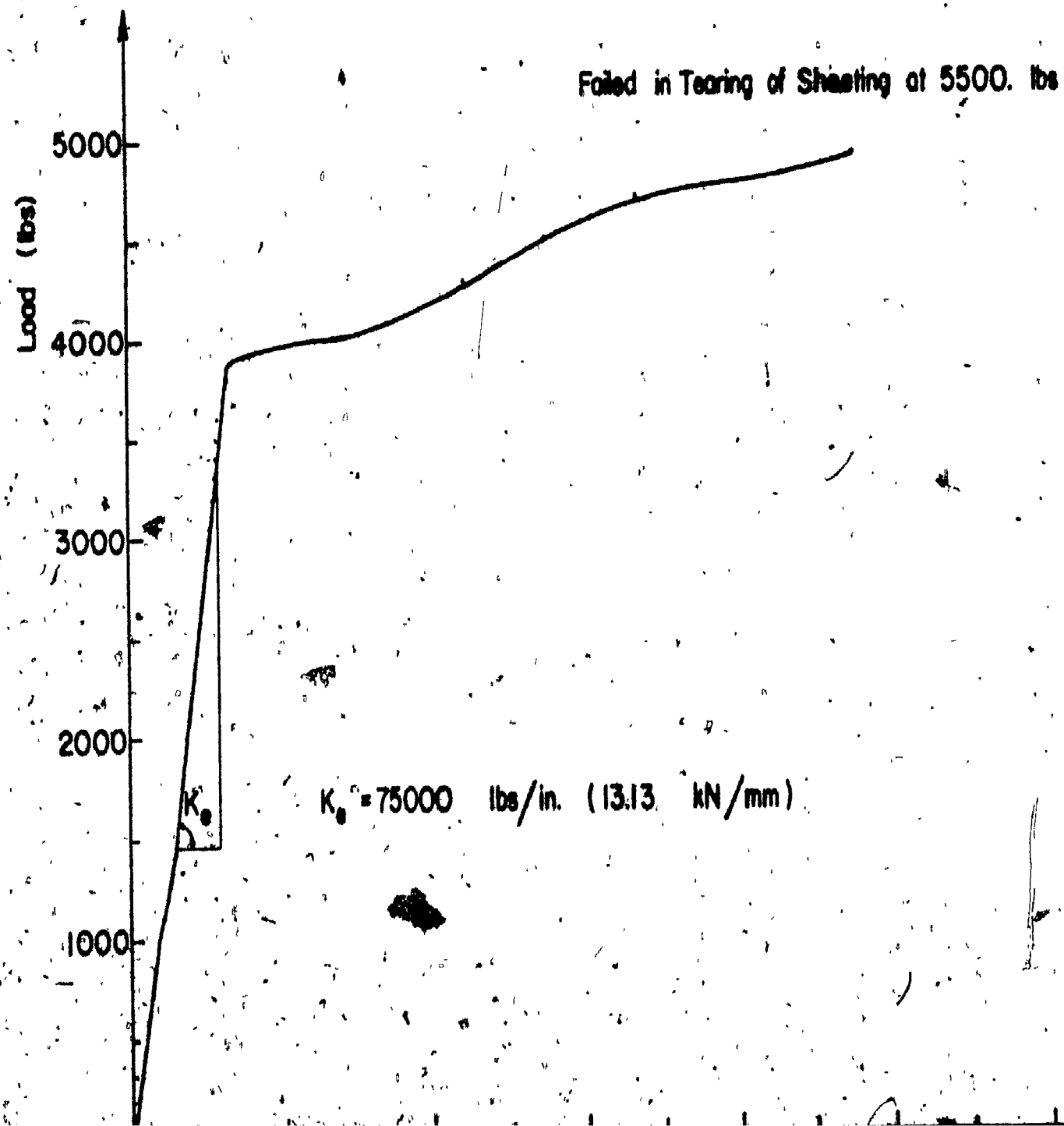
Failed in Tearing of Sheeting at 5500. lbs
Load (lbs)
5000
4000
3000
2000
1000
K_e
K_e = 75000 lbs/in. (13.13 kN/mm)

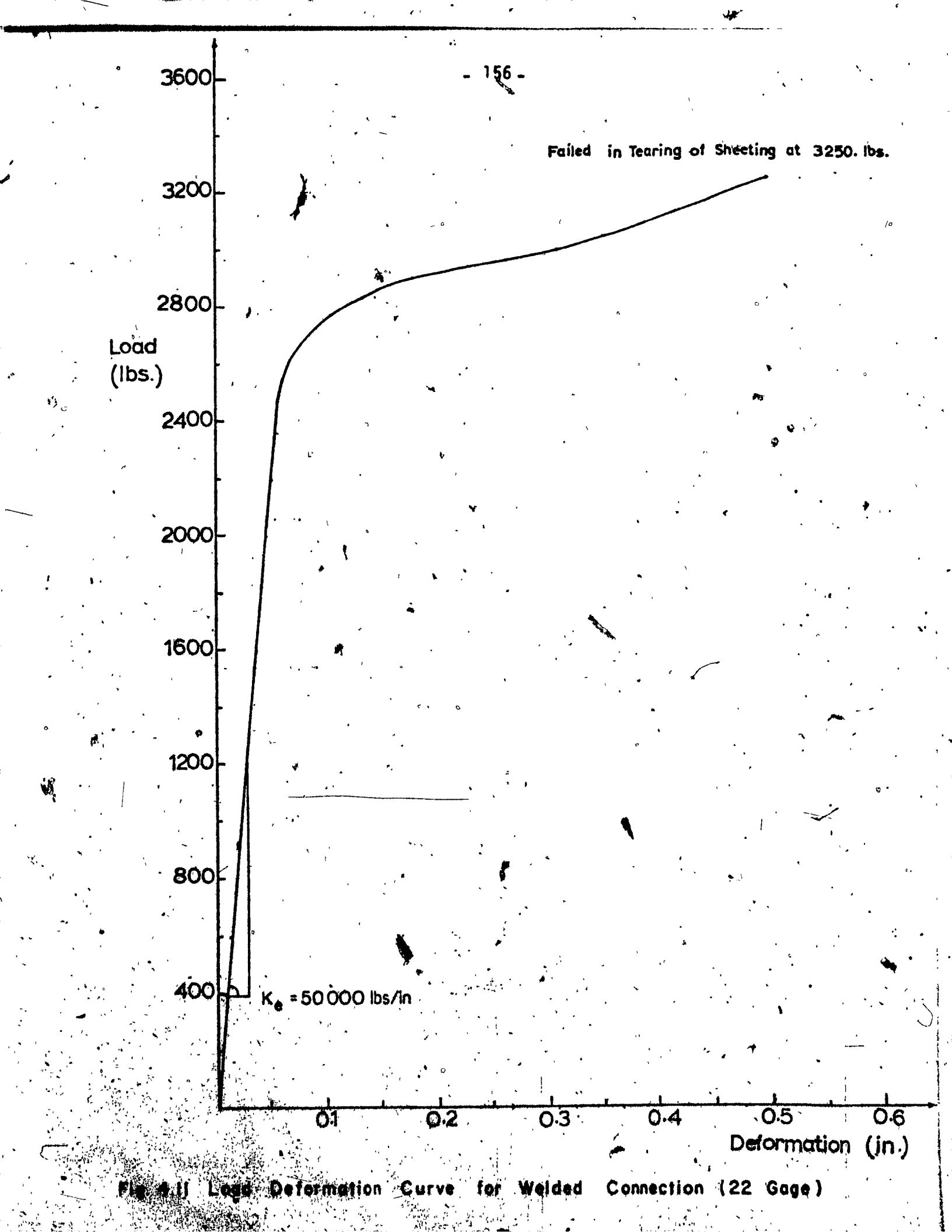

Fig 4.11 Load Deformation Curve for Welded Connection (22 Gage)

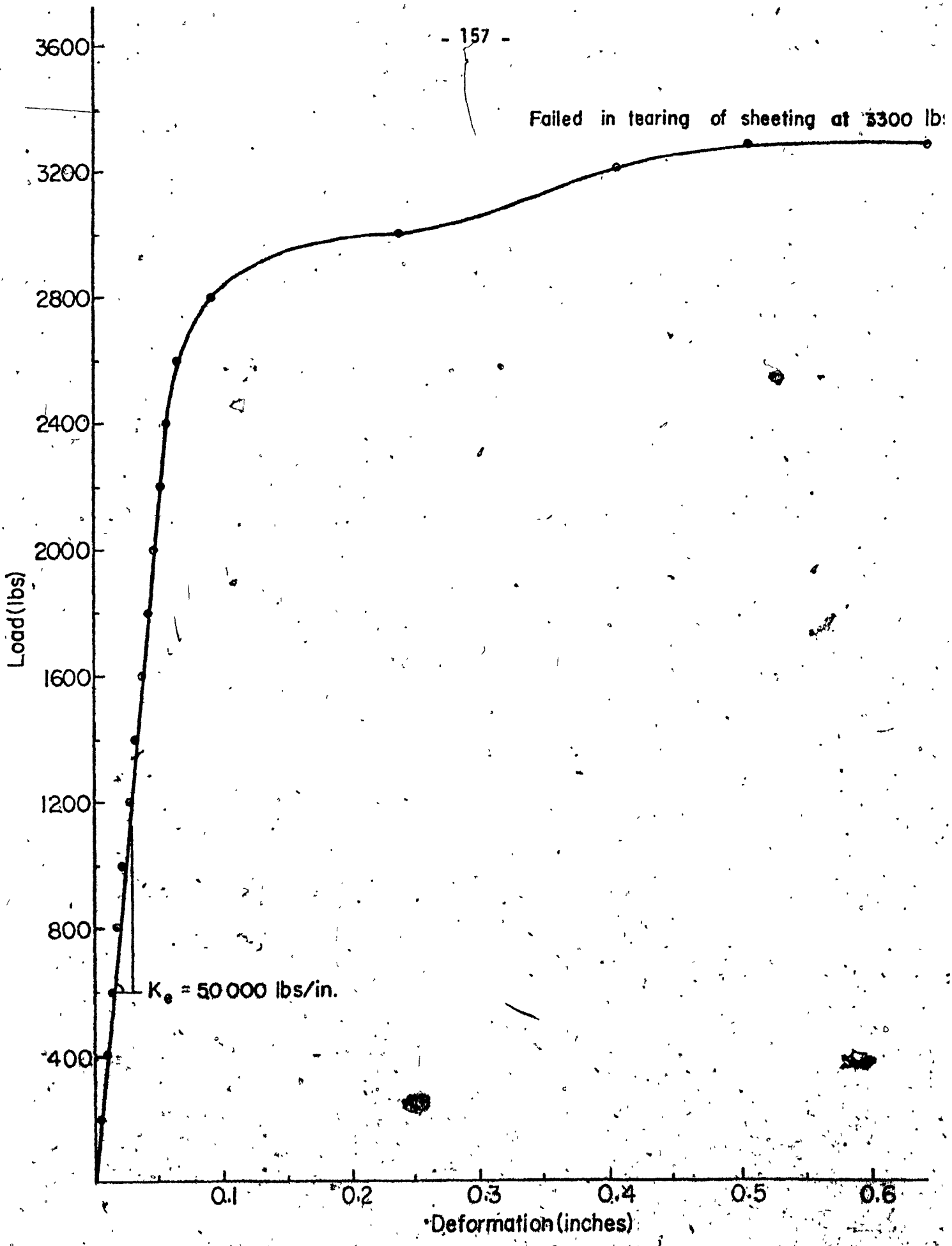

Fig. 4.12 Load Deformation Curve for Welded Connection (22 Gage)

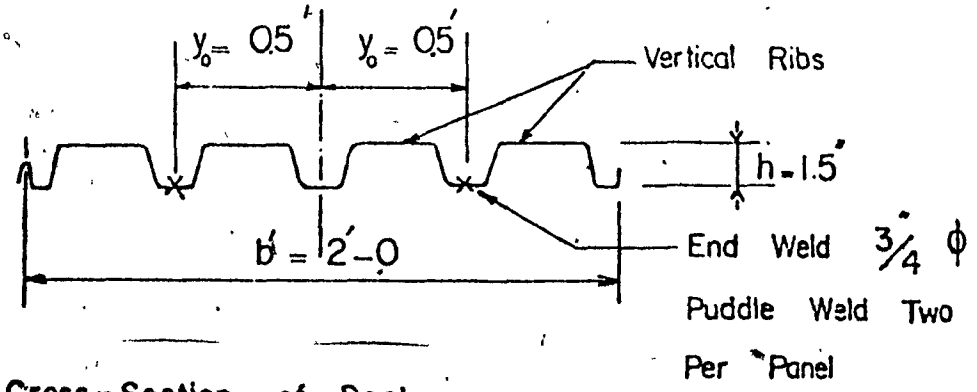

Fig. 4.14 Cross-Section of Deck

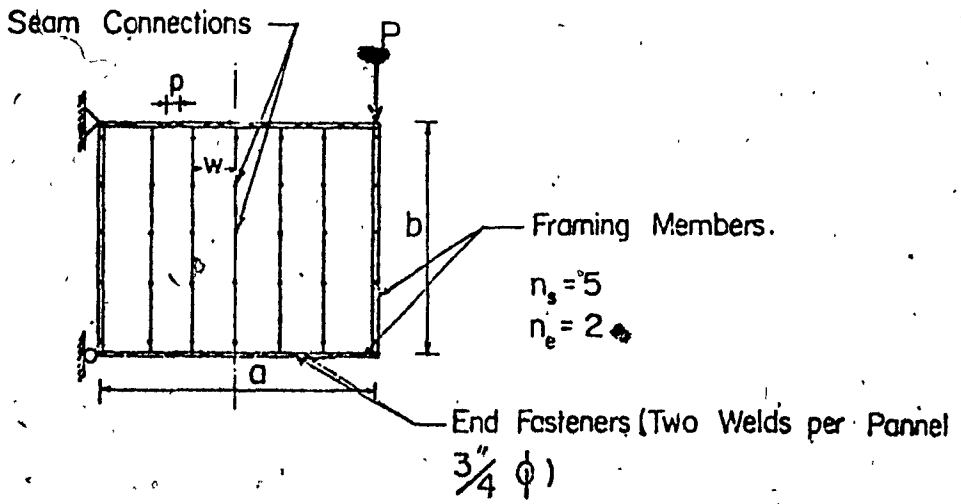

Fig. 4.13 Diaphragm Panels Fixed on All Sides

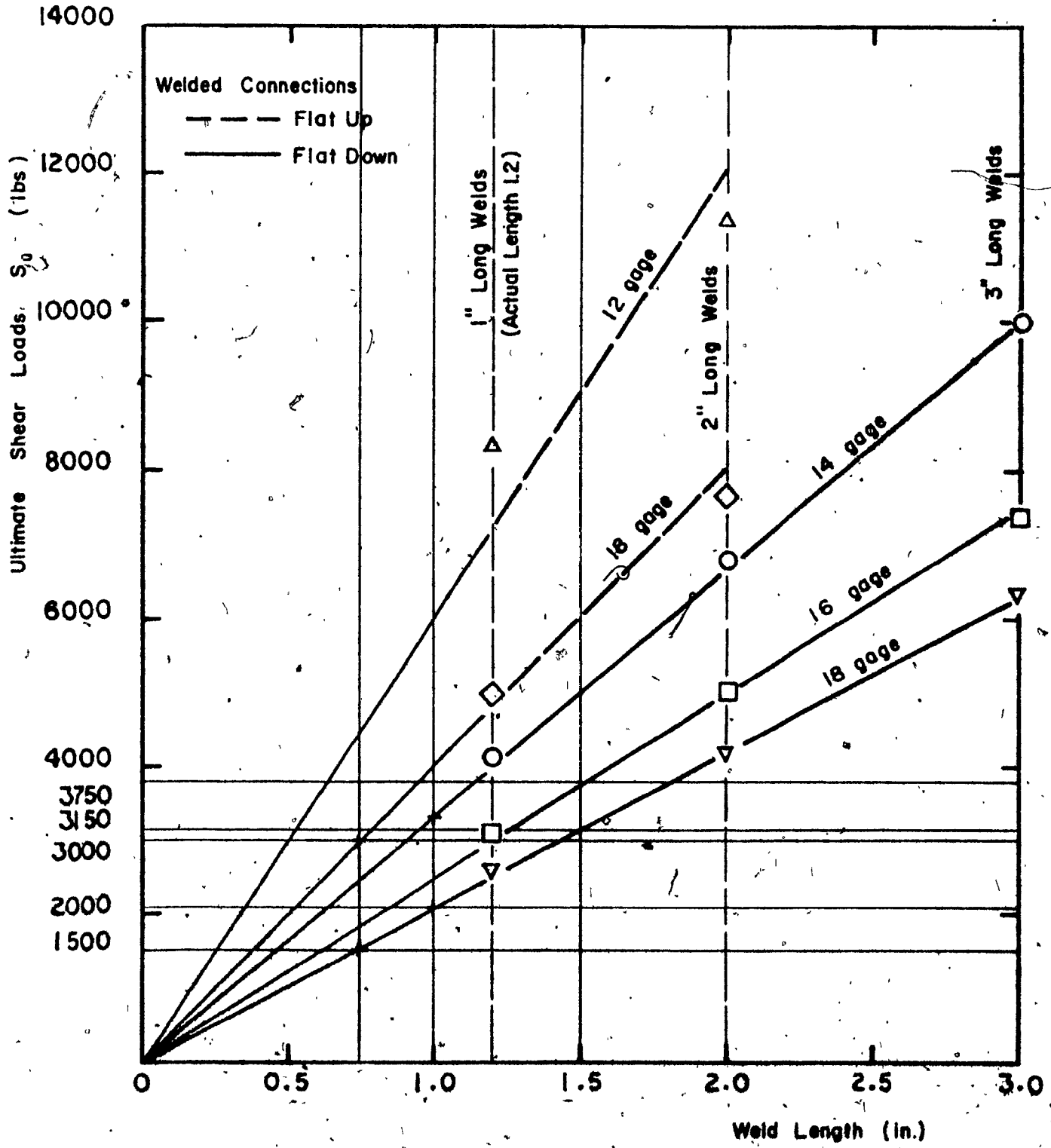

Fig. 4.14a Variation of Ultimate Shear Capacity of Welded Connections With Weld Length. (Ref. 20)

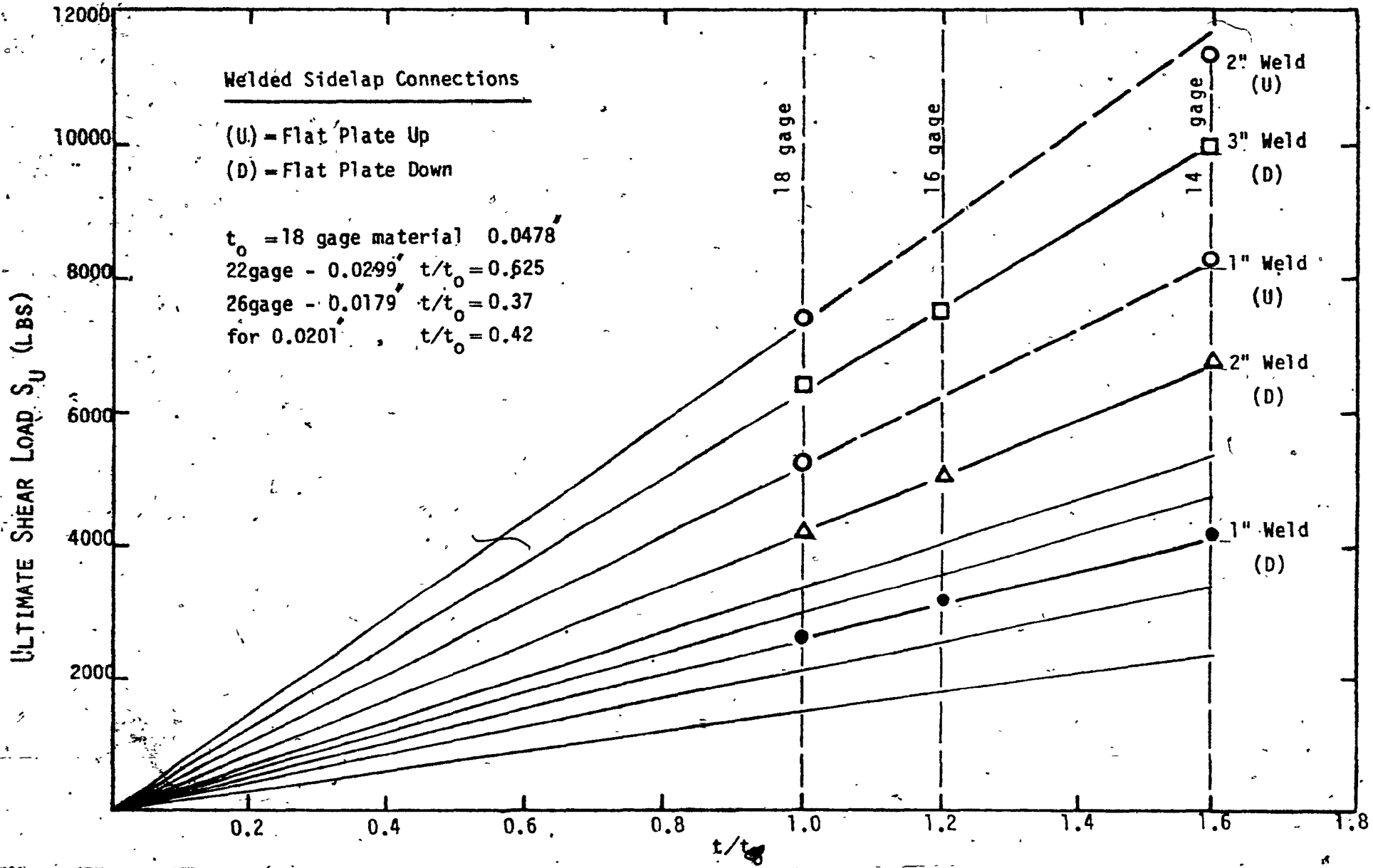

Fig. 4.15 Variation of Ultimate Shear Capacity of Welded Connections With Material Thickness. (Ref. 20)

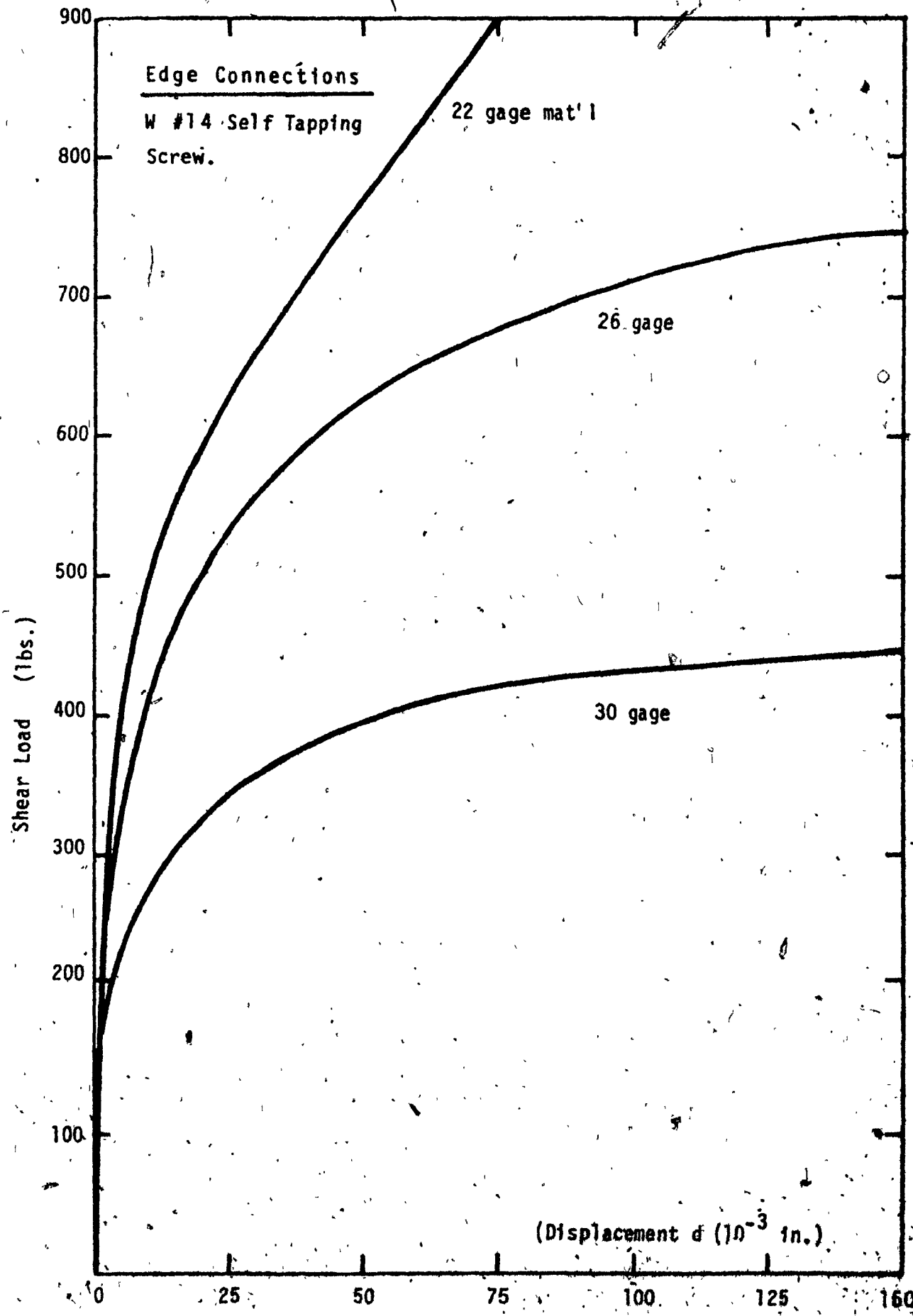

Fig. 4.16 Load vs. Slip for 14 Screw Fastened Edge Connections. (Ref. 20)

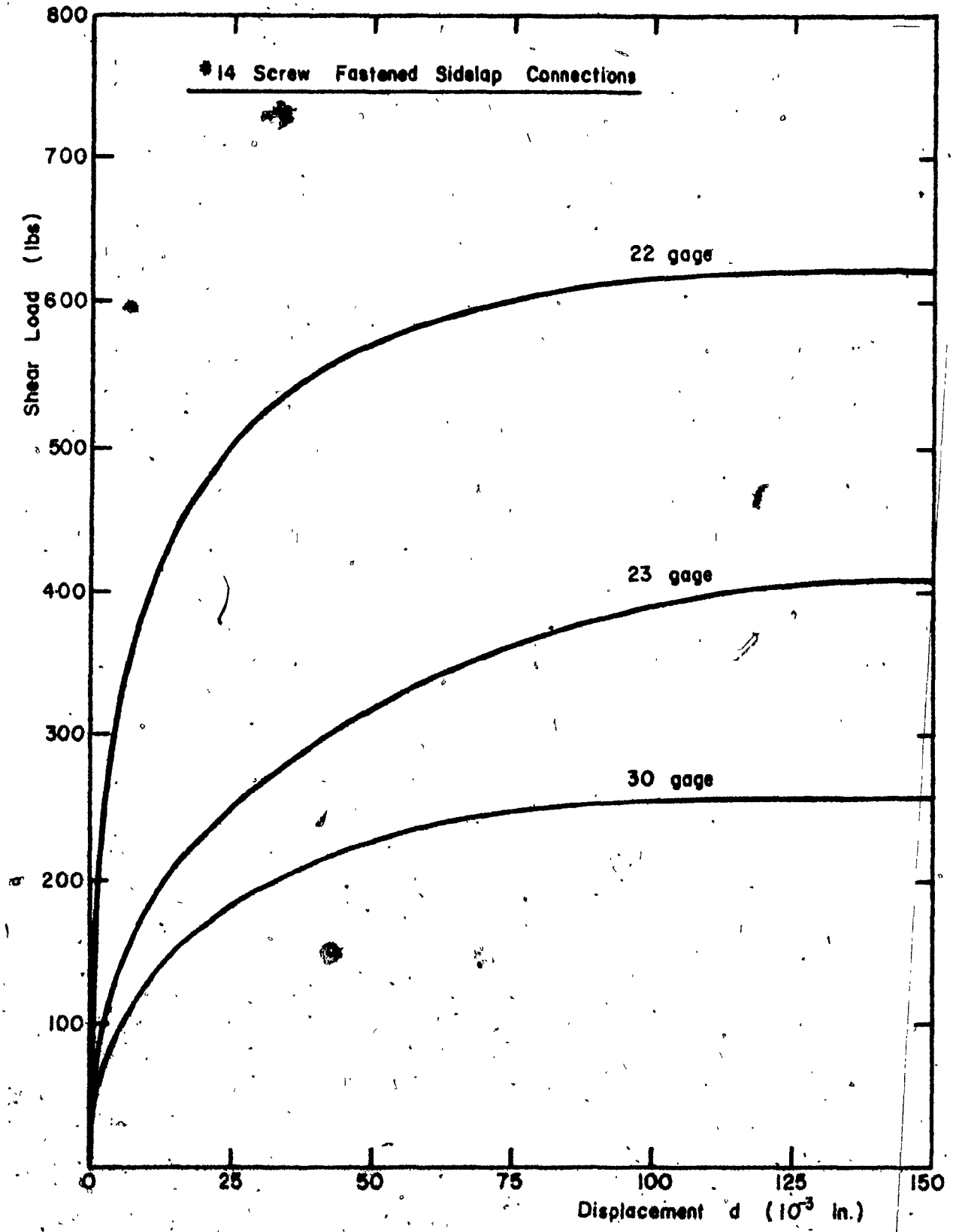

Fig. 4.17. Load vs. Slip for #14 Screw Fastened Sidelap Connection. (Ref. 20)

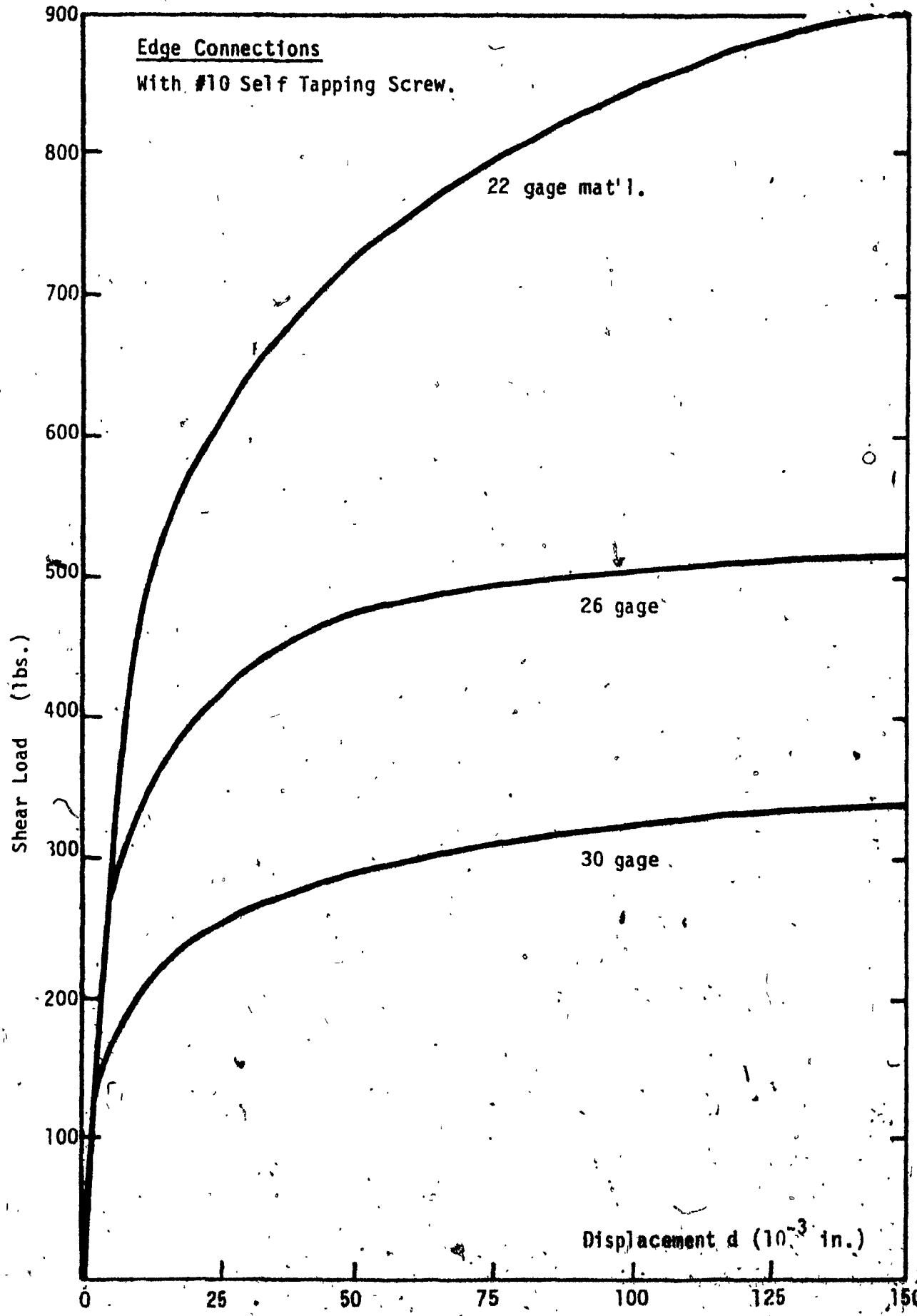

Fig. 4.18 Load vs. Slip for #10 Screw Fastened Connections (Ref. 20)

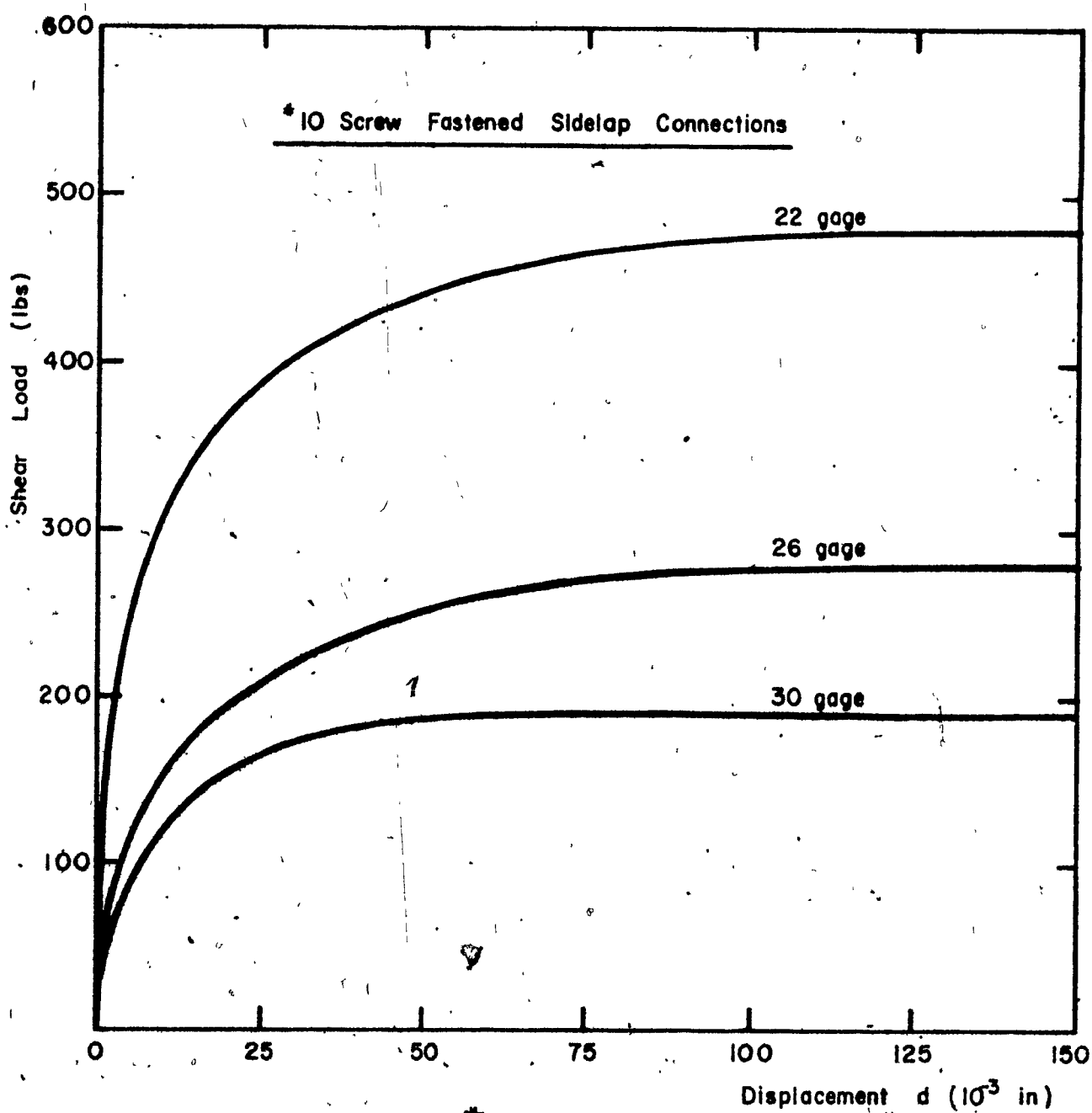

Fig. 4.19. Load vs. Slip for #10 Screw Fastened Sidelap Connections (Ref. 20)

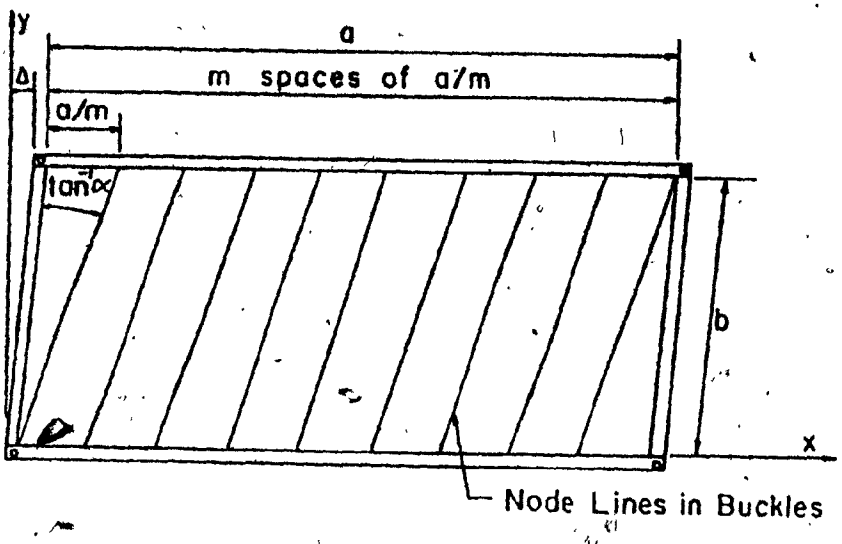

Fig. 5.1. Buckled Waves in Diaphragm (Ref. 29)

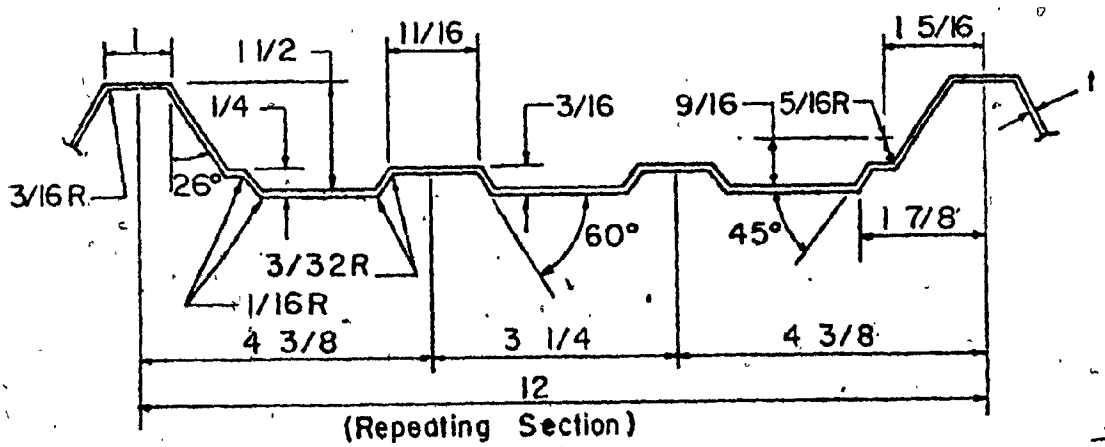

All radii are inside dimensions and all dimensions are given in inches.

Panel Properties

$I = 2.82 \times t$ in^4 (where t is the thickness of the sheet)

s = 14.06 in

q = 12.0 in

$E = 30 \times 10^6$ psi

$G = 11.5 \times 10^6$ psi

t = 0.0191 or 0.0217 in

Fig. 5.2. Cross-Section of Panel Profile (Type B). (Ref. 28)

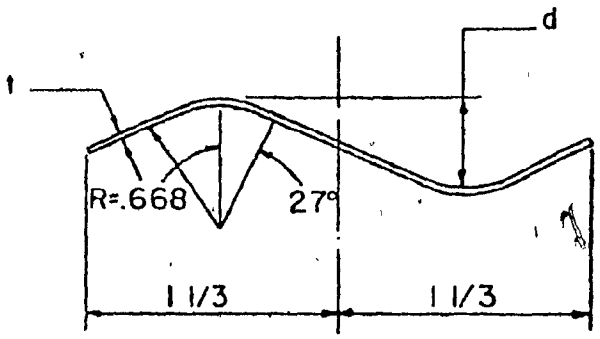

(Repeating Cross-Section)
dimensions given in inches

s = 12.9 in
q = 12.0 in
$I = .385 t$ in^4/ft (where t = thickness of the sheet)
d = .470 in (20 gage steel)
d = .496 in (24 gage steel)
$E = 30 \times 10^6$ psi
$G = 11.5 \times 10^6$ psi
t = 0.0243 or 0.0277 in

Fig. 5.3 Cross-Section of Panel Profile (Type C)
(Ref. 28)

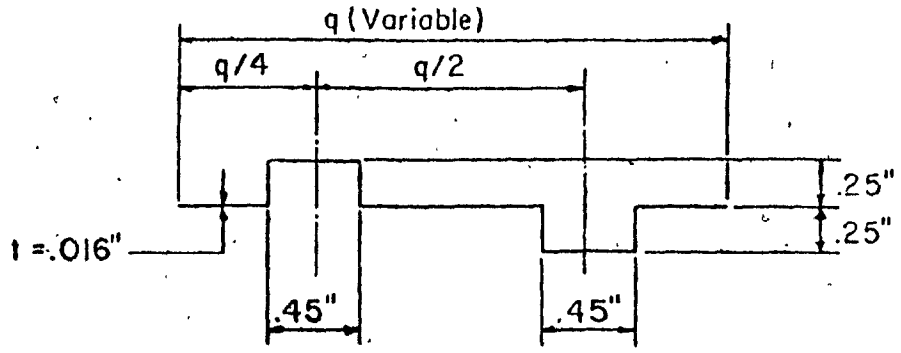

(Cross-Section of Panel)

Panel Properties

$I = 1.245 \times 10^{-3}$ in^4
q = Variable (3.48, 2.33, 5.55, 2.37, 4.79, 4.04 and 3.48 in)
s = Variable (4.42, 3.29, 6.47, 3.33, 5.71, 4.97 and 4.42 in)
$E = 10 \times 10^6$ psi
t = 0.016 in

Fig. 5.4 Cross-Section of Panel Profile (Type A)
(Ref. 28)

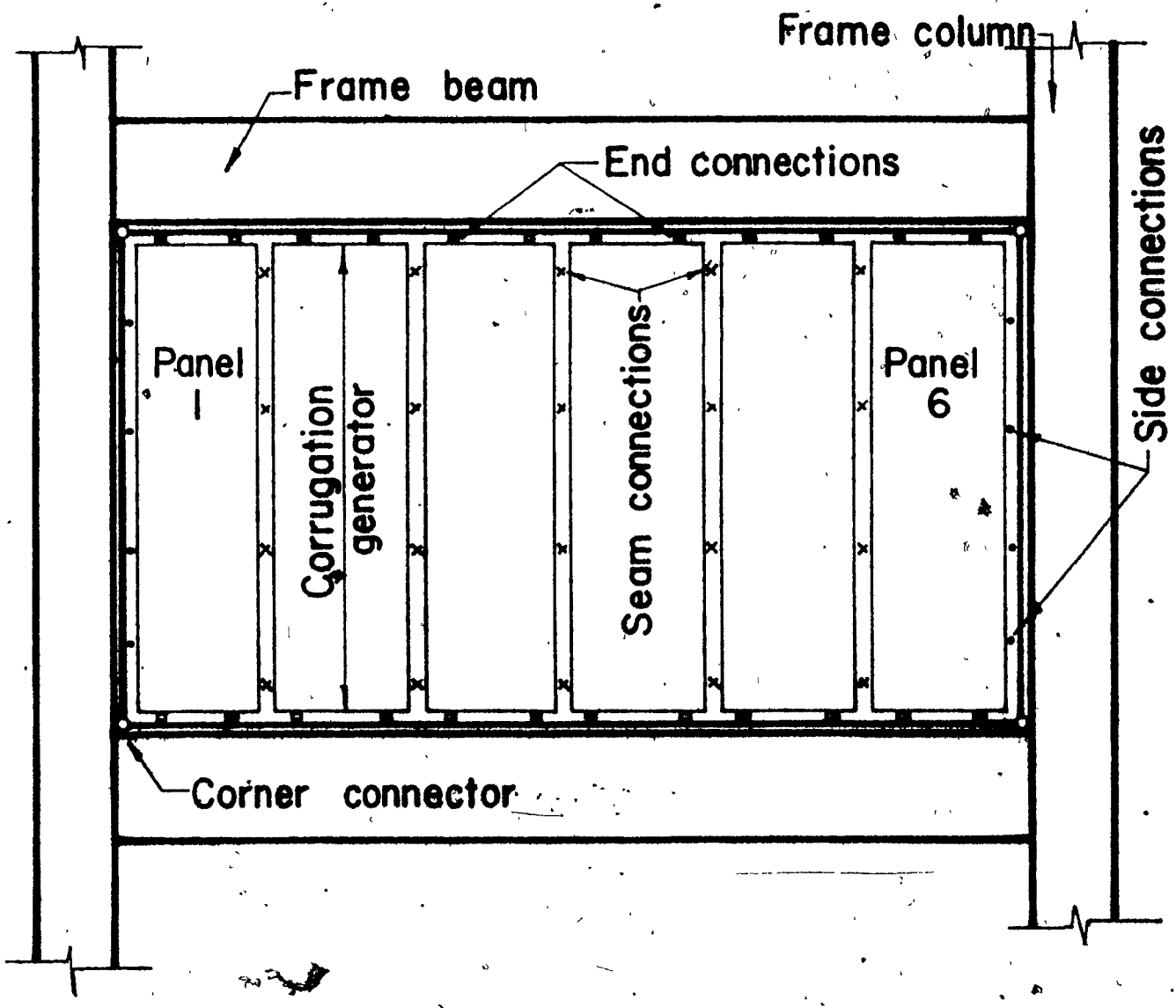

Fig 6.1 Connection Between Cladding and Frame (Ref. 38)

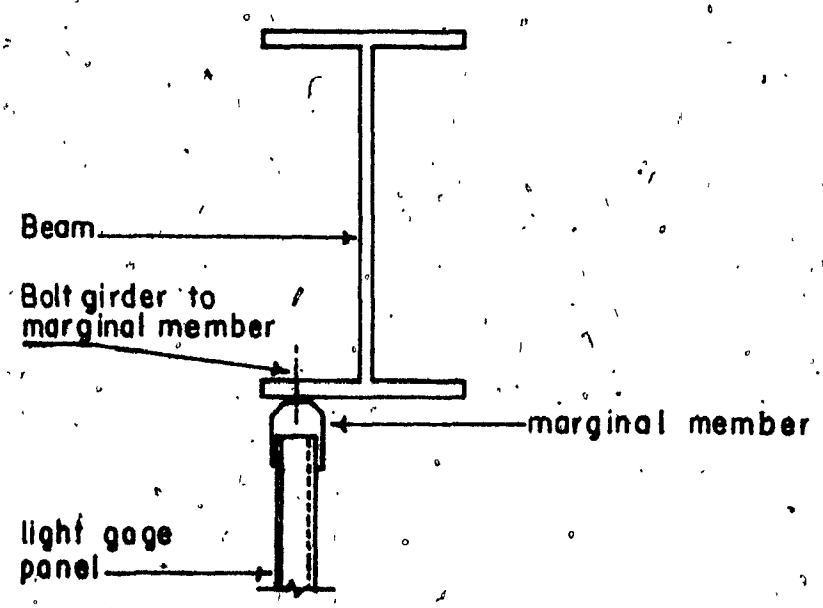

Section 'A-A' (Ref. 9)

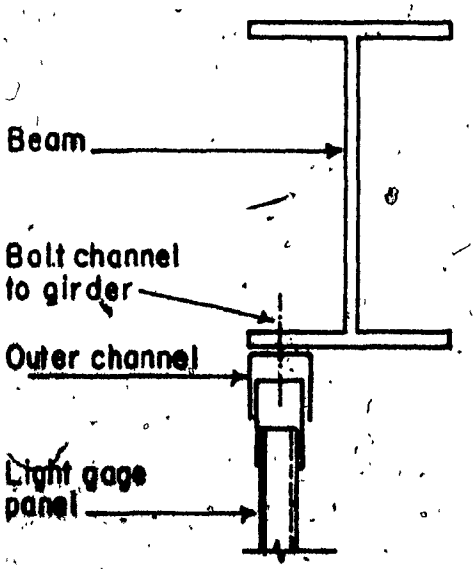

Alternate Section 'A-A' (Ref. 9)

Fig. 6.2 Details of Connection Between Cladding and Frame. (Ref. 9)

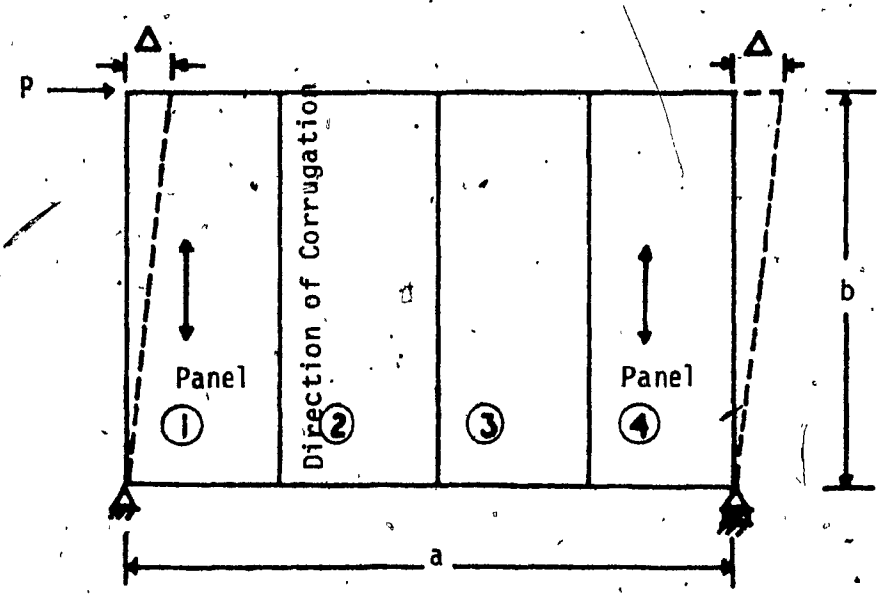

P = Shear Load on Cladding (Less Than or Equal to $0.4\,P_u$).

Δ = Shear Deflection Corresponding to Load P.

a, b = Dimensions of Cladding.

P_u = Ultimate Shear Strength of Cladding.

Shear Stiffness , $S = \frac{P}{\Delta}$ Kips/inch or Kn/mm.

Fig. 6.3. Shear Stiffness of Cladding.

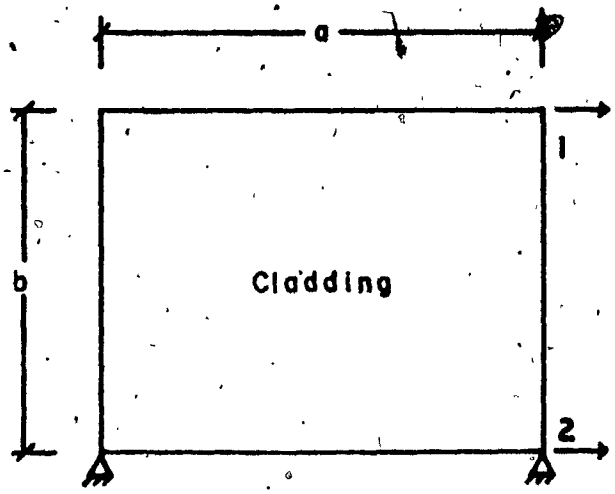

Stiffness coefficients.

Case i) $D_1 = 1$, $D_2 = 0$

$S_{11} = S \times 1$, $S_{21} = -S \times 1$.

Case ii) $D_2 = 1$, $D_1 = 0$

$S_{22} = S \times 1$, $S_{12} = -S \times 1$.

Where "S" is the shear stiffness of the cladding and is obtained as $S = \frac{G'a}{b}$

Where G' = Shear modulus of cladding.

Fig. 6.4. Displacement Coordinates 1 and 2
(No Axial Deformation of Columns)

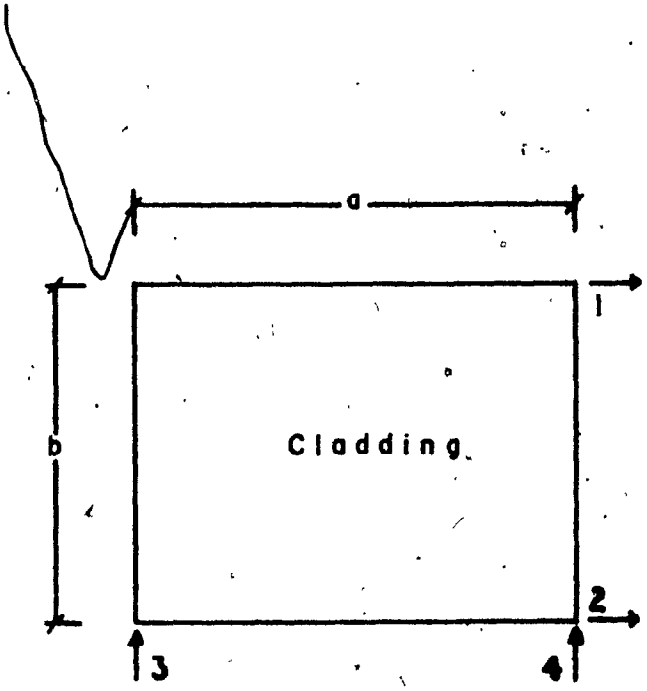

Fig. 6.5. Displacement Coordinates 1, 2, 3 and 4.
(With Axial Deformation of Columns.)

i. $D_1 = 1$, $D_2 = D_3 = D_4 = 0$. ($D_1, D_2, \ldots$ = Displacement at the joint).

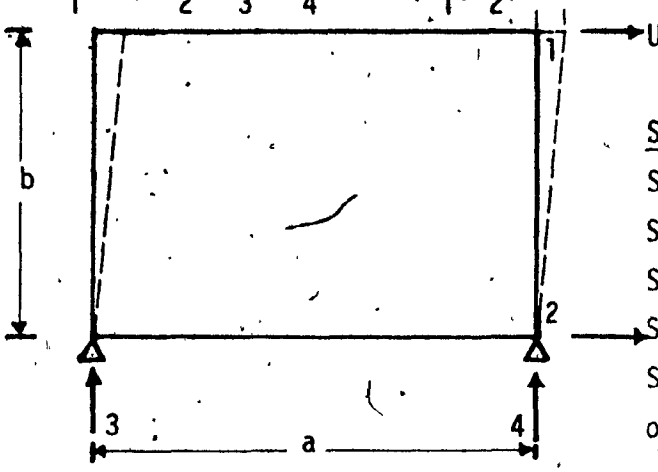

Stiffness Coefficients:

$S_{11} = Sx1$

$S_{21} = -Sx1$

$S_{31} = S.b/a.$

$S_{41} = -S.b/a$

S is the shear stiffness of the Cladding.

ii. Stiffness Coefficients for $D_2 = 1$, $D_1 = D_3 = D_4 = 0$.

For this case the coefficients may be written as:

$S_{22} = Sx1$, $S_{21} = -Sx1$, $S_{23} = -S.b/a$ and $S_{24} = S.b/a$

iii. $D_3 = 1$, $D_4 = D_2 = D_1 = 0$.

For this case, the Stiffness of the Cladding in the direction of D_3 must be known and can be obtained as: $S' = S.\frac{b^2}{a^2}$ [42]

Using this relation, the Stiffness Coefficients can be derived as follows:

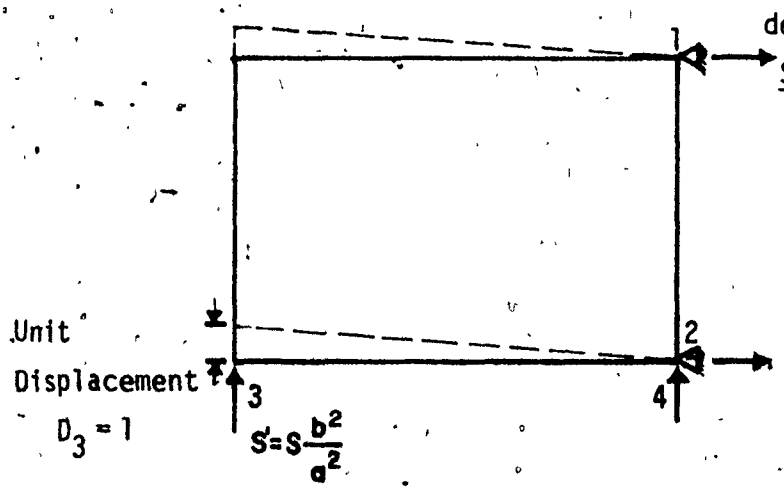

Stiffness Coefficients:

$S_{33} = S\frac{b^2}{a^2}$

$S_{34} = -S\frac{b^2}{a^2}$

$S_{32} = -S\frac{b}{a}$

$S_{31} = S\frac{b}{a}$

Similar to the above case , the stiffness coefficients for unit displacement at node 4 may be derived.

Fig. 6.6. Stiffness Coefficients With Axial Deformation Columns.

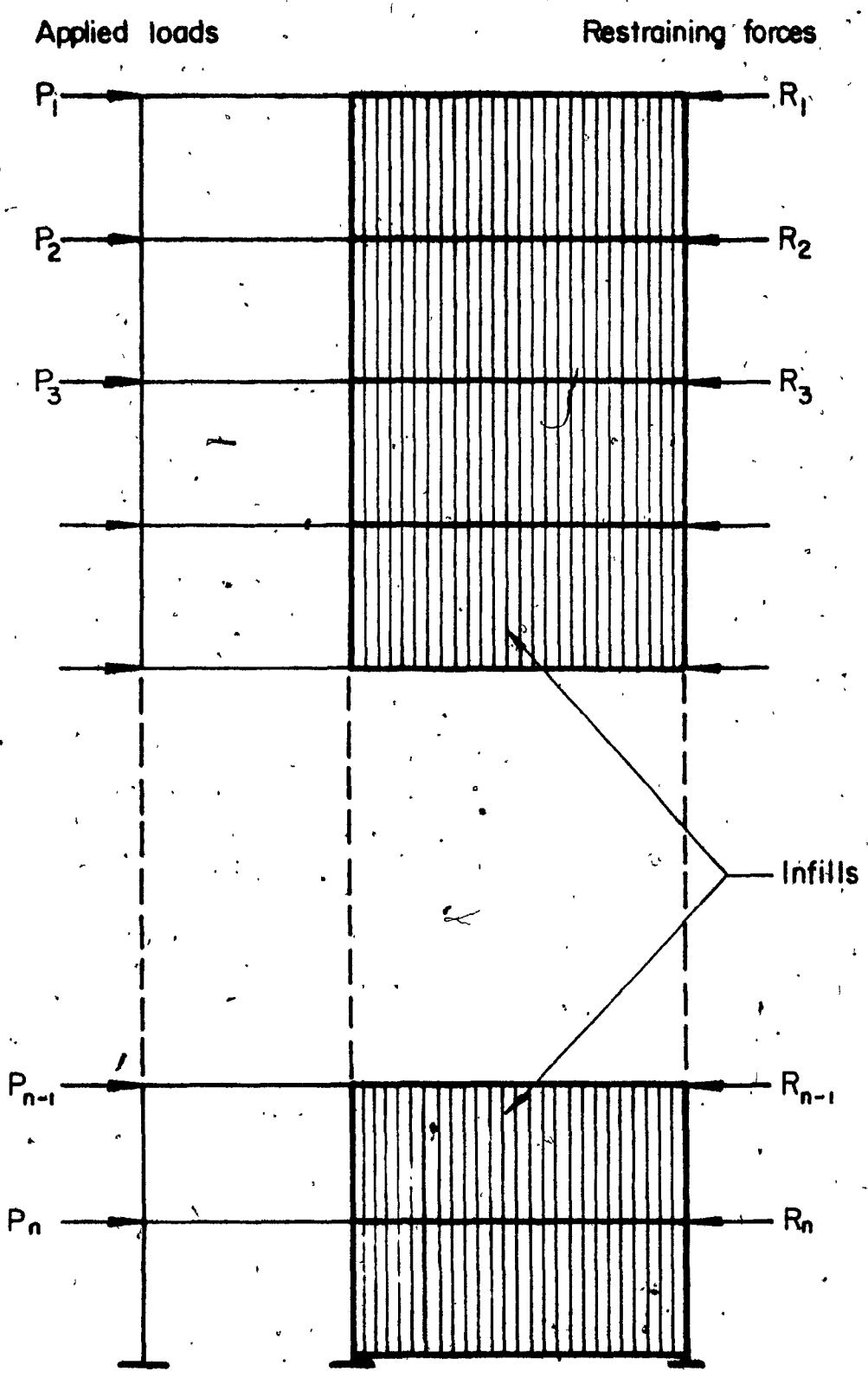

FIG. 6.7 Net Forces on Frame (P-R)

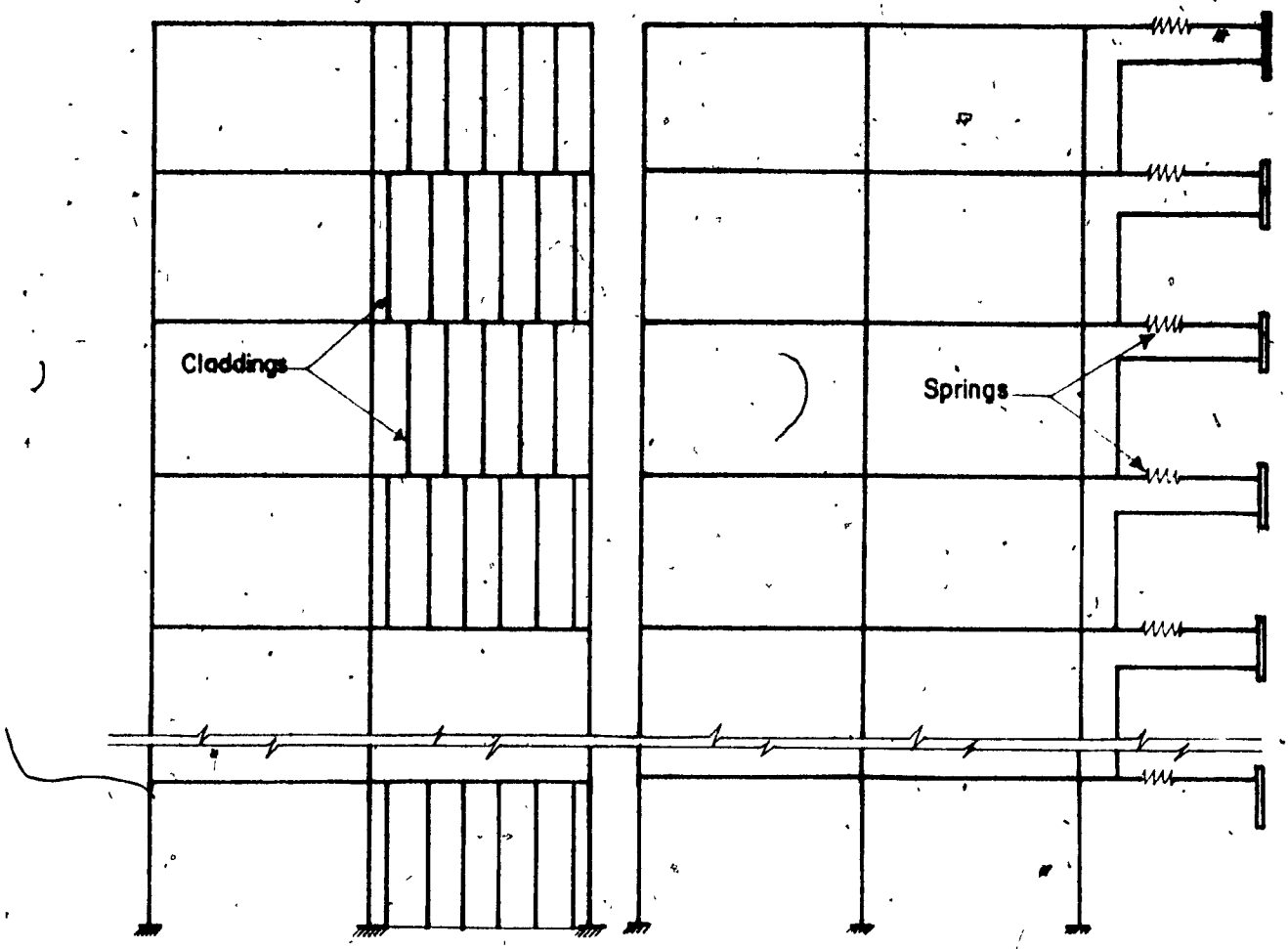

a. Frame with Claddings b. Claddings Replaced by Springs.

Fig. 6.8. Proposed Artifice for Clad Frame Analysis.

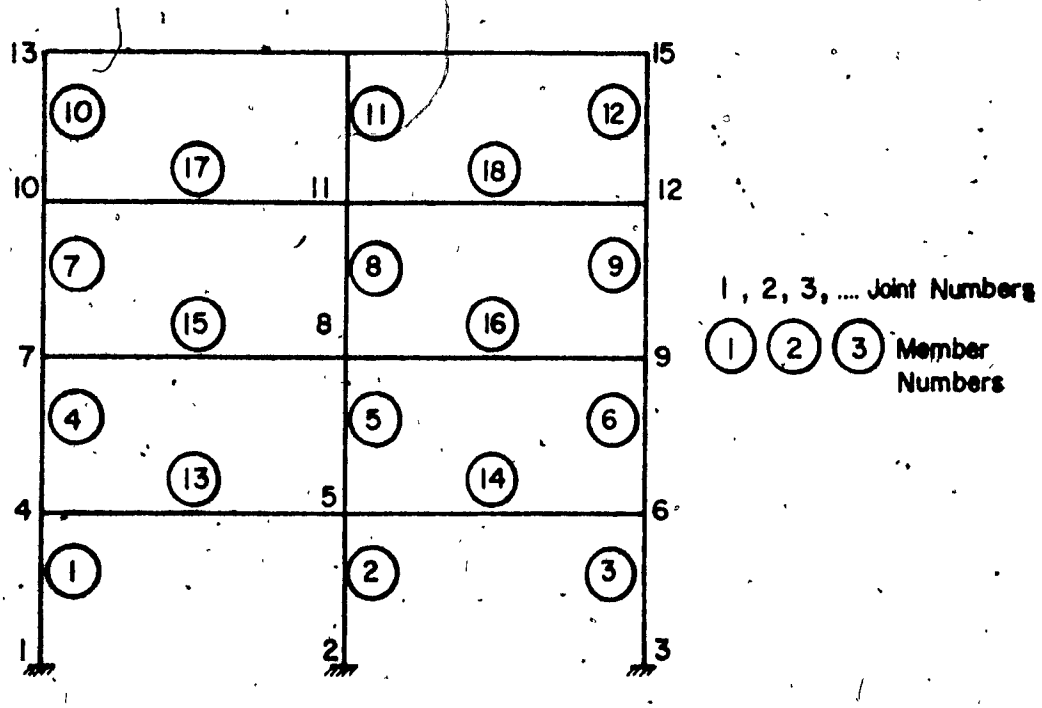

Fig. 6.9. Numbering of Joints and Members

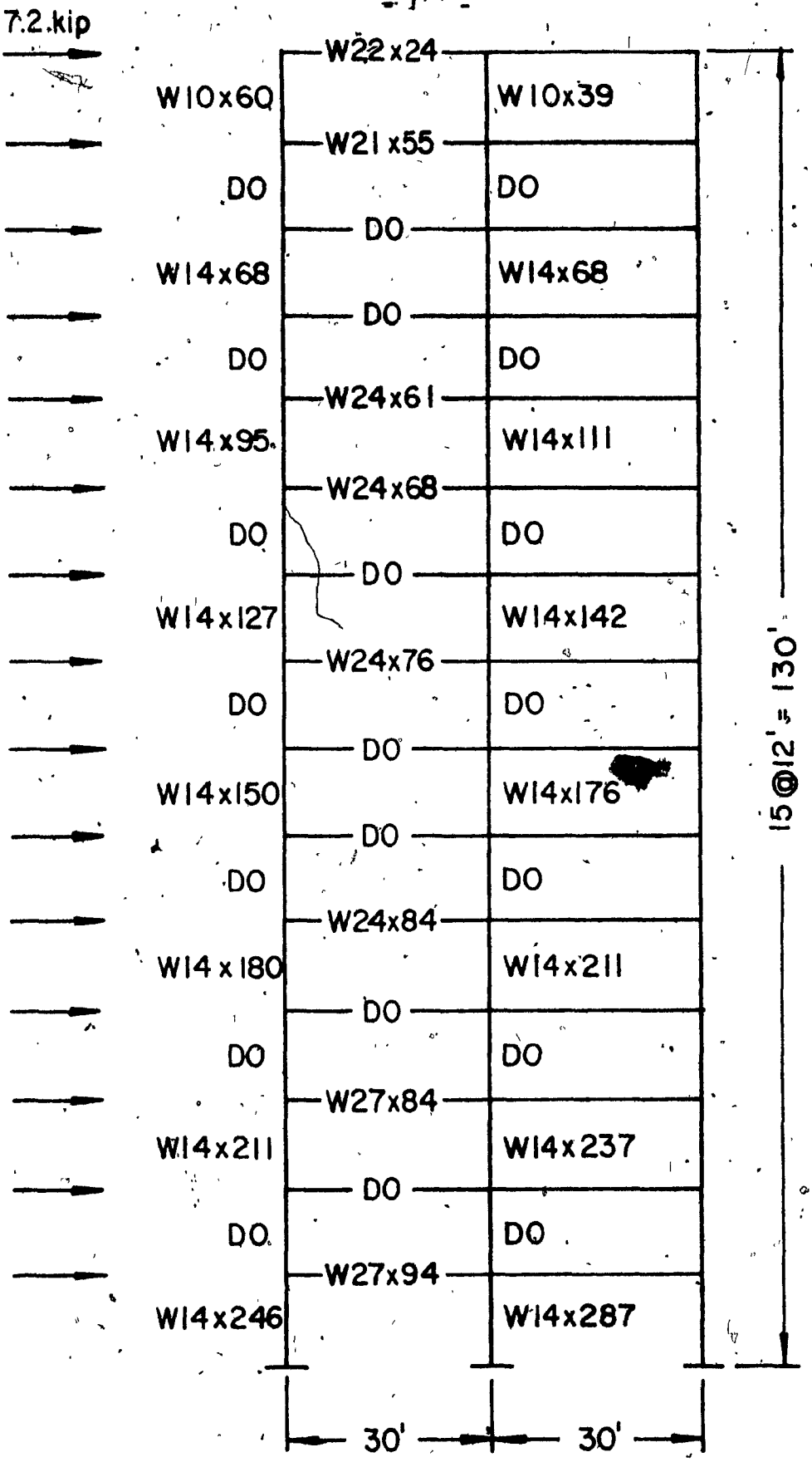

FIG. 6.10. Description of 15 Story Frame (Ref. 10)

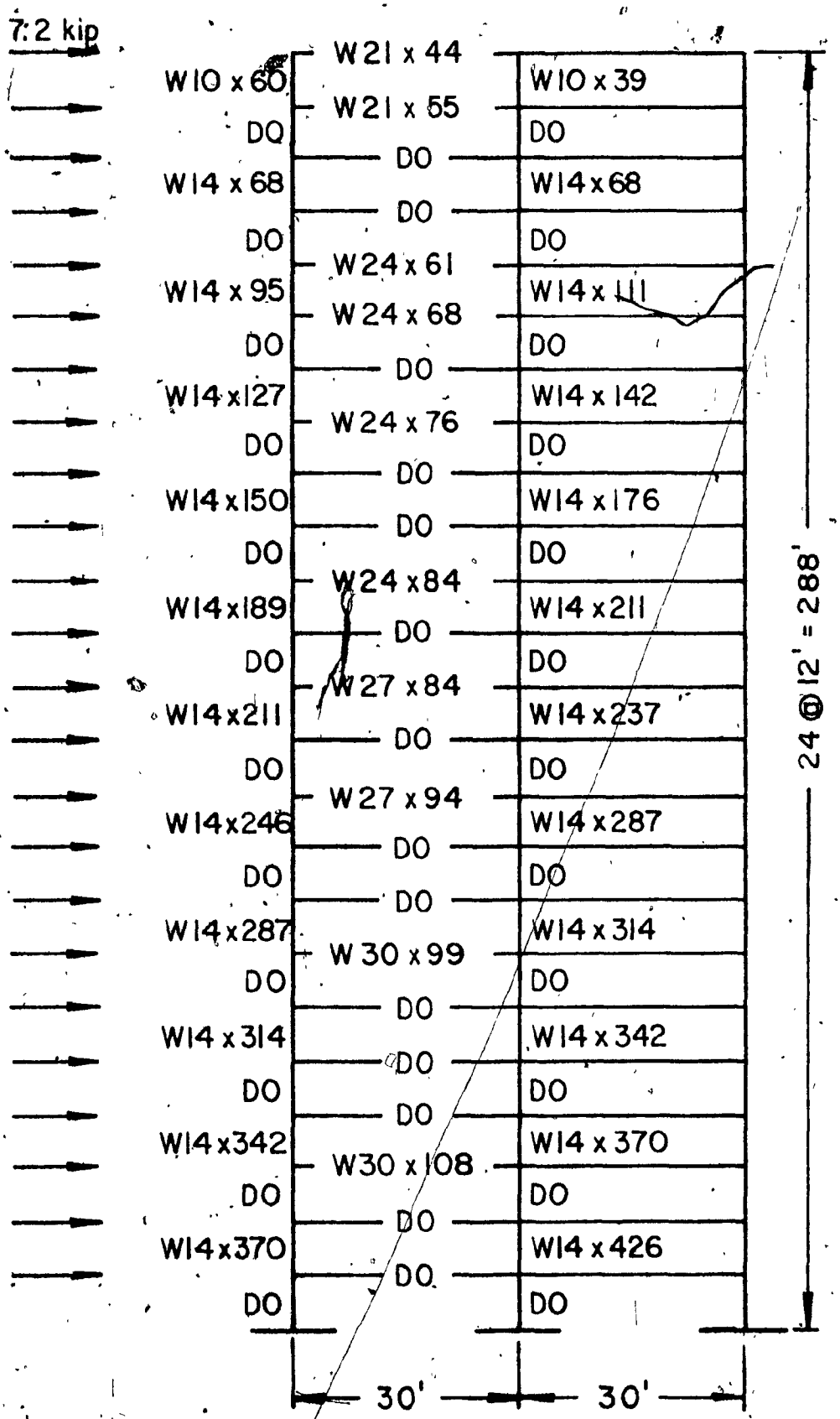

FIG. 6.11. Description of 24 Story Frame (Ref. 10)

Loading:
wind load: 7.2 kips
at each story level.

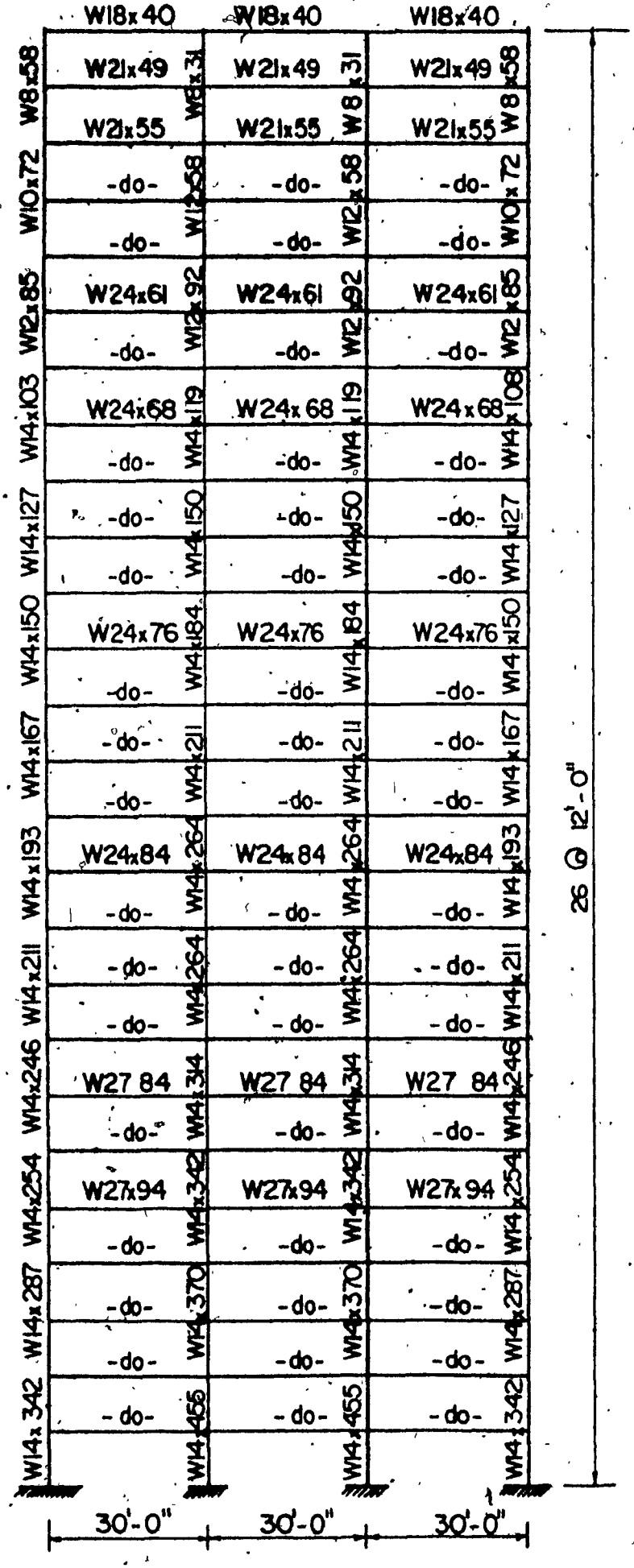

Fig.6.12. Twenty-Six-Story Frame. (Ref. 9)

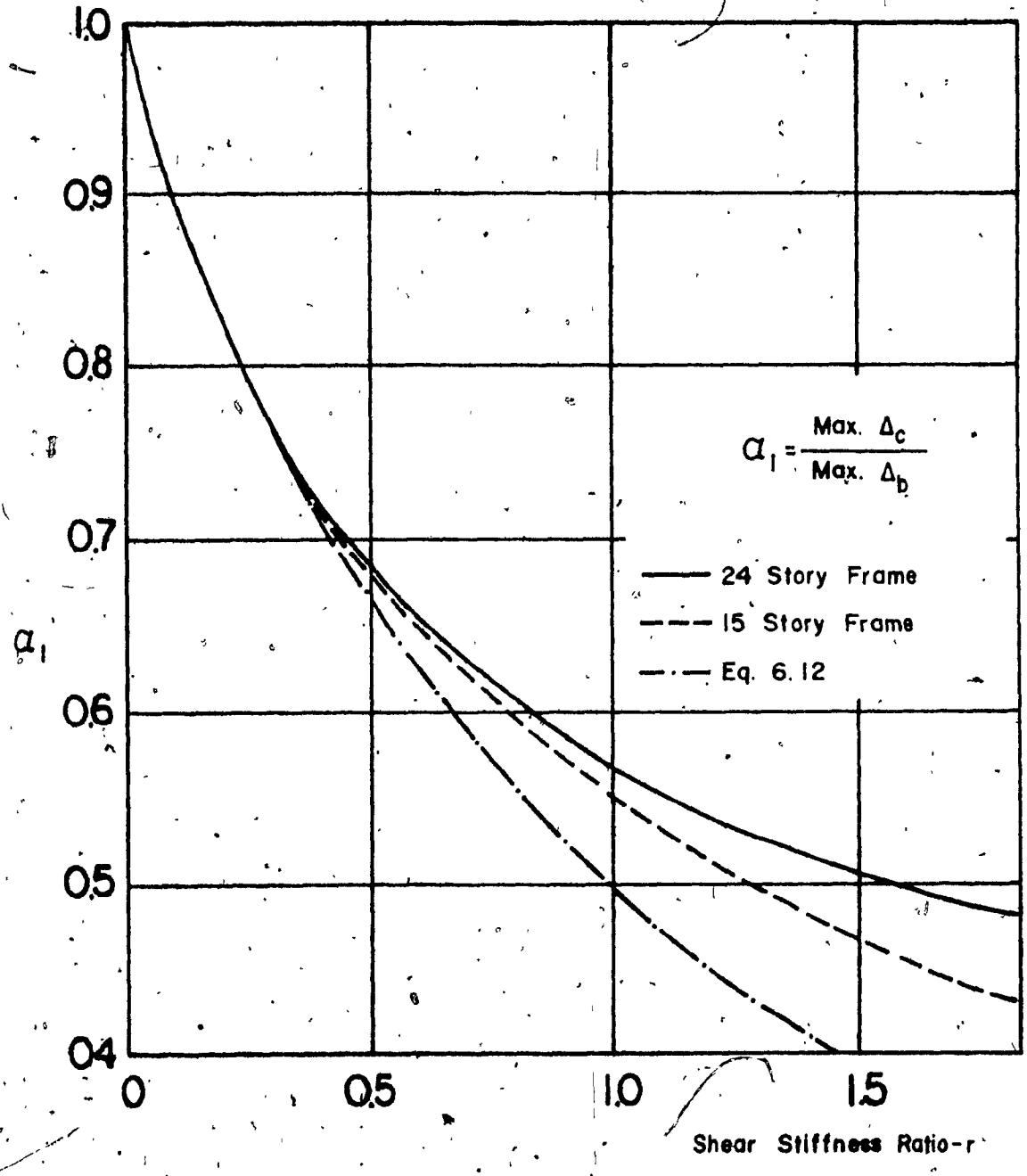

Fig. 6.13. Variation of Maximum Lateral Deflection

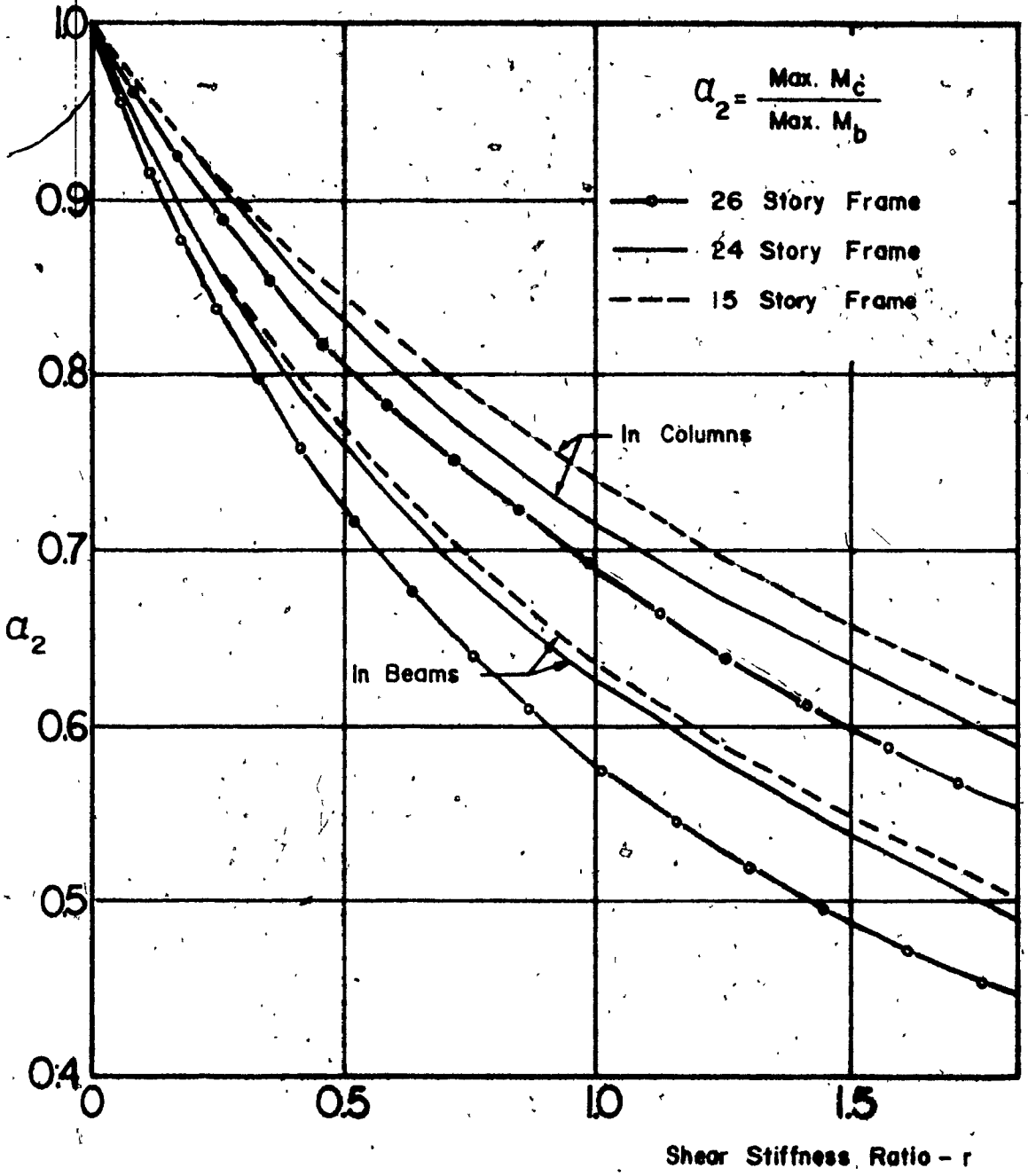

Fig. 6.14. Variation of Maximum Bending Moments.

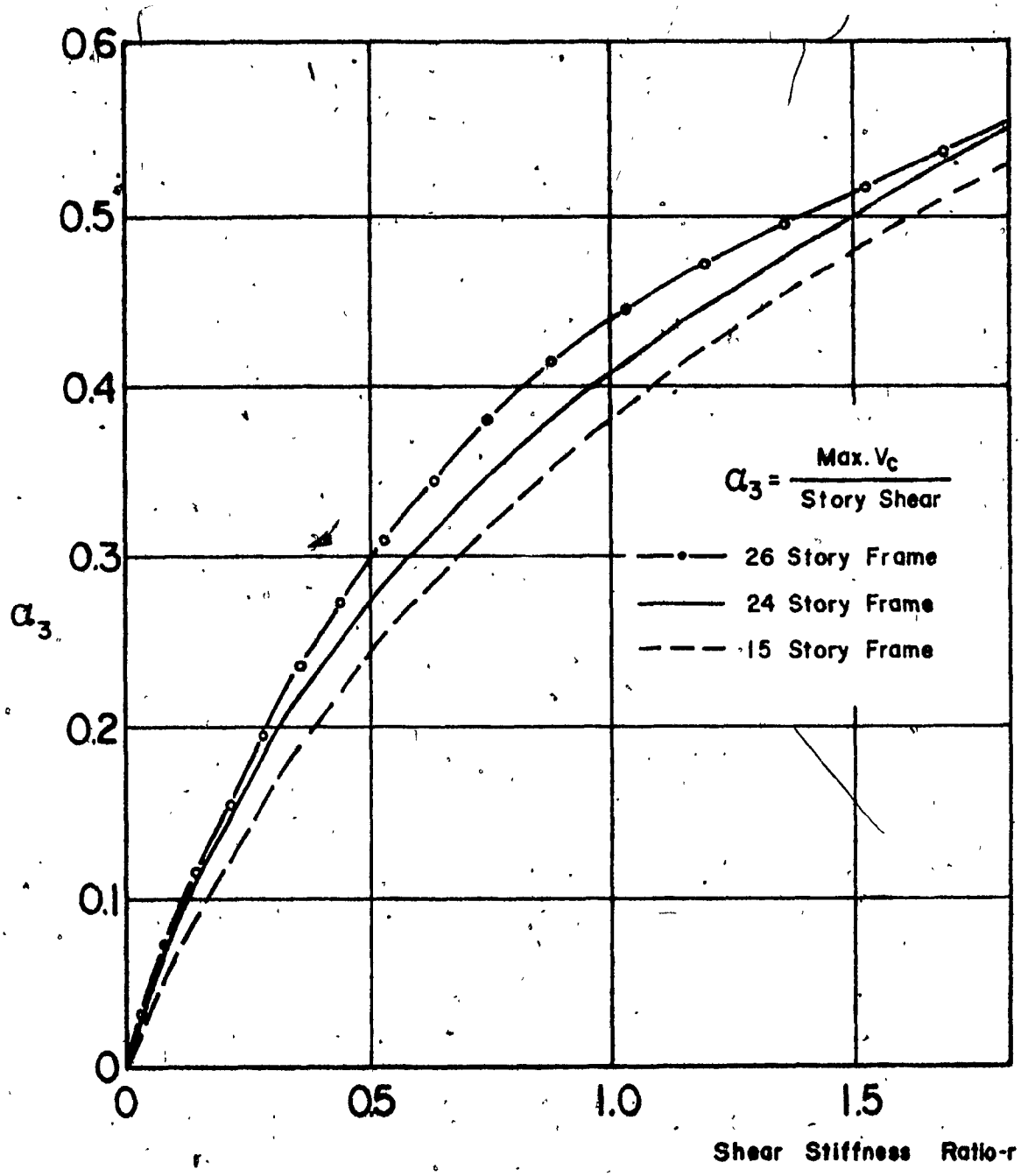

Fig. 6.15. Variation of Maximum Shear Load in Cladding.

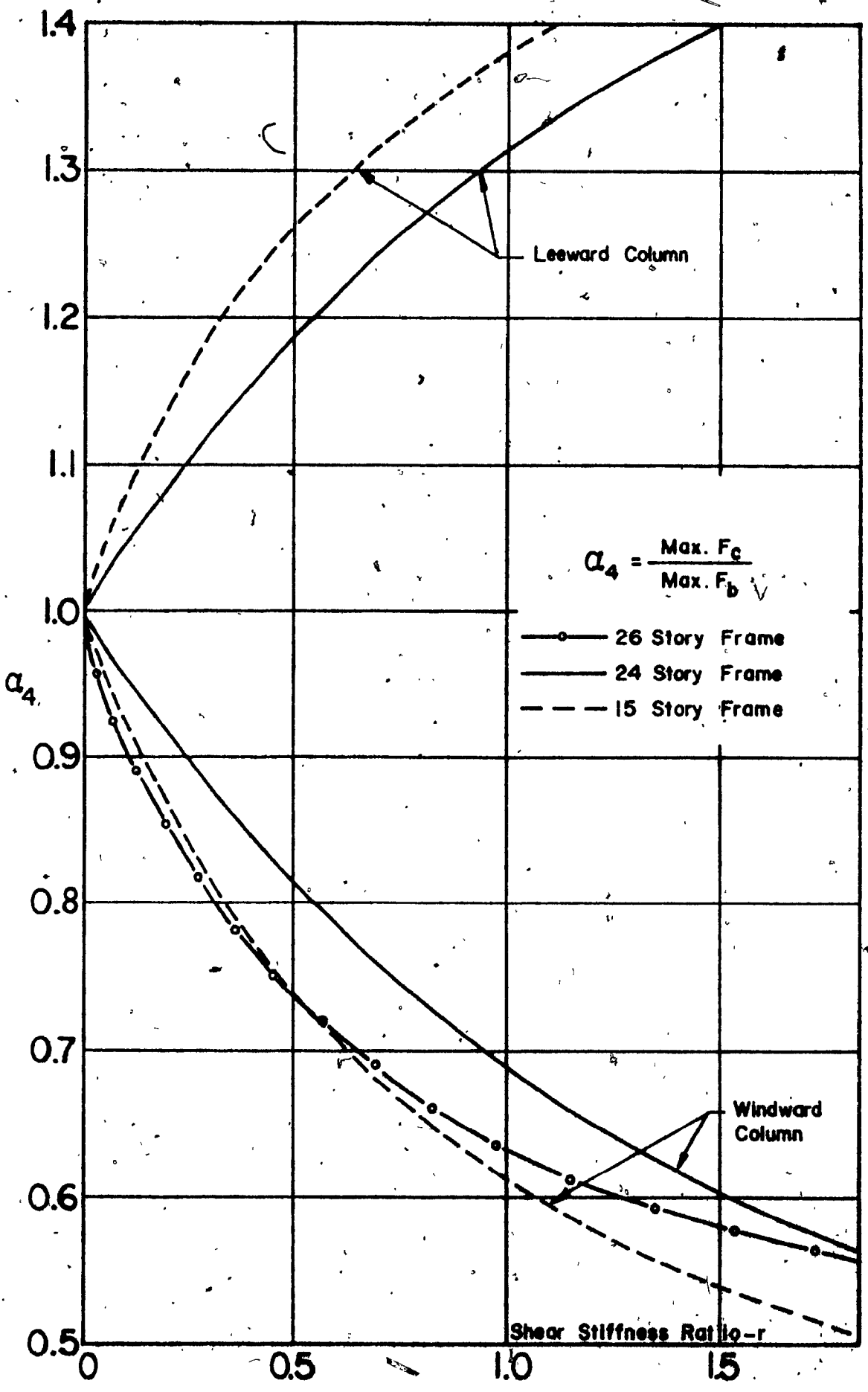

Fig. 6.16. Variation of Maximum Axial Forces in Columns.

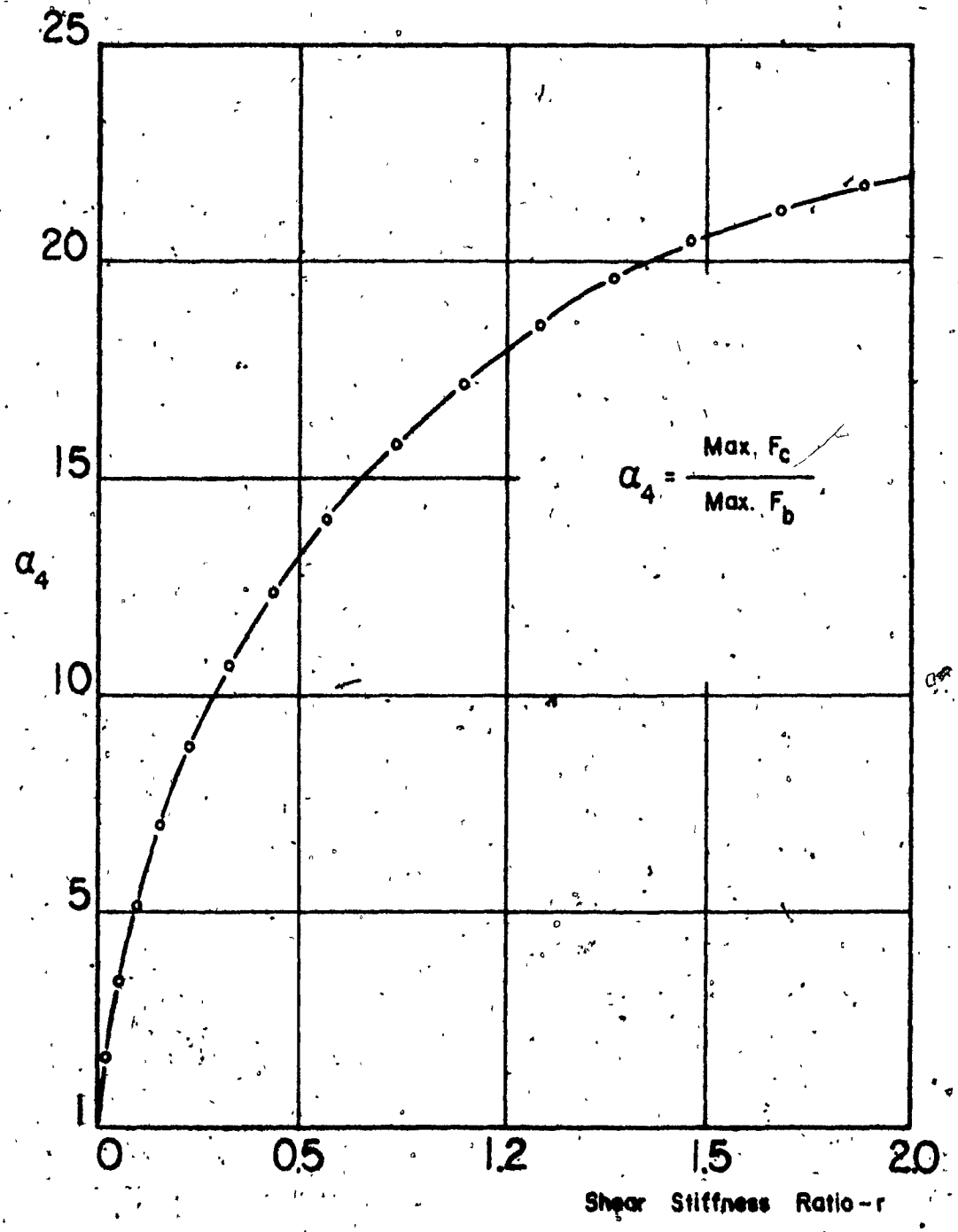

Fig. 6.17. Variation of Axial Forces in the Inferior Columns of 26 Story Frame.

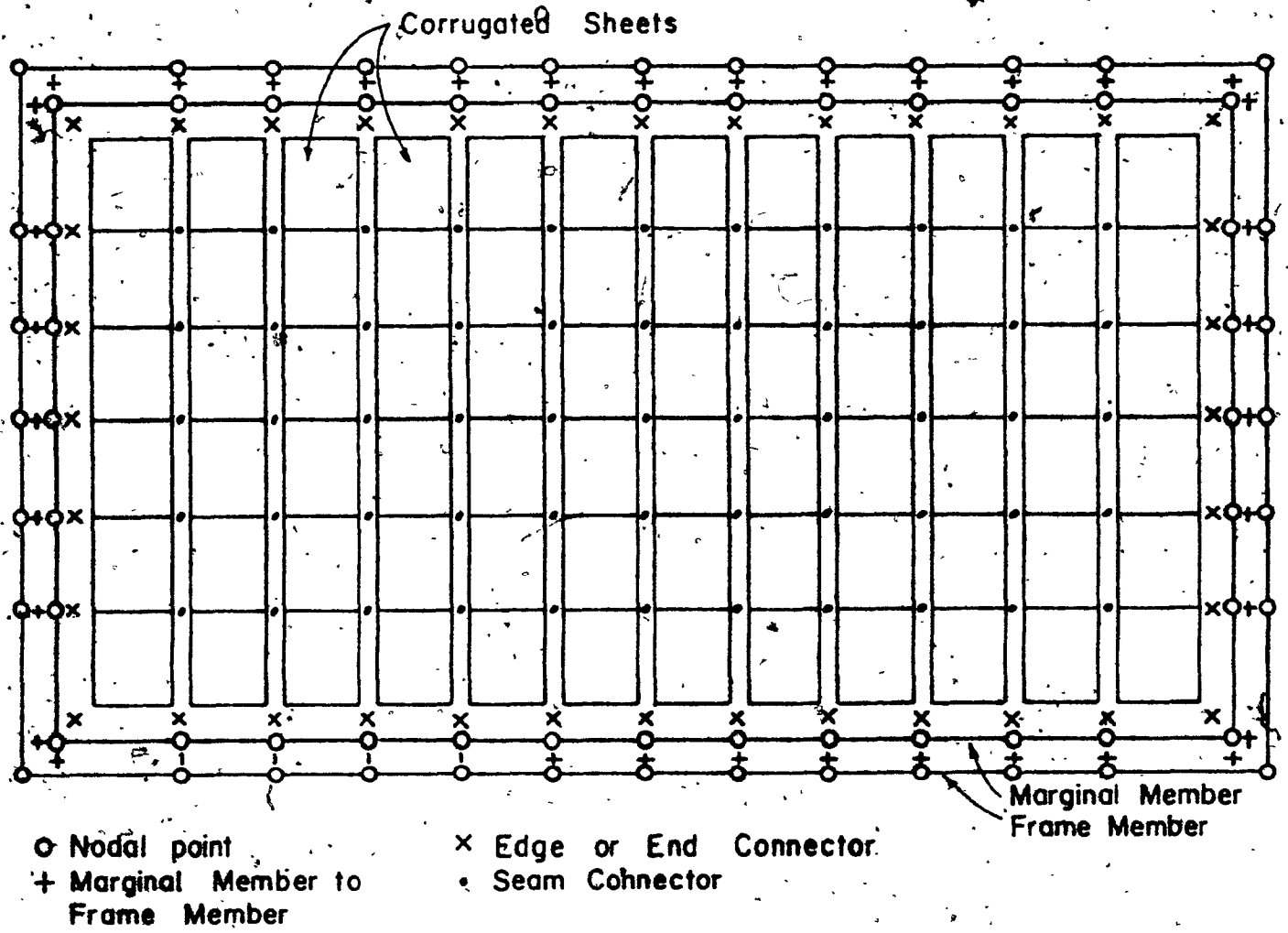

Fig. 6.18. Finite Element Model of a Typical Cladding (Ref. 20)

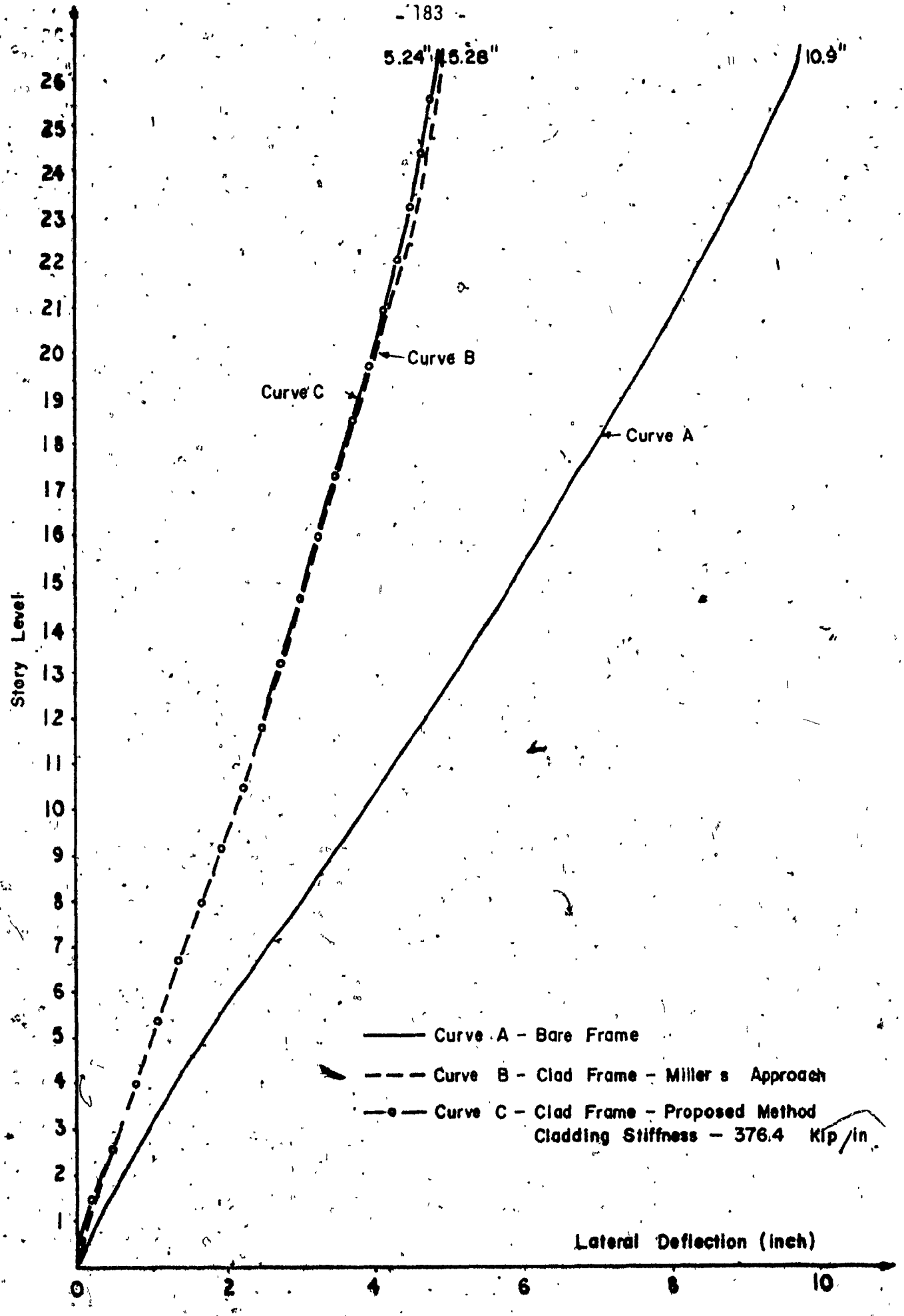

Fig. 6.19 Deflection Shapes for 26 Story Frames

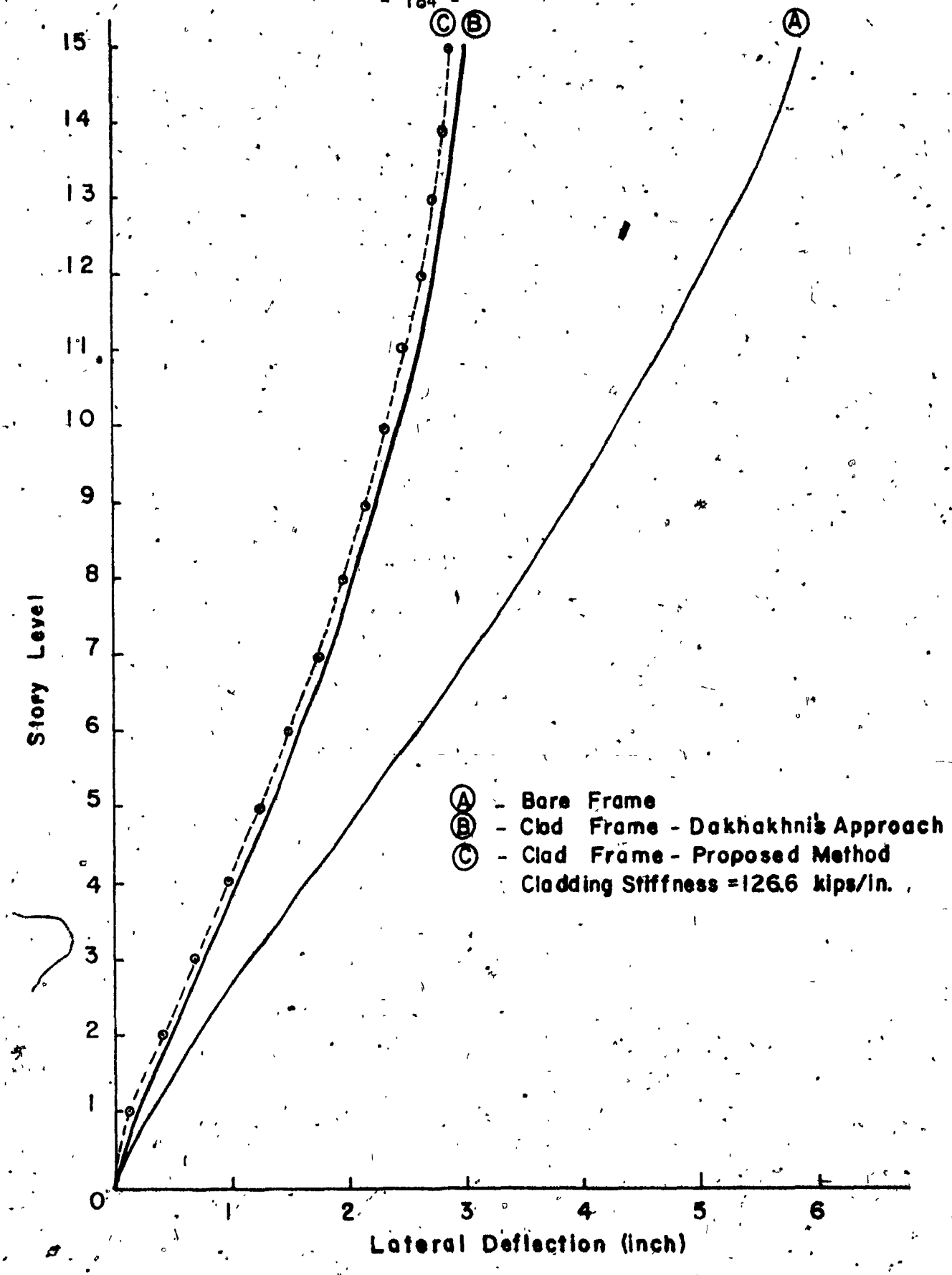

Fig. 6.20 Comparison Between Proposed Method and Dakhakhni's method for 15 Story Frame.

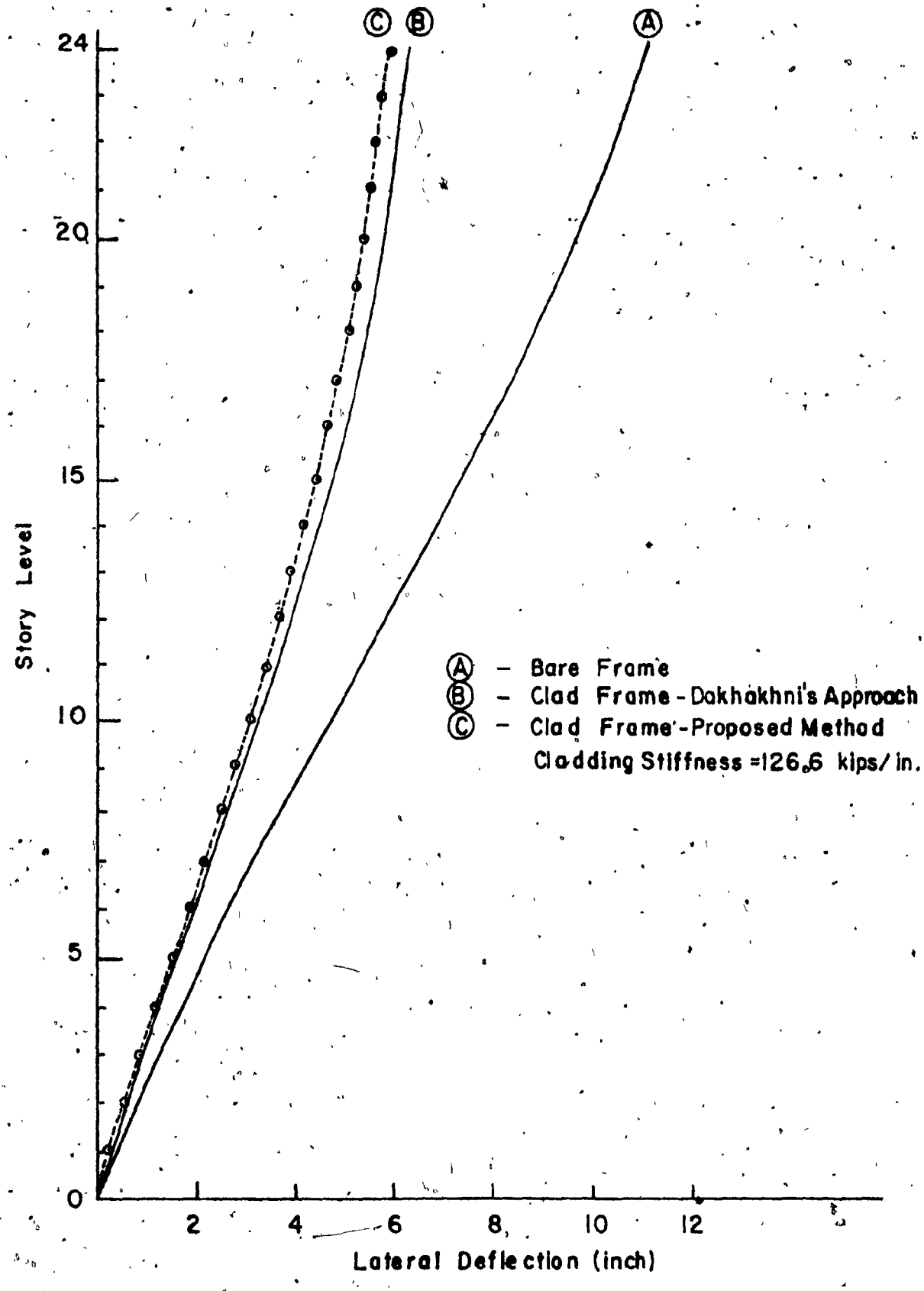

Fig. 621. Comparison Between Proposed Method and Dakhakhni's Method for 24 Story Frame.

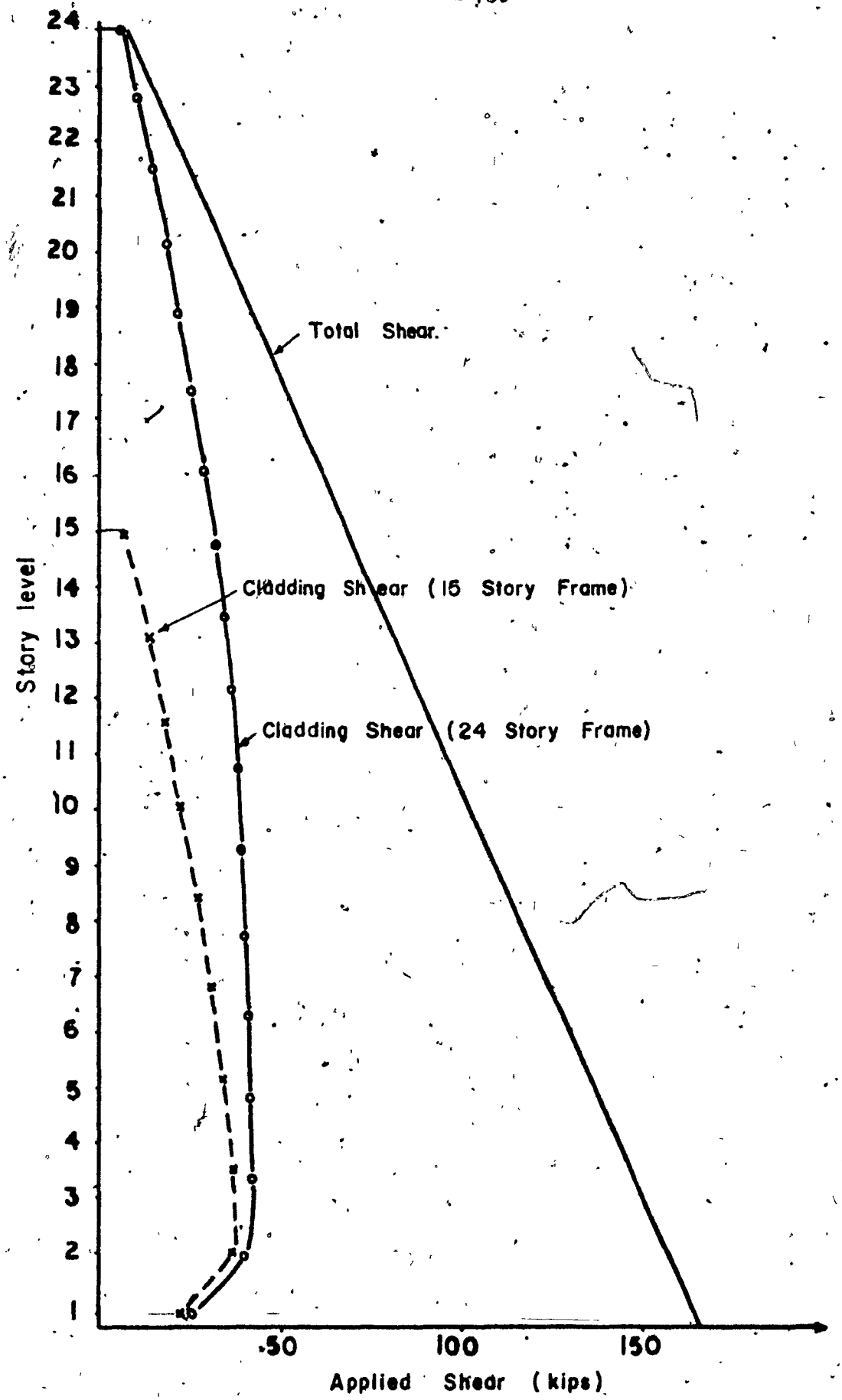

Fig. 6.22. Variation of Shear Forces in Claddings.

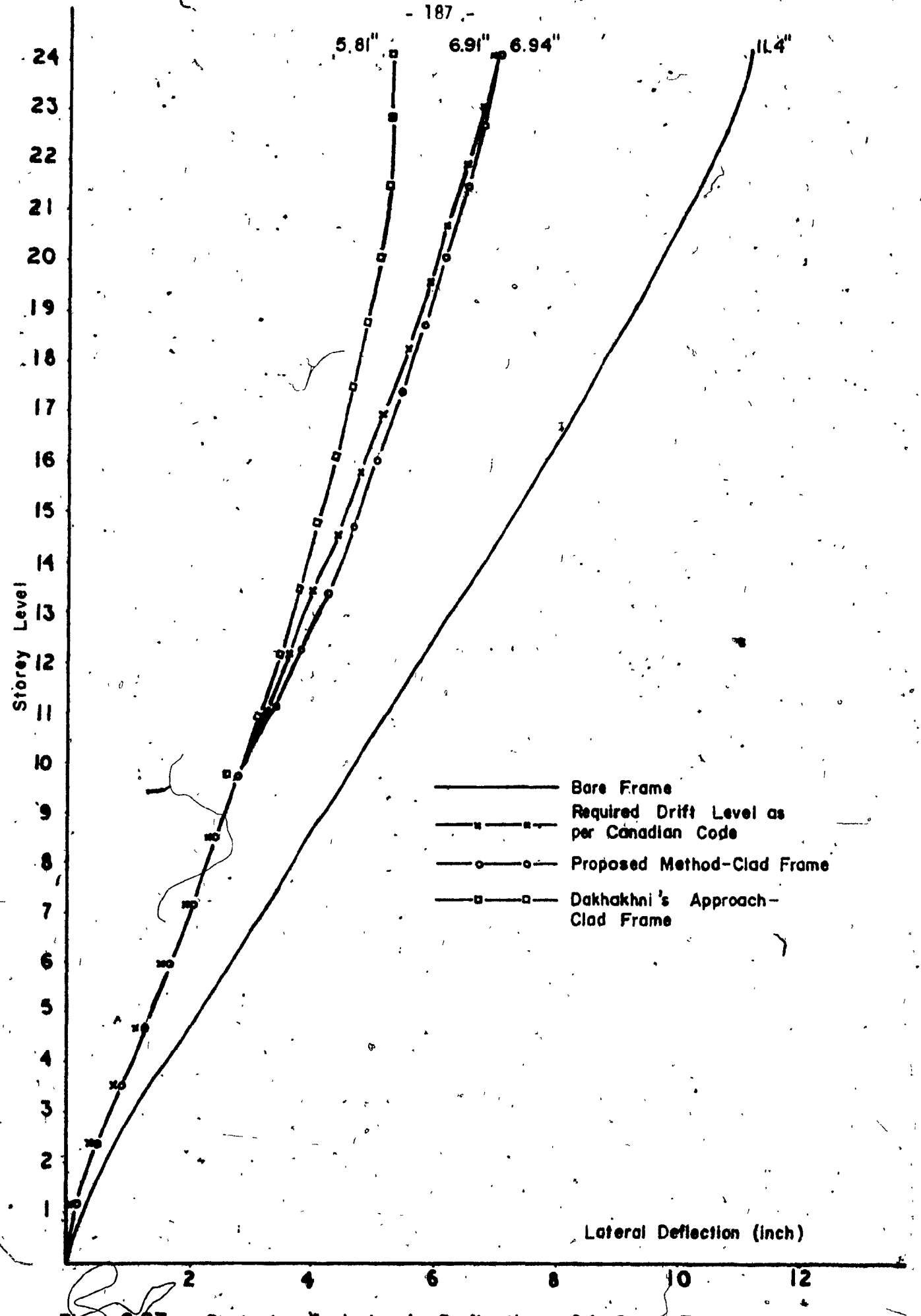

Fig. 6.23 Control of Lateral Deflection - 24-Story Frame